Elucidating Primary Human Nasal Epithelial Cell Responses to LAIV/IAV Infection in 2-Dimensional Culture Systems

Christopher James Proudlove

Submitted in the fulfilment of the requirements for the Degree of PhD, School of Infection, Immunity, and Inflammation, College of Medical, Veterinary & Life Sciences University of Glasgow, June 2023 of deposition to the library.

MRC – University of Glasgow Centre for Virus Research

Institute of Infection, Immunity, and Inflammation

College of Medical, Veterinary and Life Sciences

June 2023

Abstract

Influenza continues to represent a global health challenge, causing an estimated 650,000 deaths annually. The ability of Influenza viruses to undergo genetic drift and shift, leading to evasion of vaccination efforts, requires annual global surveillance of circulating influenza strains to best match vaccines to prevalent viral targets. Influenza vaccines can be split broadly in to two categories, Inactivated Influenza Vaccines (IIVs) and Live Attenuated Influenza Vaccines (LAIV). LAIV induces an attenuated active infection in the nasal tract, leading to specific and lasting adaptive immunity to influenza infection. Previous vaccination seasons with LAIV have found variable vaccine effectiveness (VE) with H1N1 subtypes, leading to continued studies to identify potential causes of variable VE. Madin-Darby Canine Kidney (MDCK) cells are widely used during LAIV research and development. However previous studies have found MDCK cells to be significantly more permissive to IAV than human airway cells. Here we elucidate the potential of using 2D primary human nasal epithelial (hAECn) cells in place of MDCK cells for LAIV medium-throughput assays. Using focus-forming unit (FFU)-style assay, we show that MDCK cells are significantly more permissive to LAIV than hAECn during single-cycle infection. We show that this is not a result of attachment/entry defects in hAECn cells and that LAIV A/Slovenia/2903/2015 has a higher attachment/entry efficiency than LAIV A/Bolivia/559/2013 in hAECn cells by quantifying intracellular virions 2hpi using absolute quantification digital-droplet PCR. We show by RT-qPCR that in hAECn cells, LAIV A/Slovenia/2903/2015 induces greater Myxoma resistance 1 (*MX1*) expression than LAIV A/Bolivia/559/2013. We show by 2-step RT-qPCR, that there are donor-dependent differences in *MX1* expression levels, and by pooling donors, the interferon stimulated gene (ISG) response falls within the range of the constitutive individual donors. We used open-access transcriptomic data from GTEX/Human Protein Atlas to show that constitutive expression of lung ISGs in 578 individuals is dependent on both sex and age, with males showing a higher level of differential ISG expression as a result of changing age compared to females, only Complement Factor H (CFH) showed significant difference as a result of advanced age in both females and males. Collectively, these data show hAECn cells may provide a more physiologically representative system for 2-Dimensional (2D) medium-throughput IAV/LAIV assays than MDCK cells, however, optimisation of immortalisation techniques is required to make them a cost-effective alternative to MDCK cells. Our data suggests that LAIV H1N1 strains induce different expression levels of ISG (*MX1*), we suggest this may contribute to differences in strain-specific adaptive responses and subsequent variable VE. We show that there is donor specific ISG responses (*MX1*) to LAIV, however analysis of constitutive lung ISG expression within the population show high levels of variation which may account for this. More work is required to understand the feasibility of using 2D hAECn cells to replace MDCK cells in IAV/LAIV research and development assays.

Table of contents

List of Abbreviations

IV	Influenza Virus
IAV	Influenza A Virus
IBV	Influenza B Virus
ICV	Influenza C Virus
WHO	World Health Organisation
HA	Haemaglutinin
NA	Neuraminidase
M2	Matrix Protein 2
M1	Matrix Protein 1
vRNPs	Viral Ribonucleproteins
NP	Nucleoproteins
PB1	Polymerase basic 1
PB2	Polymerase basic 2
PA	PA Polymerase Acid
SA	Sialic Acid
RBS	Receptor binding site
RdRp	RNA-dependent RNA-polymerases
NLS	nuclear localisation signals
NEP	Nuclear export protein
CDC	Centre for Disease Control
ARDS	Acute Respiratory distress syndrome
GISRS	Global Influenza Surveillance and Response System
FDA	Food and Drug Administration
NAI	Neuraminidase Inhibitor
IIV	Inactivated Influenza Vaccines
LAIV	Live Attenuated Influenza Vaccine
IGA	Immunoglobulin A
PRRs	Pattern Recognition Receptors
T-LAIV	Trivalent LAIV
Q-LAIV	Quadrivalent LAIV
VE	Vaccine Effectiveness
DIPs	Defective Interfering Particles

DVGs	Defective Viral Genomes
SIV	Simian Influenza Virus
TJs	Tight Junctions
AJs	Adherin Junctions
RIG-I	Retinoic acid-inducible gene
TLR	Toll-like Receptor
NLPR3	NOD- LRR- and pyrin domain-containing protein 3
CTD	Central carboxyl-terminal domain
CARD	Caspase activation and recruitment domains
MAVs	mitochondrial anti-viral signalling
NF-κB	nuclear factor-κB
IFN	Interferon
ISGs	Interferon Stimulated Genes
MX1	Myxovirus Resistance protein 1
IFITM	Interferon-inducible transmembrane proteins
NS1	Non-structural protein 1
DMEM	Dulbecco's Modified Eagle's Medium
SFM	Serum-Free Medium
KSFM	Keratinocyte Serum-Free Medium
CSK	Cytoskeletal buffer
PFA	Paraformaldehyde
Ethanol	Ethanol
FACS	Fluorescence-Associated Cell Sorting
MDCK	Madin-Darby Canine Kidney Cell
FFU	Focus-forming unit assay
A549	Human lung adenocarcinoma cells
HBEC3-KT	Normal Human bronchial epithelial cells immortalised with hTERT and CDK4
TCID50	50% Tissue Culture Infection Dose Assay
hAECn	Human Nasal Epithelial Cells
FACS	Fluorescence-associated cell sorting
GAPDH	Glyceraldehyde 3-phosphate dehydrogenase
PFU	Plaque-forming units
FFU	Focus-forming units
MOI	Multiplicity of infection

hpi	Hours post-infection
EpCAM	Epithelial cell adhesion molecule
IMR90	Normal human fetal fibroblast cells
WT	Wild type
HPA	Human Protein Atlas
TRIM22	Tripartite motif-containing 22
hCK	Humanised MDCK cells

List of Tables

List of Figures

Acknowledgments

I would like to thank my primary supervisor Dr Chris Boutell for his continued patience and faith in my abilities. Dr Boutell has always encouraged me to take an active role in leading my research and embracing good quality science. My time with Dr Boutell has led to growth and understanding of good scientific practise. I will proudly take forward the lessons I have learned under Dr Boutell's supervisorship to any future scientific career. I would like to thank my secondary supervisor Dr Edward Hutchinson for his valuable insight into Influenza Virology that has helped to shape my thought processes regarding influenza and LAIV biological studies.

I would like to thank Dr David Chapman (AstraZeneca). As co-supervisor from industry, Dr Chapman has been instrumental in shaping the scientific objectives and outcomes of this research project. Dr Chapman has provided a highly collaborative environment, within which scientific discussion relating to this research project was both encouraged and nurtured. These conversations have served to only increase my enthusiasm for researching the immunobiological properties of the LAIV vaccine.

Collectively, all three members of my supervisory team provided support and encouragement through the difficulties associated with the COVID-19 pandemic. Where experimental aims and objectives required adjustment, my supervisory team were instrumental in helping me shape my own thoughts and research goals to complete this research project. For this I am truly thankful.

I would like to thank the entire team within the Boutell group (CVR), whose collaborative and enthusiastic scientific ideologies helped to inspire me to produce quality research to the best of my potential. Through difficult times, these team members provided support and understanding to enable me to find a path forward, thank you Joanna Wojtus, Lauren Orr, Stephen McFarlane, Zhousiyu Yang, Victor Iliev, and Ann Orr.

Lastly, I would like to thank my wider support network, in particular my Wife, Kerry Proudlove, who has supported me throughout the long, unpredictable hours and difficult times during this research project, her support and understanding has helped make this research project possible. I would like to thank my family for their continued support in my pursuit of academic opportunities that has helped me realise my scientific interests and abilities.

Author Declaration

I, Christopher Proudlove, declare that, except where explicit reference is made to the contribution of others, this thesis is the result of my own work and has not been submitted for any other degree at the University of Glasgow or any other institution. This project was supported by Centre for Virus Research in collaboration with AstraZeneca.

COVID-19 Impact Statement

Our initial aim was to produce an immortalised airway epithelial cell culture model system by utilising telomerase-extension methods as described previously (Ramirez et al., 2004). Although the process of transducing primary hAECn cells was successfully completed by Stephen McFarlane (MRC University of Glasgow, Centre for Virus Research), we discovered that fibroblast outgrowth occurred rapidly upon serial passage (as discussed in chapter 3.2). To this end we took time to optimise FACS to positively select for epithelial cells. As discussed in chapter 3.2, we found that epithelial cell survival post-FACS was limited to 1-2 passages. Optimisation of the sorting protocol was ongoing at the onset of the Covid-19 pandemic. During lockdown, we had reduced ability to enter laboratories due to social distancing and CVR restructuring due to the pandemic. Together with our collaborators at AstraZeneca, we re-prioritised the aims and objectives of the research project to focus on how non-immortalised primary nasal epithelial cell responded to LAIV infection. Data derived from such analysis would be highly informative on the use of primary human nasal epithelial cells for IAV/LAIV assays as used in both academia and commercial biological settings. Due to the subsequent limited time, several planned experiments were unable to be completed, these include the *in vitro* validation of the GTEX-portal inter-donor differences in ISG expression that are discussed in Chapter 3.4. We would utilise two-step RT-PCR and western-blot analysis to confirm differences in ISG expression between individual donors.

I hope these circumstances are taken into consideration during the assessment of this thesis.

1. Introduction

1.1. Introduction to Influenza Viruses

1.1.1. Influenza Virus Classification and Disease Burden

Influenza viruses (IVs) belong to the family Orthomyxoviridae. These viruses are single-stranded, negative-sense RNA viruses that fall in to four main subtypes, Influenza A Virus (IAV), Influenza B Virus (IBV), Influenza C Virus (ICV) and Influenza D virus (Wright et al., 2007). IAV and IBV viruses are the causative agent of the respiratory disease 'seasonal flu'. IVs can be further categorised into subtypes. IAV subtypes are categorised by their hemagglutinin (HA) and Neuraminidase (NA) types. Within humans, there are two circulating subtypes: A(H1N1) and A(H3N2). Influenza B, unlike IAVs, are nt subtyped, bt are separated by lineage, with the two major human circulating IBV lineages being B/Yamagata and B/Victoria. ICV is less common in humans and deemed not to be of public health importance by the WHO . The World Health Organisation (WHO) report that there are an estimated 3-5 million cases of flu annually, causing an estimated 650 000 respiratory-related deaths per year (WHO, 2023b). Although Influenza can infect any age group, children are particularly at risk, with studies showing that in children under 5 years of age, there are an estimated 9,243 – 105,690 influenza-related deaths (Iuliano et al., 2018). Studies have shown that younger children (< 2 years of age) shed the greatest amount of Influenza virus during infection (Neuzil et al., 2002), indicating higher replicative potential of Influenza in the very young. As well as this high cost to human health, Influenza epidemics incur a high burden on healthcare systems. For the US alone, Influenza incurs an annual cost of an estimated $87 billion (Molinari et al., 2007). In addition to seasonal flu, Influenza can cause global pandemics owing to the highly mutagenic nature of the virus. Influenza A viruses are named according to their genus, the location of the isolate, the isolate number, the year the strain was isolated and the subtypes of the surface glycoproteins Hemagglutinin (HA) and Neuraminidase (NA). As of 2021, there were 18 different HA subtypes, and 11 NA subtypes. For IBVs, there are no surface glycoprotein subtypes (Peter M. Howley, 2020).

1.1.2. Influenza Virus Morphology

Influenza viruses (IVs) are polymorphic, existing both as filamentous and spherical virions (Badham and Rossman, 2016). IVs have a host-derived lipid envelope within which there are two surface glycoproteins; Haemagglutinin (HA) and Neuraminidase (NA), as well as small quantities of matrix protein 2 (M2) (Noda, 2011). The surface densities of HA and NA glycoproteins is determined by the influenza subtype, where H3N2 virions have been shown to have a higher proportion of glycoprotein spikes than seen in H1N1 subtypes (Moulès et al., 2011). HA and NA are not present in equal quantities on the virions surface. For H3N2 virions, HA was found to be the dominant glycoprotein, with a HA:NA ratio of 300:40 (Harris et al., 2006). The M2 protein is a ion channel that has roles in replication and homeostasis (Manzoor et al., 2017). Beneath the viral envelope there is a matrix layer formed of the matrix 1 (M1) protein, M1 has a role in maintaining virion morphology (Calder et al., 2010). At the centre of the virion lies the viral gene segments. Influenza viruses are segmented viruses, containing 8 gene segments that encode 14 viral proteins. The nature of the packaging of these segments appears to have importance in the production of new infectious virions. It has been found that IV vRNPs form a 1+7 formation, with a single vRNP surrounded by the remaining 7 in a circular pattern. Indeed, when an artificial virion omitting HA-RNP to contain only 7 out of 8 segments was used to infect human cells, host cell ribosomal RNA (rRNA) was recruited into the new virion to complete the 1+7 packaging formation (Noda et al., 2018). The segmented nature of IVs makes them ideal for reverse genetics studies, in particular, the development of Influenza vaccines that have greatly benefited from the ability to mutate, change, and reincorporate specific viral gene segments (Nogales and Martínez-Sobrido, 2016). vRNPs are composed of viral RNA bound with viral nucleoprotein (NP). At the partially complementary ends of these structure lie the polymerase complex comprising polymerase basic 1 (PB1), polymerase basic 2 (PB2) and polymerase acid (PA) (Eisfeld et al., 2015) (Zhang et al., 2019). Figure 1 shows a cartoon schematic of an influenza virion highlighting the basic structure and internal vRNPs.

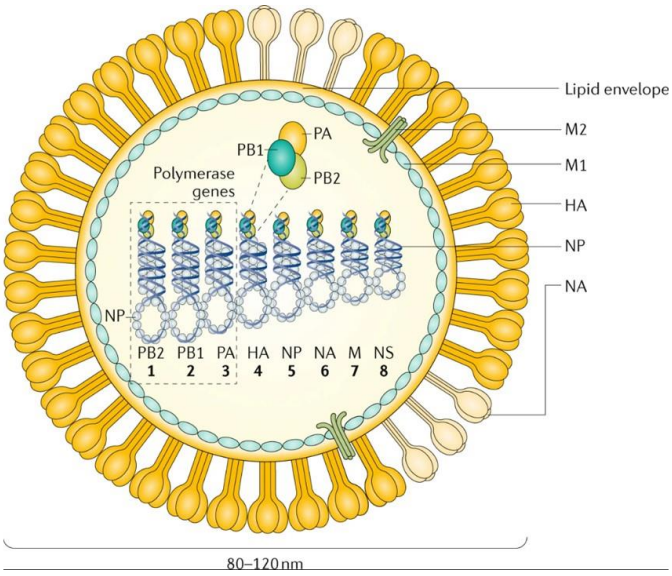

Figure 1. Morphology and Genetic Structure of an Influenza Virion. Influenza viruses are negative-sense double-stranded RNA viruses. Virions are enclosed with a host-derived lipid envelope containing two surface glycoproteins HA and NA as well as the ion channel protein: M2. Beneath the lipid envelope is the M1 protein responsible for maintaining virion structure. Within the virion there are 8 gene segments consisting of viral genomes encapsulated in viral NP (vRNPs), each vRNP contains a polymerase complex consisting of PB1, PB2 and PA subunits. Image obtained from Krammer et al. 2018 (Krammer et al., 2018).

1.1.3. Influenza Virus Replication Cycle

Influenza infection is mediated by the recognition of- and attachment to host cell surface receptors. Viral HA recognises sialic acid (SA) receptors on host cell surfaces. Influenza viruses show binding specificity to certain sialic acids. Human IVs specifically bind α(2,6) SA linkages, whereas avian and equine influenza specifically binds α(2,3). This can be seen in species specificity with the human trachea containing predominantly SA α(2,6) receptors (Couceiro et al., 1993), whereas the epithelia of Duck guts has been shown to have predominantly SA α(2,3) receptors (Ito et al., 1998). These distinctions are not definitive, mutations within HA molecules can enable changes in the HA specificity towards certain SA receptors (Palese and Shaw, 2007). This specificity is suggested to be an important barrier in cross-species transmission, limiting potential influenza pandemic events (Skehel and Wiley, 2000). It's important to note that the distribution and type of sialic acid is not heterogeneous within the human airway. Indeed, it has been shown that SA α2-6 is more common in ciliated cells of the upper respiratory tract, whereas both α2-3 and α2-6 are present on ciliated epithelial and mucus-secreting cells within the human upper airway tract, specifically the nasal tract. As well as differences in sialic acid types within the human airway, there are differences between children and adults, it has been shown that children express SA α2-3 more-so than adults. (Zhao and Pu, 2022).

Internalisation of virions begins with the cleavage of the HA precursor (HA0) to HA1 and HA2 domains. HA1 is the globular head of the HA molecular, containing the receptor binding site (RBS). At the top of the HA molecule is a highly conserved shallow depression that is the site of sialic acid binding (Weis et al., 1988). The transmembrane HA2 domain plays an important role in stabilising the HA trimer within the viral membrane (Mair et al., 2014). Internalisation of influenza virions can occur either by clathrin-dependent endocytosis (Roy et al., 2000, Chen and Zhuang, 2008) or the clathrin-independent micropinocytosis (Sieczkarski and Whittaker, 2002, de Vries et al., 2011). There are currently understood to be a number of mechanisms by which influenza virus can enter cells as summarised in Figure 2. Sialic-acid dependent entry occurs via interaction with either/both of HA and NA glycoproteins. Known receptors for SA-dependent entry include nucleolin, EGFR and CaV1.2, and more. SA-independent entry pathways can occur through DC-SIGN and MHC II pathways. Of note is that the entry mechanism for influenza virus is both cell dependent and viral strain dependent (Sempere Borau and Stertz, 2021). Once the endosomes are internalised, they are transported along microtubules, accumulating protons. This leads to a change in pH that causes HA-mediated virus-endosome membrane fusion and subsequent release of vRNPs into the cellular cytoplasm (Lagache et al., 2017).

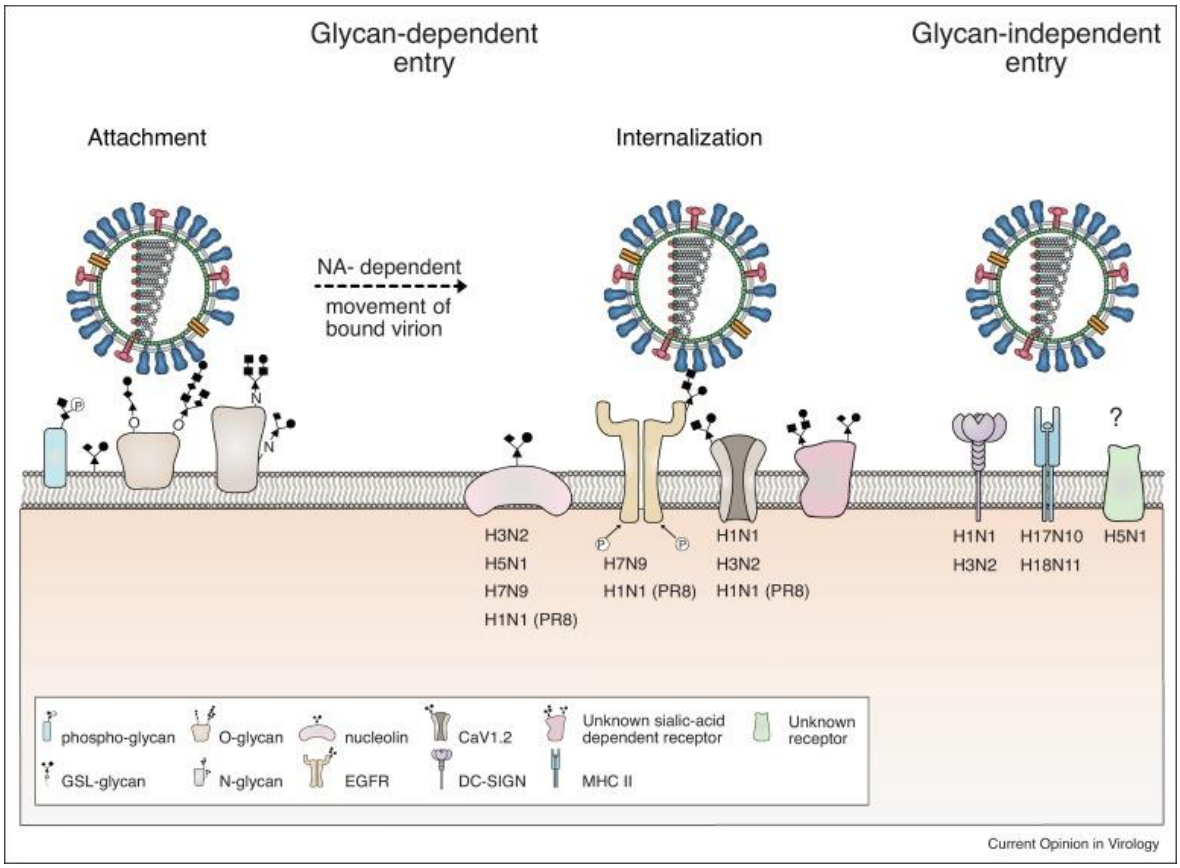

Figure 2. Influenza Virus Entry Mechanisms. Influenza virus can enter target cells through eith a glycan-dependent or glycan-independent pathway. Schematic outlines examples of known receptors as well as associated influenza strain. Adapted from Borau et al. 2021. (Sempere Borau and Stertz, 2021).

Once in the cytoplasm, vRNPs utilise the cells importin-α-importin-β nuclear import pathway to directs vRNPs into the nucleoplasm (Dou et al., 2018). Nuclear import of vRNPs require direct activity of nuclear importins, all 8 influenza segments have been shown to contain nuclear localisation signals (NLS). However, viral NP NLS have been shown to be necessary and solely sufficient for import in to the nucleus (Peter M. Howley, 2020). Viral RNA transcription and replication occurs in the host-cell nucleus using viral RNA-dependent RNA-polymerases (RdRp). Viral RdRp contains three proteins, PB1, PB2 and PA. Viral mRNA has been found not to contain a native 5'-cap, as is present with cellular mRNA, (Plotch et al., 1978). Instead, influenza virions undergo 'cap-snatching', whereby the endonuclease activity of PB2 cleaves cellular mRNA to release the cap structure. This process is crucial for replication as the cellular cap section is required for viral transcription (Li et al., 2001).

Nuclear export requires host cell nuclear export protein (NEP). It is understood that NEP forms a complex with viral M1 and newly synthesised vRNPs (Peter M. Howley, 2020, O'Neill et al., 1998). Newly synthesised vRNPs are transported to the cellular membrane for virion assembly, incorporating a host-cell lipid membrane. Packaging of new virions is thought to occur via one of two mechanisms, first, random packaging of each of the eight segments have the same signalling sequence for packaging that will lead to random packaging of each virion, increasing the likelihood of infectious virion generation. The second model, 'selective incorporation model' suggests that each segment has specific, individual activity, leading to independent packaging of individual RNPs into newly forming virions (Peter M. Howley, 2020) After viral budding, the virion must be released from the cellular plasma membrane, to do this, viral NA cleaves sialic-acid residues from viral glycoproteins, allowing for virion release and continuation of infection (Palese et al., 1974). The replication cycle of influenza viruses is summarised in figure 3.

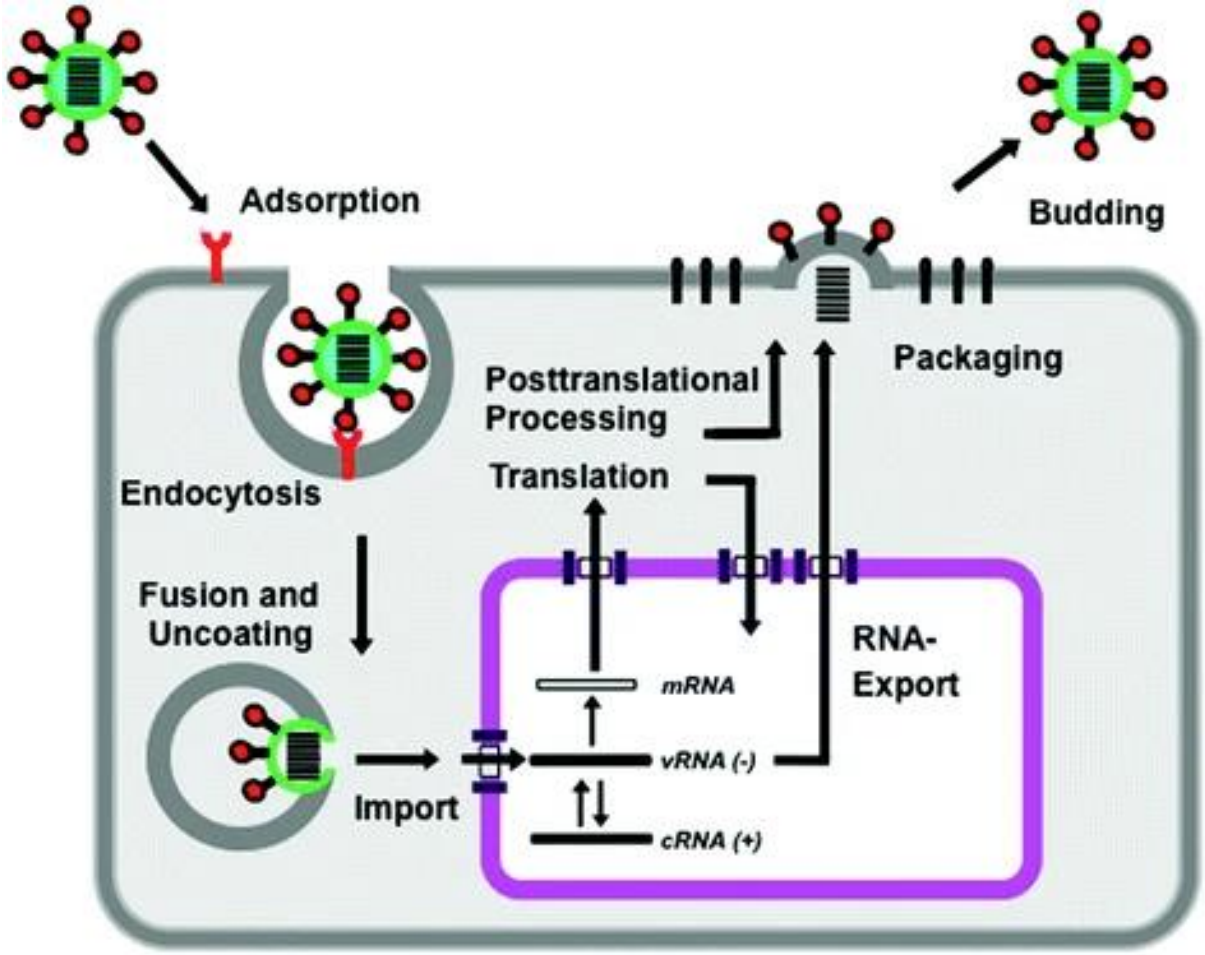

Figure 3. Summary Schematic of Influenza Virus Replication Cycle. Influenza viruses attach to surface glycoproteins of host cells before undergoing adsorption and endocytosis. pH-mediated virion fusion to endosome membranes is followed by vRNP uncoating into the cell's cytoplasm. Nuclear import of vRNPs is required for cRNA formulation for viral genome replication. Viral mRNA is produced within the nucleus and is subsequently exported into the cytoplasm for translation of new vRNPs. Packaging of progeny IAVs occurs at the cell membrane whereby budding occurs followed finally by release of new influenza virions. (Adapted from Pleschka S. 2013 (Pleschka, 2013)).

1.2. Influenza Pathology

Influenza is the causative agent of 'flu'. Mild flu symptoms, as defined by the Centre for Disease Control (CDC), include fever, coughing, sore throat, runny/stuffy nose, muscle aches, headaches, fatigue, and nausea/diarrhoea. Acute cases can lead to pneumonia, either by influenza infection directly, or co-infection with bacteria. Additionally, infection of the lower lung can lead to an extreme pro-inflammatory response and potential sepsis (CDC, 2022a). One of the most acute pathologies of influenza infection is what's known as a 'cytokine storm'. Cytokine storms occur as a result of an over-active pro-inflammatory response that leads to excessive production of cytokines, leading to acute respiratory distress syndrome (ARDS) (Short et al., 2014). Cytokines are small proteins that are responsible for signalling between cells during an immune response (Gu et al., 2021, Liu et al., 2016). Cytokine storms can lead to sever pathologies, including organ damage, and in extreme cases can be potentially fatal (Herold et al., 2015). Severity of disease is associated with certain at-risk groups with particular co-factors, including obesity, advanced age, and pregnancy. Additionally, it has been found that underlying genetics can determine disease outcomes, with variation in baseline expression of genes that confer controls on intracellular viral replication (Clohisey and Baillie, 2019). According to the CDC, between 2010 and 2020, the annual number of illnesses resulting from flu were an estimated 9 million to 41 million, resulting in between 140,000 and 710,000 hospitalizations. The number of deaths attributed to flu were estimated to be between 12,000 and 52,000 within the US. This high illness burden necessitates continued research into the biology of influenza infection, therapeutics for treatment to limit severe illness and associated immunopathology's, and improved vaccination strategies to prevent severe disease in vulnerable individuals.

1.3. Clinical Relevance of Influenza: - Seasonal and Pandemic Flu

During the constant arms race between pathogens and host immunity, influenza viruses have two major defence mechanisms to avoid host immunological responses to infection; antigenic drift, and antigenic shift (2018). Antigenic drift is characterized by the slow accumulation of point mutations within the viral genome (Both et al., 1983). These point mutations are possible because influenza viruses lack the proof-reading machinery during vRNA replication (Steinhauer et al., 1992). When these point mutations build in the antigenic HA and NA glycoproteins, this can lead to viral escape from host adaptive immune responses, thus conferring replicative advantage to virions with these mutations (Wiley et al., 1981). Where antigenic drift is characterized by the slow accumulation of single nucleotide polymorphisms (SNPs), antigenic shift is defined by the complete replacement of genome segments. This mechanism necessitates co-infection with influenza strains with different host reservoirs. For this reason, only similar IAV subtypes are known to undergo antigenic shift as they have a wide range of host reservoirs (Cox and Subbarao, 2000). The resulting novel IAV strains can replicate with increased efficiency as there is limited immunity in the wider population.

This increased ability to replicate can lead to influenza pandemics. The 1918 pandemic (Spanish Flu) is attributable to the ability of avian influenza A(H1N1) to jump species barriers from host reservoir to humans, and subsequently undergo human-human transmission through a process of spill-over event (Nicholson et al., 2003). Other pandemics have emerged including in 1957, 1968, 1977 and 2009 (2018).

The mutagenic nature of Influenza viruses has significant ramifications for anti-Influenza vaccination strategies. To best match vaccine strains to currently circulating Influenza strains, the World Health Organization (WHO) through its Global Influenza Surveillance and Response System (GISRS), monitor circulating influenza strains on an annual basis. These data are used to recommend Influenza strains to be incorporated in to Influenza vaccines for each flu immunisation season (WHO, 2023a).

1.4. Vaccination Strategies Against Influenza

1.4.1. Inactivated Influenza Vaccines

There are a number of vaccines that have been developed to protect against seasonal flu. Anti-flu vaccines come in three forms, inactivated influenza vaccines (IIVs), Live Attenuated Vaccines (LAIV) and mRNA vaccines. Table 1 summarises vaccines approved by the FDA in the USA as of 2023.

IIVs work to introduce an adaptive immune response to Influenza antigenic HA and sometime NA (Wong and Webby, 2013). Specifically, IIVs have been shown to induce both a local and systematic immune response, characterized by a dominant IgG antibody response (Cox et al., 1994), with VE increasing with multiple doses as shown in children between 6-23 months, where 2 doses of IIV leads to higher HAI titres (Wall et al., 2021). This phenomenon is suggested to result from reduced exposure to virus in these younger children, as shown by older children showing robust HAI titres after a single dose.

Table 1. Anti-Influenza Vaccines Approved by the USA FDA as of 2023. Data collated from FDA (FDA, 2023), available at: **https://www.fda.gov/vaccines-blood-biologics/vaccines/vaccines-licensed-use-united-states**

Product name (Trade Name)	Year First Licensed	Manufacturer	Target Patient Demographics	Delivery Method	Inactivated/Attenuated
Fluad Quadrivalent	2020	Seqirus	65+ yrs	Intramuscular Injection	Inactivated
Afluria Quadrivalent	2016	Seqirus	18+ yrs	Intramuscular Injection	Inactivated
Flucelvax Quadrivalent	2016	Seqirus	6 months +	Intramuscular Injection	Inactivated
FluLaval	2006	ID Biomedical Corporation of Quebec	6 months +	Intramuscular Injection	Inactivated
FluMist Quadrivalent	2003	AstraZeneca	2 yrs – 49 yrs	Nasal Spray	Live Attenuated
Fluarix Quadrivalent	2012	GlaxoSmithKline Biologicals	6 months +	Intramuscular Injection	Inactivated
Fluzone Quadrivalent	2014	Sanofi Pasteur Inc.	6 months +	Intradermal Injection	Inactivated

1.4.2. Live Attenuated Influenza Vaccines

The Live Attenuated Influenza Vaccine (LAIV, Flumist/Fluenz) is an active, temperature-attenuated anti-flu vaccine that is delivered via a nasal spray (AstraZeneca, 2023). In the US, Flumist/Fluenz is recommended for persons aged 2 years – 49 years (Carter and Curran, 2011). In the UK, LAIV is used for annual school vaccination programmes. School vaccination provides direct protection against flu for this age group, although studies have shown that such a school vaccination program confers protection to family members also (King et al., 2006). LAIV infection and replication occurs in the nasopharynx, working on the principle of 'infect to protect'. The restriction of replication to the upper respiratory airway prevents severe pathologies associated with lower-respiratory tract infections. During the production of LAIV, reverse genetics technologies are utilised to incorporate antigenic HA and NA glycoproteins on a backbone containing proteins and gene segments from influenza strains containing mutations limited replication to 33ºC. LAIV is produced as a quadrivalent formulation, containing two IAV strains (H1N1 and H3N2) and two IBV strains from the B/Yamagata and B/Victoria lineages (Barr and Jelley, 2012), in the temperature attenuated backbones from A/Ann Arbor/6/60 (Jin et al., 2003) and B/Ann Arbor/1/66 (Hoffmann et al., 2005) respectively. A/Ann Arbor/6/60 temperature attenuation is conferred by amino acid substitutions in 10 loci within viral proteins PB1, PB2 and NP (Jin et al., 2003), for B/Ann Arbor/1/66, temperature attenuation is conferred by mutations of viral PA (Donabedian et al., 1987).

LAIV induces both an antibody and T-cell immune response in the nasopharyngeal tract. Where LAIV B-strains induce both an IgA and T-cell response, LAIV A-strains have been shown to predominantly induce a T-cell response with a reduced antibody response (Ambrose et al., 2012). Such B- and T-cell responses have been shown to provide protection for up to 1 year in children (Mohn et al., 2015). Where adaptive immune responses to LAIV have been characterised, less is known about the specific innate immune responses to LAIV. This is important as it has been shown that a robust adaptive response requires the activation of innate immunity (Medzhitov and Janeway, 1997). Interestingly, a comparative study of LAIV and matched wild-type strains showed that in 3D-differentiated nasal cells, LAIV strains induced a stronger host-cell innate immune response, including the up-regulation of a number of genes including pattern recognition receptors (PRRs) RIG-I and TLR-3, as well as STAT-1, IRF-7, MxA and IP-10 (Fischer et al., 2014). With LAIV being quadrivalent, the impact of co-infection with 4 LAIV strains on such early innate immune responses remains unclear.

Flumist/Fluenz was first approved for use in 2003 in the US (Barberis et al., 2016). Early LAIV formulations were produced as a trivalent formulation, containing A/H1N1, A/H3N2 and B influenza viruses (Jackson et al., 1999). In 2012, the WHO and European Medicines Agency (EMA) recommended that an additional B strain should be added to the formulation to combat mismatches seen between the T-LAIV B strain and circulating IBVs. With LAIV now becoming quadrivalent (Q-LAIV), containing A,H1N1, A/H3N2, B/Yamagata and B/Victoria strains (Tisa et al., 2016). Vaccine effectiveness (VE) of LAIV has, in some previous seasons (2013-14, 2015-16) (Caspard et al., 2016, Caspard et al., 2017), been sub-optimal. For the 2016-17 immunisation season the USA Advisory Committee on Immunization Practices (ACIP) voted that the Flumist/Fluenz should not be used for persons aged 2 to 17 years. They state that during the 2015 - 2016 immunisation season, LAIV had a vaccine effectiveness of 3% compared to that of IIV (62%) for the comparable vaccination seasons (ACIP, 2016). In 2018, ACIP, upon review, recommended that LAIV be re-introduced as an option for influenza vaccination in the US for the 2018-19 vaccination season (Grohskopf et al., 2018).

Given the sub-optimal effectiveness conferred by LAIV during some certain previous seasons (2013-14, 2015-16) (Caspard et al., 2016, Caspard et al., 2017), efforts are being made to elucidate underlying causes of variable VE. VE studies by Hawksworth et al. 2020 have shown that there are strain-specific differences in relative replication rates within 3D-differentiated human airway cells. Interestingly, demonstrate that LAIV A/Bolivia/559/2013 has a relatively lower replication effectiveness than a comparative H1N1 strain (LAIV A/Slovenia/2019/2015) (Hawksworth et al., 2020). These data are supported by another study by Dibben et al. 2021 where it was found that LAIV A/Bolivia/559/2013 has a reduced replicative fitness compared to other LAIV strains when infected as a part of a trivalent or quadrivalent formulation (Dibben et al., 2021). Together, these data suggest that different strains of LAIV have different rates of replication, and that inter-strain competition in a multi-valent formulation can compound this difference. These data provide a hypothesis that strain-dependent differential replication rates can contribute to strain-specific variation in VE, what remains to be seen is how these impacts upon the ability of each LAIV strain to induce an innate immune response and subsequent protective adaptive response. Other internal AstraZeneca studies have begun to shed light on the comparative immunogenicity of LAIV strains. A common phenomena of Influenza replication is the production of defective interfering particles (DIPs) that contain defective viral genomes (DVGs). These DVGs have been shown to be immunogenic, eliciting innate immune responses equal to, or greater than fully intact influenza viruses (Wu et al., 2022). Due to this, studies have been undertaken to determine the relative amounts of DVGs in different LAIV strain monovalent formulations, and their relative contribution to the activation of innate immunity. Ayaz et al. showed that for a number of LAIV strains, including LAIV A/Slovenia/2903/2015 and LAIV A/Bolivia/559/2013, that there was no

significant difference in the number of DVGs, between sample preparations and that the immunogenicity of DVGs associated with each strain to not induce a statistically different innate immune response between high and low DVG abundances (Ayaz et al., 2021).

1.4.3. mRNA Vaccines to Influenza

mRNA vaccines have been touted as a cost-effective alternative to current IIVs and LAIV vaccines (described above). mRNA vaccines come in two varieties, self-amplifying and non-amplifying. Non-amplifying mRNA vaccines do not require the entrance of the vaccine into the host cell nucleus, making use instead, of cytoplasmic transcriptomic machinery to produce the relevant antigens that are presented on the cell surface, leading to both a humoral and T-cell immune response. mRNA vaccines use lipid nano particles (LNP) as a delivery mechanism to enter target cells (Chivukula et al., 2021). These vaccines are promising as they are comparably easy to produce and with the absence of the requirement for replication, the potential for a highly multivalent mRNA vaccine is a promising step forward towards a universal flu vaccine. Indeed recently, a formulation of influenza mRNA vaccine containing 20 IAV strains was tested and proved effective against all 20 IAV strains in ferrets (Arevalo et al., 2022). These mRNA vaccines do however present challenges for long lasting protection. Indeed in 2019, a randomized control trial in adults found that mRNA vaccines consisting of H10N8, and H7N9 IVs to only show a strong humoral immune responses, with no cell-mediated immunity being observed (Feldman et al., 2019). Although mRNA vaccines show promise, as has been the case with mRNA vaccines developed and used widely during the SARS-COV-2 pandemic (LactMed, 2006), further work is required to understand what benefits mRNA anti-influenza vaccines would incur beyond those currently available IIV and LAIV technologies.

1.5. Anti-Influenza Therapeutics

A number of drugs have been developed for the treatment of Flu, in the US there are four drugs that have been approved by the Food and Drug Administration (FDA) and are recommended by the CDC: Rapivab (peramivir), Relenza (zanamivir), Tamiflu (oseltamivir phosphate) and Xofluza (baloxavir marboxyl) (CDC, 2022b). In the UK, oseltamivir and Zanamivir are the chosen drugs recommended by the UK government (2021). Of the drugs named above, peramivir, zanamivir and oseltamivir are neuraminidase inhibitors (NAI). (McClellan and Perry, 2001, Elliott, 2001, 2019). The NAIs act to block the release of newly formed virions from the infected cell surface, effectively blocking further infection events and halting viral spread (McKimm-Breschkin, 2013). Baloxavir in contrast, acts to block viral transcription by blocking the 'cap-snatching' ability of influenza to obtain host-derived RNA fragments that act as a primer for transcription (Dufrasne, 2021). Although such treatments exist, there has long been efforts to offer prophylaxis in the form of annual vaccination strategies.

1.6. Immunity to Influenza

1.6.1. Physical Barriers to Influenza Infection

Upon entry into the airway, influenza virus faces a number of physical barriers to infection. Lining the epithelial surface is a mucus layer up to 50 μm in thickness (Fahy and Dickey, 2010). Mucus contains mucins that competitively bind influenza HA. This is counteracted by viral NA that acts to cleave mucin-HA interactions. A study using simian influenza virus (SIV) found that NA can degrade mucins to promote the movement of SIV through mucus (Yang et al., 2014). This has been demonstrated for human IAVs too, whereby it was shown that IAV interacts with human mucus in a dose-dependent manner, similar to the SIVs, IAVs were able to negate the competitive binding potential of mucins to HA through cleavage of mucin sialic acids by viral neuraminidase (Cohen et al., 2013). As well as overcoming the mucus barrier in the airway, epithelial cells present their own physical barrier in the form of three junctions: tight junctions (TJs), adherins junctions (AJs) and desmosomes. The formation of TJs helps to stabilize cell-to-cell contact through interactions with the cytoskeleton, which promotes inter-cellular signalling (LeMessurier et al., 2020) Avian IVs have been shown to disrupt this process through NS1 binding to a key TJ domain (PDZ), destabilizing the TJ and modulating cellular ability to signalling (Golebiewski et al., 2011).

1.6.2. Microbiome as an Anti-Influenza Barrier to Infection

The microbiome of the upper and lower airway tract presents another barrier to influenza infection. It has been found in murine models that the effect of the microbiome on influenza infection potential results from priming of the immune system, indeed when the microbiome was disrupted through administration of antibiotics, there was a significant change in macrophage response both type I and type II interferons (Ichinohe et al., 2011). Interestingly age appears to determine the relative effectiveness of the microbiome to regulate influenza infection (Lee et al., 2019a). Although the gut microbiota has been well characterised in its role in host immune responses, less in known about the effect of the lung microbiome on respiratory illnesses. Takeshi Ichinohe et al. showed in 2021 that the microbiome of the lung regulates adaptive T cell, and antibody responses to influenza (Ichinohe et al., 2011). Additionally, they showed that the presence of the lung microbiota leads to a steady state induction of pro-inflammatory interleukins (IL-1β and IL-18) (Ichinohe et al., 2011). If an infective influenza virion can successfully reach its target cell, it will begin the process at internalisation. Once within the cell, the host cell intrinsic and innate immune responses will act to regulate their infectious potential.

1.6.3. Intrinsic Immunity to Influenza Viruses

Intrinsic immunity can be defined as acting as antiviral host restriction factors that are present within the host cell prior to infection, acting directly on the invading virus to restrict the initiation or progress of infection. A number of such proteins have been found to act against Influenza. The interferon induced transmembrane genes that belong to the IFITM family of genes (IFITM1, 2 and 3) IFITM proteins were identified to have anti-influenza (Brass et al., 2009). Studies that knocked out IFITM3 saw a significant rise in IAV replication, whilst over-expression of IFITM3 led to significant curtailing of IAV (Brass et al., 2009). Although the mechanism of IFITM3 anti-IAV activity remains elusive, two potential mechanisms have been proposed. Firstly, it was suggested that IFITM3 acts to prevent viral entry into the cytoplasm through reducing the cellular membranes fluidity by increasing levels of cholesterol leading to a block of hemifusion. The second mechanism suggests that IFITM3 instead acts to inhibit viral release after hemifusion with the surface membrane (Wellington et al., 2019).

Other intrinsic immune proteins shown to be active against influenza viruses include the IFN-induced protein with tetratriopeptide repeats (IFIT) proteins. These proteins are located within the cytoplasm and bind to viral RNA containing a 5’-ppp motif. The direct binding of IFIT proteins to viral RNA in a manner similar to the PRR RIG-I. however, instead of induction an interferon

response, binding of IFIT to vRNA inhibits downstream viral replication processes (Yan and Chen, 2012). Similar to IFIMT3, the full mechanism of IFIT anti-Influenza activity remains elusive.

1.6.4. Innate Immune Responses to Influenza Viruses

Incoming and replicating Influenza virions are detected by host cells using pattern-recognition receptors (PRRs). There are three predominant PRRs that sense Influenza, retinoic acid-inducible gene (RIG-I), Toll-like receptors (TLRs), and NOD- LRR- and pyrin domain-containing protein 3 (NLPR3) receptors (Malik and Zhou, 2020). RIG-I acts to detect double-stranded RNA, influenza genomes have been shown to have a 'panhandle' structure owing to partially complementary sequences in the 5' and 3' ends (Schlee et al., 2009). RIG-I has a central carboxyl-terminal domain (CTD) that contains a binding pocket with recognition sites for RNA 5'-PPP or 5'-2PP groups as well as 2'-O groups. Inactive RIG-I proteins contain caspase activation and recruitment domains (CARDs). Once incoming RIG-I agonists come in to contact with RIG-I CTDs, CARDs are displaced. CARDs from multiple activated RIG-Is oligomerise and subsequently interact with mitochondrial anti-viral signalling protein (MAVS) that leads to downstream antiviral signalling (Kowalinski et al., 2011). There are many TLRs, with two in particular known to recognise Influenza RNA; TLR3 and TLR7. TLR3 recognises double-stranded RNA within endosomes of infected cells, as dsRNA is not produced by IAV during infection, the current ligand for TLR3 is currently unknown (Iwasaki and Pillai, 2014). TLR7 in contrast, recognises single-stranded RNA of Influenza virions within endosomes of infected cells. TLR7 activates transcription factors nuclear factor-κB (NF-κB), triggering a pro-inflammatory immune response, and interferon regulatory factor 7 (IRF7), inducing type 1 interferons (IFNs) (Diebold et al., 2004). NLRP3 form the inflammasome, activated via a number of pathways including cell damage caused by influenza infection, unlike TLRs and RIG-I, NLPR3 is not involved in direct anti-Influenza responses, instead activation of NLRP3 inflammasomes leads to increased tolerance to infection and recruitment of immune T and B cells to sites of infection (Iwasaki and Pillai, 2014).

PRR activation leads to interferon production that in turn causes the expression of a number of interferon-stimulated genes (ISGs) that have anti-viral properties, here we describe a number of ISGs that have well characterised anti-Influenza activity (as reviewed by Iwasaki et al. 2014 (Iwasaki and Pillai, 2014)).

Myxovirus resistance proteins (MX) protein is encoded for by the *MX1* gene in humans. This GTPase is a known interferon-inducible gene that restricts influenza A virus within the cytoplasm of infected cells (Pavlovic et al., 1992), however the direct mechanism of influenza restriction in human is not fully understood (Peter M. Howley, 2020). Similarly, the host interferon-inducible transmembrane (*IFITM*) proteins (*IFITM1-3*) have been shown to restrict IAV infection through prevention of viral fusion to host membranes. These membrane-bound proteins are present throughout the cellular membrane, although the details of their mechanism is poorly understood (Peter M. Howley, 2020). Interferon-stimulated gene 15 (*ISG15*) acts to block dimerization of viral NS1, leading to impaired ability of NS1 to interact with importin α, preventing nuclear import of influenza virus, a step required for IAV transcription and replication. NS1 is a known viral antagonist of the human innate immune response to IAV, *ISG15* works to inhibit this activity of IAV-NS1 (Peter M. Howley, 2020).

The recognition of viral PAMPs by host PRRs lead to the promotion of humoral and cellular responses as mentioned above. As a part of this response, cytokines are produced, many of these are pro-inflammatory, this pro-inflammatory response can lead to immunopathology and severe outcomes in such a condition known as the ‘cytokine storm’. Many cytokines are produced in response to viral infection, and these can be categorised in to two broad categories: primary and secondary cytokines. Primary cytokines can be defined as those that are directly induced by viral infection, whereas secondary cytokines can be defined as those induced during downstream processes, often induced by other cytokines (Guo and Thomas, 2017). Primary and secondary cytokines of note are shown in figure 4. There are a number of well characterised pro-inflammatory cytokines, the unchecked expression of which has been shown to be pivotal in the induction of a cytokine storm, such examples include Tumour Necrosis Factor-α, Inerleukin-6 as reviewed by Gu Y, et al. 2021 (Gu et al., 2021).

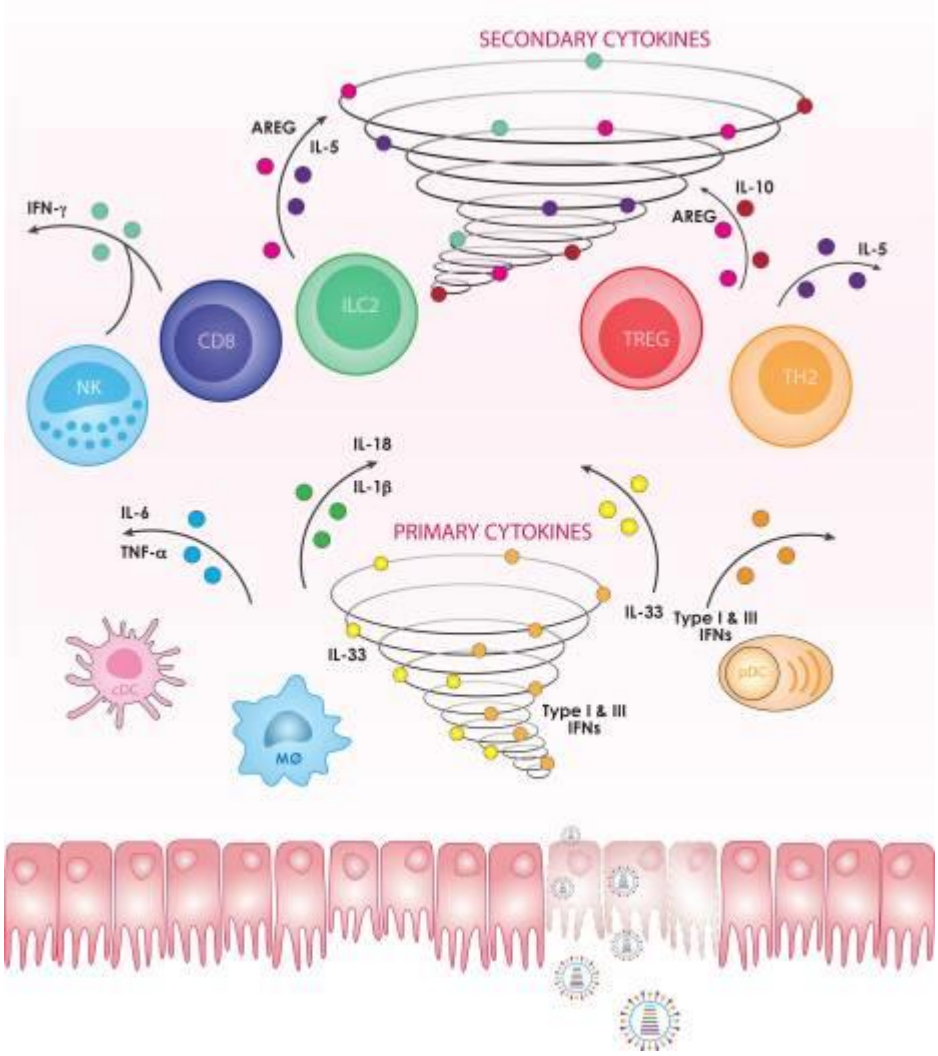

Figure 4. **Primary and Secondary Cytokines Involved in Influenza Virus Infection**. Incoming influenza virions are recognised by host PRRs that lead to the transcription of primary cytokines. These cytokines have a number of anti-viral effects including the activation of secondary cytokines. The cells attributed to the release of specific cytokines are also indicated. Adapted from Guo Xi et al 2017 (Guo and Thomas, 2017).

1.6.5. IAV vRNPs Act as an Immune Response Antagonist

Just as the human host cell has intrinsic and innate immune response to infection, IAV has developed the means to antagonise these responses. Viral NS1 has been well studied for its ability to antagonise the host innate immune response. It achieves this by binding to viral single-stranded RNA that is the target for PRRs such as RIG-I. If virions are not recognised by PRRs then downstream production of IFN responses will be negated (Albrecht and García-Sastre, 2008). Further to this, NS1 was shown to bind to TRIM25, an E3 ligase that has roles in the ubiquitination of RIG-I and subsequent downstream signalling. NS1 has other cellular targets that regulate the IFN-inducible immune response to infection showing that it has a broad range of targets aiding in viral escape from detection and subsequent eliciting of a host response (Peter M. Howley, 2020). IAV PB1-F2 protein, like NS1 is an immune antagonist. PB1-F2 interacts with the RIG-I/MAVs pathway, regulating downstream activation of NF-κβ signalling. in addition, PB1-F2 binds to proteins of the mitochondrial membrane, causing pore formation and subsequent apoptosis of the infected cell, although this was seen to be a phenomena predominantly of infected immune cells rather than epithelial cells (Peter M. Howley, 2020). PA-X is a viral protein that is the result of a ribosomal frameshift in PA leading to the formation of a unique C-terminus that has endonuclease activity that targets host mRNA, shutting off the production of many host genes including those that regulate influenza infection (Peter M. Howley, 2020).

There is a continual arms race between host anti-viral proteins and influenza immune antagonist proteins. Understanding how influenza virus's evade host immune pathways may provide insights in to novel therapeutic and prophylactic treatments.

1.6.6. Adaptive Immune Responses to Influenza

The adaptive immune response to influenza infection can be split in to two main responses: humoral, and cellular immune response. During the humoral response, antibodies are made to a number of viral proteins. Anti-HA antibodies have been shown to block viral attachment to the cell surface, inhibiting entry and internalisation. In contrast, anti-NA antibodies actively block viral shedding from the cell surface, this leads to a reduction in severity of disease but does not completely block influenza infection. Beyond making antibodies to viral surface glycoproteins, antibodies are produced against viral M2, although high amounts of anti-M2 antibody are required to inhibit viral replication. As well as these membrane-bound viral proteins, a number of internal viral proteins can be targets of antibody responses such as M and NP proteins, however these are non-inhibitory to infection (Peter M. Howley, 2020). In terms of the cellular response to influenza, $CD8^+$ T-cells have been shown to play roles in reducing the severity of disease (Sridhar et al., 2013), the specific role of T cell responses to IV infection is difficult to study owing to such cells only being present in the peripheral blood for a few days post-infection (Peter M. Howley, 2020).

1.7. In Vitro Studies of IAV and LAIV; Which Cell Model to Choose?

1.7.1. MDCK cells; advantages and disadvantages to use *in vitro* IAV studies.

In vitro studies of Influenza require the use cell culture model systems, the choice of which must be made on the basis of a number of factors; 1) permissibility to infectious agent replication, 2) relative cost of both cells and associated cell culture reagents such as maintenance media, 3) relevance to the biological question being asked by the assay. Madin Darby Canine Kidney Cells (MDCK) are a continuous epithelial cell line derived from the kidney of a female Cocker-Spaniel in 1958 (ATCC). MDCK cells have long been used for Influenza research as they have been shown to be capable of enabling viral replication. This makes MDCK cells useful for use in *in vitro* replication assays such as with the plaque-forming unit assay as well as standard replication assays (Gaush and Smith, 1968, Kongsomros et al., 2021, Frensing et al., 2016). The permissive nature of MDCK cells to Influenza virus makes them a useful cell line for the development and manufacture of cell-based Influenza vaccines (Audsley and Tannock, 2004, Doroshenko and Halperin, 2009, Genzel and Reichl, 2009, Green, 1962). Beyond this, MDCK cells are also used during the development and manufacture process of egg-derived Influenza vaccines such as with LAIV, whereby MDCK cells are often used to determine potency levels of LAIV strains through assays such as the Focus-Forming Unit (FFU) assay (Hawksworth et al., 2020).

Due to their ability to enable multi-cycle influenza infection, and their cost-effective nature owing to their continuous growth, MDCK cells are a low-cost choice for medium-throughput studies. However, using cells of canine origin for studies of viruses attributable to human disease has become a topic of study, with studies showing that MDCK cells are significantly more permissible to Influenza replication than human lung epithelial cells (A549 and HBEC3-KT) (Charman et al., 2021). To maintain the permissibility of MDCK, but increase their physiological comparability to human airway cells, alternative forms of MDCK cells have been engineered, including MDCK-SIAT1 and humanised MDCK (hCK) cells that incorporate higher expression levels of SA α2-6 receptors (Byrd-Leotis et al., 2022). What is less understood is how the host cell response to Influenza differs between MDCK cells and human airway cells.

1.7.2. Other commonly Used Cell Lines for Influenza Research

The specific sialic acids that IVs exhibit has led to formulation of MDCK cells that better reflect the SA-α2-6 targeted by human influenza viruses. To this extent, MDCK-SIAT1 cells have been developed that over-express SA-α2-6 on their surface (Oh et al., 2008). Indeed MDCK-SIAT1 cells have shown a higher effectiveness in isolation of human IVs relative to standard MDCK cells (Oh et al., 2008), interestingly this study found that the genetic stability of viral HA remained intact, a phenomenon not always true for IV infection in conventional MDCK cells. MDCK-SIAT1 cells share many of the same benefits and drawbacks as of conventional MDCK cells (as described above). To this end, airway epithelia cells are often chosen to better reflect the human airway. One such commonly used cell line is the A549 cells, these cells are derived from a lung adenocarcinoma (Giard et al., 1973), as such they hold inherent genetic variability (Isaka et al., 2003). In fact, within a given stock of A549 cells, there may well be multiple subpopulations of cells, adding further to the inherent variation (Croce et al., 1999). The effect of the genetic instability owing to the carcinomic nature of A549 cells makes undertaking any host cell response analysis particularly difficult. Other cell lines have developed to circumvent this issue. Human bronchial epithelial cells that been immortalised through telomerase extension (Ramirez et al., 2004) (HBEC3-KT) provide a primary-like airway cell culture model that is cost effective, physiologically representative of the human airway system (lower respiratory tract), and free from genetic instability and variability seen in cells such as A549. When undertaking research and development of the attenuated vaccine (LAIV), the temperature attenuation of infective vaccine strains limits replication to the upper respiratory tract, predominantly the nasopharyngeal airways (Hawksworth et al., 2020). With this in mind, we suggest that the ideal cell line would indeed be that of immortalised nasal epithelia.

When discussing the relative relevance of cell types for surrogates of the *in vivo* human airway for 2D respiratory virus research, it is important to note that not all epithelial cells are equal. In general, lung respiratory system is pseudostratified columnar epithelial (Kia'i and Bajaj, 2023), meaning although there is a single layer of cells, the nuclei are not situated along the same plane. Giving the appearance of multiple cellular layers. Within the human respiratory system, not all parts of the human airway consist of equal proportions of epithelial cell type. Figure 5 shows how the epithelia of the lung change from the predominantly ciliated, undifferentiated, and secretory epithelia of the large airways, to type I and type II alveolar epithelia in the Alveoli. These type I and II epithelia are a merger of epithelial cells seen in the large and small airways. (Crystal et al., 2008). The nasal tract is predominated by ciliated epithelia and mucosal secreting cells, these act to dislodge and transport incoming debris/pathogens that get trapped within the mucous secreted by the secretory cells (Sobiesk and Munakomi, 2023). As well as different make-up of cell types throughout the human airway, we must consider how these cells may differ in their relative expression of surface receptors used readily by influenza virus as discussed in section 1.6.4. such considerations can aid in the choice of which cell line best represents the in vivo system being replicated in vitro. This forms the basis for choosing primary human nasal epithelial cells for the study of LAIV, where active replication of this cold-adapted live virus is limited to the nasal tract (Hawksworth et al., 2020).

NASAL CELLS

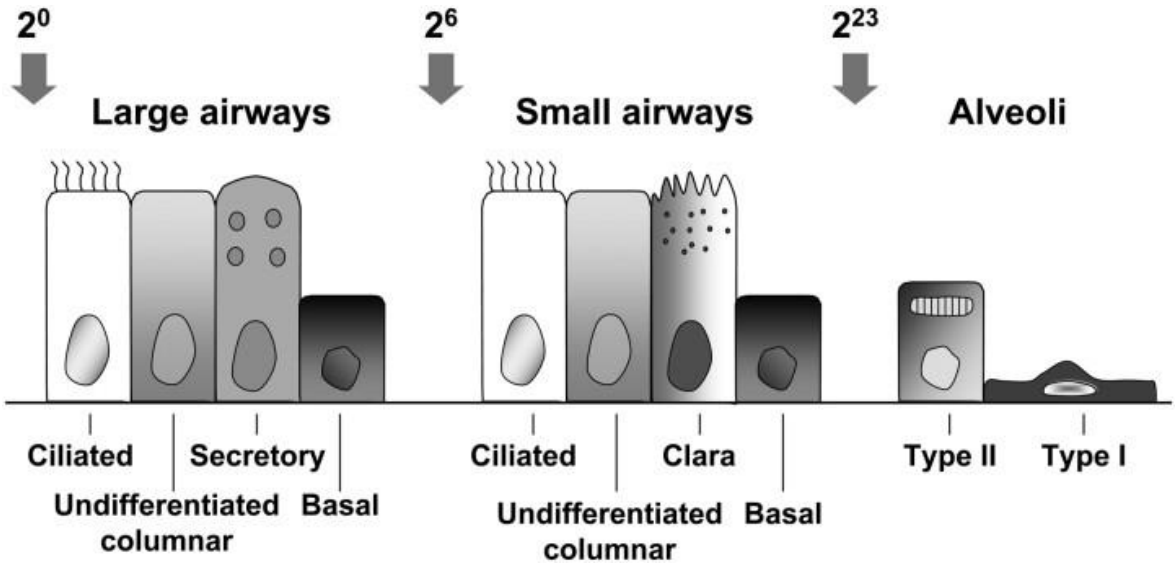

Figure 5. Epithelial Cells of the Human Airway. Epithelial cell type prominent in large airways with no branching (2^0 branches – 2^5 branches), small airways at 2^6-2^{23} branches and 2^{24} branches onwards. adapted from (Crystal et al., 2008).

1.8. Thesis Study Aims

3D-differentiated airway epithelial cells have been and continue to be used in the studies on influenza virus and associated host responses (Lawko et al., 2021). Where these cell model systems provide a physiology more applicable to the human airway than many other 2-dimensial cell cultures such as MDCK, A549 and HBEC3-KT, they are highly cost-ineffective for high-throughput bioassays typically used both within academic IAV studies, and LAIV development and research such as TCID50 and FFU assays. To this extent, MDCK and A549 cells are used commonly in IAV/LAIV studies and development. We aim to understand whether primary human nasal epithelial cells in 2D can be used as a high throughput 2D culture system to conduct regular bioassays in a physiological environment closer representing that of the upper airway tract that LAIV is specifically targeting, and non-complicated influenza infection occurs.

Aim 1. We aim to corroborate findings by Charman et al. 2019 (Charman et al., 2021) showing that human airway epithelial cells are significantly restrictive to influenza infection than MDCK cells and expand this to elucidate the relative permissivity to LAIV of primary hAECn cells. We will utilise plaque forming unit (PFU) assays and focus-forming unit (FFU) assays to compare multi-cycle and single-cycle infection potential of IAV respectively. We will compare MDCK cells to A549 and HBEC3-KT cells. We will expand this premise to primary hAECn cells and LAIV. We will compare the relative permissivity of hAECn cells and MDCK cells two LAIV strains: LAIV A/Slovenia/2903/2015 and LAIV A/Bolivia/559/2013, strains with documented high and low VE respectively (Coelingh et al., 2015, Dibben et al., 2021). We will determine the relative levels of viral entry to determine whether each LAIV strain has equal attachment/entry efficiencies, and whether LAIV virions enter MDCK cells and hAECn cells at equal or different levels.

Aim 2. We will elucidate hAECn host-cell innate immune responses to LAIV. We will build on the finding by Dibben et al. showing LAIV A/Bolivia/559/2013 has reduced replicative fitness compared to LAIV A/Slovenia/2903/2015 in human airway cells. We hypothesise that differential replicative fitness will lead to differential activation of innate immune responses. Using two-step RT-qPCR, we will quantify ISG expression in hAECn cells in response to LAIV A/Slovenia/2903/2015 and LAIV A/Bolivia/559/2013.

Aim 3. We aim to compare the innate immune activation of hAECn cells from 3 different donors in response to LAIV A/Slovenia/2903/2015 infection. Using primary hAECn cells in 2D will require the use of cells derived from either individual or pooled donors, we aim to elucidate any differences in ISG expression that may exist between cells from individual donors or combined pooled cultures comprising equal quantities of these constituent donors. We will utilise two-step RT-qPCR to quantify the relative expression of two highly characterised ISGs that are well known for their anti-IAV activity, MX1 and OAS1 (Iwasaki and Pillai, 2014).

Aim 4. We aim to study inter-person variation in constitutive expression of lung ISGs within the wider population. Studying inter-donor differences in host-responses to LAIV infection is limited in the sample number of donors that are practically possible for *in vitro* studies. In order to understand how individuals, differ in their potential responses to LAIV vaccination and IAV infection, we will utilise open-access transcriptomic data from GTEx portal (Carithers et al., 2015) to compare the constitutive expression of ISGs in the lung of 578 individuals. We will determine the effect of sex and age on ISG baseline expression, thereby providing preliminary data on the level of genetic variation of airway (lung) ISGs prior to specific IAV/LAIV infection/vaccination.

Together, this thesis aims to investigate the pros and cons of utilising primary 2S hAECn cells for IAV and LAIV vaccine immunological research. We will elucidate and discuss any challenges and important considerations for using such a culture systems in IAV vaccine development.

2. Materials and Methods

2.1. Materials

2.1.1. Cells

Table 2. Cells used throughout this thesis.

Cell Line	Tissue Origin	Donor Details	Company	Passage Range (Upper limit)
Madin Darby Canine Kidney Cell (MDCK)	Canine Kidney	N/A	Donated by professor Palmarini Laboratory (CVR)	<50
A549	Human Lung	N/A	Public Health England	<25
Human Embryonic Kidney (HEK) 293T	Human Lung Fibroblast		Public Health England	<15
Human Bronchial Epithelial Cells (HBEC3-KT)	Human Lung (Bronchial)	N/A	Boutell Group (CVR)	<25
Primary human airway cells (nasal) (hAECn) AB0608 (D1)	Human Nasal Airway	Male, 50, Caucasian	Epithelix	<12
Primary human airway cells (nasal) (hAECn) AB0541 (D2)	Human Nasal Airway	F, 57, African	Epithelix	<12
Primary human airway cells (nasal) (hAECn) AB0784 (D3)	Human Nasal Airway	M, 35, Caucasian	Epithelix	<12

2.1.2. Cell Culture Media

Table 3. Cell culture media used in this thesis.

Media	Additives	Company
Dulbecco's modified Eagle's medium (DMEM)	10% FCS, 100 units/mL penicillin, and 100µg/mL streptomycin	ThermoFisher Scientific
Serum-free Dulbecco's modified Eagle's medium (SFM)	100 units/mL penicillin, and 100µg/mL streptomycin	ThermoFisher Scientific
Keratinocyte Serum-Free Media (KSFM)	25mg bovine pituitary extract and 2.5µg human recombinant epidermal growth factor (supplied by manufacturer) plus 100 units/mL penicillin, and 100µg/mL streptomycin	ThermoFisher Scientific
Human Airway Epithelial Cell Media (hAEC)	N/A	Epithelix

2.1.3. Cell Culture Dissociation Reagents

Table 4. Cell Culture Dissociation Reagents

Reagent	Concentration	Company	Reference/Catalogue Number
Trypsin	5% (in Versene)	ThermoFisher	-
TrypLE	1X	ThermoFisher	12604021

2.1.4. Antibodies

Table 5. Notes on antibodies used throughout this study

Antibody	Primary/Secondary/ Conjugated	Company	Reference	Dilution
Mouse anti-NP	Primary	Abcam	Ab20343	1:2,000
Sheep anti-HA	Primary	NIBSC	16/304	1:1,000
Mouse anti-EpCAM Alexa-Fluor 488	Conjugated	Abcam	Ab253268	1:200
Donkey anti-mouse Alexa-fluor 555	Secondary	ThermoFisher Scientific	A-31570	1:1,000
Donkey anti-sheep Alexa-fluor 555	Secondary	ThermoFisher Scientific	A-21436	1:1,000
Goat Anti-mouse HRP	Secondary	Sigma-Aldrich	A4416	1:1,000

2.1.5. Viruses

Table 6. Notes on viruses used throughout this study

Strain	Origin	Propagation Method
A/WSN/1933 (H1N1)	Boutell Group (CVR)	Cell (MDCK)
A/California/07/2009 (H1N1	Hutchinson Group (CVR)	Cell (MDCK)
A/Puerto Rico/2008 (H1N1)	Boutell Group (CVR)	Cell (MDCK)
WT A/Slovenia/2903/2015 (H1N1)	AstraZeneca	Egg
WT A/Bolivia/559/2013 (H1N1)	AstraZeneca	Egg
LAIV A/Slovenia/2903/2015 (H1N1)	AstraZeneca	Egg
LAIV A/Bolivia/559/2013 (H1N1)	AstraZeneca	Egg

2.1.6. Oligonucleotides

Table 7. Oligonucleotide Details. Sequences and associated fluorophores (Fluor)/quenchers for primers and probes used in this study. 'Uknown' indicates Oligos where no sequence data is available.

Name	Sequence (5' – 3')	Fluor	Quencher	Company	Reference
OligoDT	Unknown	N/A	N/A	Qiagen	N/A
Uni12	AGCAAAAGCAGG	N/A	N/A	ThermoFisher	N/A
RT IAV	CCGAGATCGCACAGAGACTT	N/A	N/A	ThermoFisher	N/A
IAV Seg7 Fwd Primer	AAGACAAGACCAATCYTGTCACCTCT	N/A	N/A	ThermoFisher	N/A
IAV Seg7 Rev Primer	TCTACGCTGCAGTCCYCGCT	N/A	N/A	ThermoFisher	N/A
IAV Seg7 Probe	TCACGCTCACCGTGCCCAGTG	FAM	BHQ1	ThermoFisher	N/A
GAPDH (MDCK) Fwd Primer	ACATCATCCCTGCTTCCAC	N/A	N/A	ThermoFisher	N/A
GAPDH (MDCK) Rev Primer	TGCCTGCTTCACTACCTTC	N/A	N/A	ThermoFisher	N/A
GAPDH (MDCK) Probe	CCTGCCGCCTGGAGAAAGCTGCCAA	FAM	BHQ1	ThermoFisher	N/A
GAPDH	Unknown	FAM	Uknown	ThermoFisher	4333764F
MX1	Unknown	FAM	Unknown	ThermoFisher	Hs00895608_m1
OAS1	Unknown	FAM	Unknown	ThermoFisher	Hs00973635_m1

2.1.7. Molecular Assay Kits

Table 8. Notes on Molecular Assay Kits used throughout this Study

Kit	Company	Reference/Catalogue No.
RNeasy Viral RNA Extraction Kit	Qiagen	52906
RNeasy Total RNA Extraction Kit	Qiagen	74134
Reverse Transcription Kit	ThermoFisher	N8080234
TaqMan Fast Universal PCR Master Mix (2X) no AmpErase UNG	ThermoFisher	4366072
MicroAmp Fast Optical 96-Well Reaction Plate, 0.1 mL	ThermoFisher	4346907
ddPCR Supermix for Probes (No dUTP)	Bio-Rad	1863023
DG8 Cartridges for QX200/QX100 Droplet Generator	Bio-Rad	1864008
DG8 Gaskets for QX200/QX100 Droplet Generator	Bio-Rad	1863009
Droplet Generation oil	Bio-Rad	1863005
ddPCR 96-Well Plates	Bio-Rad	12001925

2.1.8. Buffer Compositions

Table 9. Notes on Buffers used throughout this Study

Buffer	Composition
PBS-T	1X PBS + 0.01% Tween-20
CSK	2mL 250mM HEPES (pH 7.0) + 1mL 5M NaCl + 5.31g sucrose + 0.3mL 500mM $MgCl_2$ + 1mL 250mM EGTA (pH 8.0) + dH_2O (to 50mL total)
Avicel	25mL SFM + 25mL 2.4% Avicel + 0.5ml 1% DEAE dextran + 0.781mL 7.5% $NaHCO_3$ + 2.5mL FCS
IF fix and permeabilise solution	9mL CSK buffer + 0.5mL 10% Triton-X-100 + 0.5mL 33.3% PFA/EtOH
ICC fix and permeabilise solution	9mL 5% milk solution (100mL PBS-T + 5% skimmed milk) + 0.5% 10% Triton-X-100 + 0.5ml 33.3% PFA/EtOH

2.2. Methods

2.2.1. Routine Passaging of MDK, A549 and 293-T Cells

MDCK, A549 and 293T cells were grown to ~75-80% confluence. Cells were washed twice with Versene. Cells were overlaid with Trypsin (5% in Versene) and incubated at 37ºC + 5% CO_2 until 90+% of cells have detached. Cells were quenched with maintenance media (DMEM + 10% FCS + 100 units/ml penicillin and 100µg/ml streptomycin). And split at a ratio for desired date of next passage.

2.2.2. Routine Passaging of HBEC3-KT Cells

HBEC3-KT cells were grown to ~75-80% confluence. Cells were washed once with Versene then overlaid with TrypLE. Cells were incubated at 37ºC + 5% CO_2 until >90% cells detached. Cells were quenched with maintenance media (KSFM). Cells were pelleted by centrifugation at 188 rcf for 5 minutes. Supernatant was removed and cells resuspended in maintenance media. Cells were split at a 1 in 5 ratio into fresh tissue culture flasks for routine passaging.

2.2.3. Routine Passaging of Primary hAECn Cells

Primary hAECn cells were obtained from Epithelix (Epithelix, 2023). Cells were grown to ~70% confluence in hAEC maintenance media at 37ºC + 5% CO^2. Cells at desired confluence were washed once with Versene and overlaid with TrypLE dissociation agent. Trypsinisation undertaken at 37ºC + 5% CO^2 until 10% cells are left attached to tissue culture flask. Remaining attached cells washed of using hAEC media. Cells were collected and pelleted by spinning at 188 rcf for 5 minutes. Cell pellet was re-suspended in hAEC media and split in a ratio of 1:3 for routine passaging.

2.2.4. Plaque Forming Efficiency (PFE) Assay

MDCK, A549 and HBEC3-KT cells were grown to confluence in 12-well tissue culture plate (Costar 3513). Virus (A/WSN/1933, A/California/07/2009, A/Puerto Rico/2008) was serially diluted 1 in 10 in serum-free DMEM (SFM). Cells were washed with SFM. 200µl inoculum was added to each well and incubated for 1 hour at 37ºC + 5% CO_2 for viral adsorption. Inoculum was removed and cells were overlayed with semi-solid Avicel overlay. Cells were incubated for 48 hours further at 37ºC + 5% CO_2. Cells were fixed and permeabilised with 5% Triton-X + 5% paraformaldehyde (PFA) for 10 minutes at room temperature. Cells underwent immunocytochemistry (ICC) using primary mouse anti-NP (ab20403) at 1 in 2,000 dilution for 1 hour at room temperature. Followed by a 1 hour incubation at room temperature with anti-mouse hrp secondary antibody at 1 in 1,000 dilution. Plaques were visualised using TrueBlue peroxidase staining (Insight, 50-70-02) at room temperature for <10minutes. Plaques were imaged using EpsonScan software/hardware. Plaques were counted manually by eye. Plaque-forming units/ml (PFU/ml) were calculated thus: No. Plaques/(inoculum dilution x inoculum volume).

2.2.5. Focus-Forming Units (FFU) Assay (A/WSN/1933, A/California/07/2009, A/Puerto Rico/2008)

MDCK cells were grown to confluence in 48-well tissue culture plate (Costar 3548). Virus stocks were serially diluted 1in10 in SFM. 50µl inoculum was added to cells and cells were incubated for 1hour at 37ºC + 5% CO_2 for virus adsorption. Inoculum was removed and replaced with SFM. Cells were further incubated at 37ºC + 5% CO_2 for 5hours. Cells were fixed with 5% Triton-x + 5% PFA in PBS + 2% FCS at room temperature for 10 minutes. Cells were stained with mouse anti-NP (ab20403) at 1in2000 for 1hour at room temperature. Cells were counter-stained with secondary donkey anti-mouse (Fluor 555) + DAPI (1 in 2,000) for 45 minutes at room temperature. Foci were detected using Celigo hardware/software. Linear regression analysis was carried out to determine the dilutions of virus resulting in foci counts within the linear range. We define Foci as a cell positive for antigen (DAPI + NP). FFU/ml was calculated thus: No. Foci/(inoculum dilution x inoculum volume).

2.2.6. Focus-Forming Unit (FFU) Assay for LAIV Strains

Methodology was adapted from AstraZeneca standard operating procedure (SOP) for LAIV FFU assay. MDCK cells were grown to confluence in 48-well tissue culture plate (Costar 3548). Virus stocks were serially diluted 1in10 in SFM. 50µl inoculum was added to cells and cells were incubated for 1hour at 33ºC + 5% CO_2 for virus adsorption. Inoculum was removed and replaced with SFM. Cells were further incubated at 33ºC + 5% CO_2 for 19hours. Cells were fixed with 5% Triton-x + 5% PFA in PBS + 2% FCS at room temperature for 10minutes. Cells were stained with sheep anti-HA (ab20403) at 1 in 2,000 for 1hour at room temperature. Cells were counter-stained with secondary donkey anti-sheep (Fluor 555) + DAPI (1 in 2,000) for 45minutes at room temperature. Foci were detected using Celigo hardware/software. Linear regression analysis was carried out to determine the dilutions of virus resulting in foci counts within the linear range. We define Foci as a cell positive for antigen (DAPI + NP). FFU/ml was calculated thus: No. Foci/(inoculum dilution x inoculum volume).

2.2.7. Immunofluorescence to Determine Relative Antigen Presentation (A/WSN/1933 and A/California/07/2009)

MDCK, A549 and HBEC3-KT cells were grown to confluence in 48-well tissue culture plate (Costar 3548). Virus stocks prepared at MOI of 1.0 (PFU/ml determined in MDCK cells) in SFM. 50µl inoculum was added to cells and cells were incubated for 1hour at 37ºC + 5% CO_2 for virus adsorption. Inoculum was removed and replaced with SFM. Cells were further incubated at 37ºC + 5% CO_2 for 5hours. Cells were fixed with 5% Triton-x + 5% PFA in PBS + 2% FCS at room temperature for 10minutes. Cells were stained with mouse anti-NP (ab20403) at 1 in 2,000 for 1hour at room temperature. Cells were counter-stained with secondary donkey anti-mouse (Fluor 555) + DAPI (1in2000) for 45minutes at room temperature. Foci were detected using Celigo hardware/software. Total cell number was obtained via obtaining DAPI-positive counts. NP-positive cells were determined by obtaining counts of fluorescence with both DAPI and NP. The percentage of cells that were positive for viral NP was calculated.

2.2.8. Immunofluorescence to Determine Relative Antigen Presentation (WT A/Slovenia/2903/2015, WT A/Bolivia/559/2013, LAIV A/Slovenia/2903/2015 and LAIV A/Bolivia/559/2013)

MDCK, A549 and HBEC3KT cells were grown to confluence in 48-well tissue culture plate (Costar 3548). Virus stocks were prepared at MOI 0.5 (FFU/ml determined in MDCK cells) in SFM. 50µl inoculum was added to cells and cells were incubated for 1hour at 33ºC + 5% CO_2 for virus adsorption. Inoculum was removed and replaced with SFM. Cells were further incubated at 33ºC + 5% CO_2 for 19 hours. Cells were fixed with 5% Triton-x + 5% PFA in PBS + 2% FCS at room temperature for 10 minutes. Cells were stained with sheep anti-HA (ab20403) at 1 in 2,000 for 1hour at room temperature. Cells were counter-stained with secondary donkey anti-sheep (Fluor 555) + DAPI (1 in 2,000) for 45 minutes at room temperature. Foci were detected using Celigo hardware/software. Total cell number was obtained via obtaining DAPI-positive counts. NP-positive cells were determined by obtaining counts of fluorescence with both DAPI and NP. The percentage of cells that were positive for viral NP was calculated.

2.2.9. Flow Cytometry

In order to determine the proportion of cells within the immortalised hAECn (hAECnT) produced by Steven McFarlane (CVR) that were epithelial cells, mouse anti-EpCAM Alexa-fluor 488 conjugated antibody was used to target the epithelial cell adhesion molecule (EpCAM) epithelial cell marker. 293T fibroblasts were used as a negative control. HBEC3-KT cells were used as a positive control. hAECnT cells were continually passaged up to passage 11. At each passage, $1x10^6$ cells were maintained in suspension and stained with mouse anti-EpCAM 488 (1 in 200) + DAPI for 1 hour at room temperature. DAPI was used as a dead/non viable cell marker. As DAPI cannot enter impermeable cells, it will only enter dead cells that have a compromised and permeable membrane. Using GUAVA easyCyte HT BG system (Merk) hardware, cells were analysed for EpCAM positivity. The proportion of cells positive for EpCAM was determined using FlowJo software.

2.2.10. Fluorescence-Associated Cell Sorting (FACS)

HBEC3-KT and hAECnT cells were trypsinised using standard tissue culture protocols. Cells were incubated in suspension with conjugated mouse anti-EpCAM 488 antibody at 1:200 dilution for 1 hour. Cells were pelleted by centrifugation at 200 rcf for 5 minutes and washed by re-suspension in 1x PBS. Cells were pelleted once again by centrifugation at 200 rcf for 5 minutes. Cells were re-suspended in 5mL x PBS and subjected to FACS sorting using FACS-Aria hardware and software. EpCAM-positive cells and EpCAM-negative cells were collected in to separate 15mL falcon tubes. Cells were subsequently seeded in to 60 mm tissue culture dishes and placed in to 37ºC + 5% CO_2 for growth. Cells undertook media changes every 48 hours and passaged as per standard cell passage protocol. FACS results are represented as cell gating graphs with forward and side scatter plots used for cell population selection as well as forward vs FITC scatter plot for selection of EpCAM-positive cells. Number of cells positively selected for by FACS is recorded and shown. DAPI was used to exclude dead/non-viable cells.

2.2.11. Digital-Droplet PCR (ddPCR) for Absolute Quantification of Virus

Viral RNA was extracted from 100µl of virus stock using RNeasy kit (QIAGEN #52906). Reverse transcription PCR was carried out using 150ng/reaction viral RNA and the following thermocycle conditions: Primer anneal – 25ºC for 10min, Extension – 37ºC for 60min and inactivation – 95ºC for 5min. cDNA was serially diluted 1in10 in nuclease-free water (NFW). 40µl PCR reactions were set-up using ddPCR Supermix for Probes (No dUTP) (Bio-Rad #1863023), Seg7 Fwd Primer (5'-AAGACAAGACCAATCYTGTCACCTCT-3'), Seg7 Rev Primer (5'-TCTACGCTGCAGTCCYCGCT-3') and Seg7 Probe (5'TCACGCTCACCGTGCCCAGTG-3'). ddPCR reaction beads were produced using 21µl reaction + 70µl ddPCR Droplet Oil (Bio-RAD #1863005). PCR was carried out using the following thermocycle: 1 cycle: denature – 95ºC for 20s. 40 cycles: Anneal – 95ºC for 3s, extend – 60ºC for 30s. copies/ml (IAV-Segment 7) were calculated for each cDNA dilution. cDNA dilutions that resulted in copies/ml within a linear range were determined. Copies/ml were then calculated as an average of these.

2.2.12. Virus Attachment/Entry Efficiency Assay

MDCK and hAECn D1 (AB0608), and hAECn D2 (AB0541) were grown to confluence in 24-well Costar tissue culture plates (Costar #3526) at 37ºC + 5% CO_2. LAIV A/Slovenia/2903/2015 and LAIV A/Bolivia/559/2013 inoculums were prepared at MOI 0.5 (copies/ml derived from ddPCR absolute quantification). Virus was adsorbed on to cells via a 1hour incubation at 33ºC + 5% CO_2. Inoculum was removed and cells were overlayed with SFM + cycloheximide (CHX) to prevent viral gene transcription. After a further 1hour incubation at 33ºC + 5% CO_2, cells were washed with SFM and trypsinised to remove any surface-bound virions and obtain cells in suspension. Cells were pelleted by spinning at 200 rcf for 5 minutes and supernatant containing free virions removed. Total RNA was extracted (RNease, QIAGEN #74134). cDNA synthesis was carried out with OligodT and Uni12. ddPCR was carried out (as per methodology described previously) for GAPDH (4333764F), MDCK-GAPDH (FWD 5'- ACATCATCCCTGCTTCCAC-3', REV 5'-TGCCTGCTTCACTACCTTC-3' and probe 5'- CCTGCCGCCTGGAGAAAGCTGCCAA-3') and LAIV Segment 7 (as stated in section 2.2.12). Total number of intracellular virions (IAV-Segment7) relative to total number of cells (GAPDH) was calculated for each cell type.

2.2.13. Determination of the Effect of Demographics on Constitutive Expression of Lung ISGs

To determine the level of variation in constitutive expression of lung ISGs within the wider population, we first obtained a list of 100 ISGs to use as a starting point for analysis. A study by Shaw et al. 2017 (Shaw et al., 2017) aimed to elucidate ISGs common amongst 10 mammalian species. We isolated the ISGs from Homo sapiens and ranked them in descending order of gene expression level in response to interferon challenge. We chose 100 ISGs as a manageable number of genes for bioinformatic analysis in the absence of time and training for coding software to handle larger data sets. With these 100 ISGs, we used open access data from GTEX Portal, a study undertaken to elucidate the genomic, transcriptomic, and proteomic mapping of tissues throughout the human body (Carithers et al., 2015). We chose to focus on lung ISGs as we wanted to determine the variation in baseline expression of ISGs within the cells/tissues most closely resembling the *in vivo* infection target of IAV/LAIV. We would ideally have chosen to study the upper respiratory/nasal tract; however, these data were not available in the GTEX study. Collectively we had 578 samples total. We aimed to understand our sample demographics using information available, Sex and Age. GTEX Portal samples are placed into age cohorts (20-29, 30-39, 40-49, 50-59, 60-69 and 70-79). We found that for females, there were only 4 samples in the age cohort of 70-79. So as not to bias our results with statistically low sample power, we combined age cohorts 60-69 and 70-79 for both females and males, increasing sample size power for these ages collectively. nTPMs obtained from GTEX Portal have been pre-normalised to transcript copy length. We chose to undertake no further normalisation so as not to bias our results.

We first obtained nTPMs for all 100 ISGs for females and males separately and ran Mann-Whitney tests to determine whether there is a statistically significant difference in expression level of our 'ISGome'. We next aimed to test each individual ISG for differential constitutive expression between females and males. We collected nTPMs for each individual ISG and ran Mann-Whitney statistical test for each to determine which ISG, if any, are differentially expressed as a result of sex.

To determine the effect of changing age on constitutive expression of lung ISGs, we combined the nTPMs for each age cohort in females and males collectively, using multiple comparison ANOVA (Kruskal-Wallis), we determined whether changing age was responsible for any differential expression. We next separated males and females and ran multiple comparison ANOVA (Kruskal-Wallis) in order to determine whether any differential expression of individual lung ISGs as a result of age is common amongst males and females, or whether there is a sex-dependent effect of age on lung ISG constitutive expression.

We chose two ISGs (CFH and JAG1) that showed a significant effect of age on expression levels in the lung and TRIM25 as a negative control gene that showed no statistically significant effect of age on lung expression. With these we expanded our analysis to determine whether the observed difference was a result of up-regulation or down-regulation in response to changing age. Having elucidated the MX1 and OAS1 expression profile of primary hAECn cells to LAIV infection, we here wanted to understand whether there is natural variation in these genes at a baseline constitutive level. Therefore, we obtained nTPM data for both *MX1* and *OAS1* and performed the pipelines as described above.

2.2.14. Dose-Response Determination of ISG Response to LAIV

LAIV A/Slovenia/2903/2015 was prepared at MOI's 10, 5, 1, 0.1 and 0.01 (Copies/ml determined by ddPCR absolute quantification on virus stocks). Total RNA was extraction (QIAGEN #74134) and cDNA synthesis undertaken using OligodT reverse transcription primer and the TaqMan reverse transcription kit (ThermoFisher, #N8080234). Real-time qPCR was undertaken to quantify GAPDH (Thermofisher 4333764F), MX1 (Thermofisher Hs00895608_m1) and OAS1 (Thermofisher Hs00973635_m1). delta-delta cT analysis was undertaken, normalising ISG cT to GAPDH cT. Fold increase calculated relative to mock.

2.2.15. RT-qPCR to Determine ISG Response to LAIV/IAV

hAECn cells from three different donors D1, D2 and D3 (see Table 2 for details) were grown to 80% confluence in 24-well Costar plate (Costar, #3526). LAIV A/Slovenia/2903/2015 and LAIV A/Bolivia/559/2013 inoculums were prepared at MOI of 5.0 (copies/ml determined by ddPCR absolute quantification on virus stocks). Virus was adsorbed on to cells for 1hour at 33ºC + 5% CO_2. Inoculum was removed and cells were overlayed with SFM + 0.02% BSA. Cells were incubated for a further 11 hours at 33ºC + 5% CO_2. Total RNA was extracted from cells (QIAGEN RNeasy #74134) and cDNA synthesis undertaken using OligodT reverse transcription primer and the TaqMan reverse transcription kit (ThermoFisher, #N8080234). Real-time qPCR was undertaken to quantify GAPDH (Thermofisher 4333764F), MX1 (Thermofisher Hs00895608_m1) and OAS1 (Thermofisher Hs00973635_m1). delta-delta cT analysis was undertaken, normalising ISG cT to GAPDH cT. Fold increase calculated relative to mock.

2.2.16. Innate Immune Response (MX1) to LAIV A/Slovenia/2903/2015 in Pooled-Mixed hAECn Donors and Individual Constitutive hAECn Donors

We seeded primary hEACn cells from three independent donors (see Table 2 for details). We also created a pooled cell culture by seeding equal numbers of each donor collectively. Once cells reached 80-90% confluence, we infected cells with LAIV A/Slovenia/559/2015 at MOI 5.0 (copies/ml determined by ddPCR absolute quantification on virus stocks) and incubated at 33ºC + 5%CO_2 for 1 hour to enable adsorption. We replaced inoculum media with maintenance media and allowed for 11 hours further incubation at 33ºC + 5% CO_2. We extracted total RNA from the cells using Qiagen RNease extraction kit as per manufacturers' instructions. We used the universal reverse-transcription primer (Uni12) to generate cDNA for downstream PCR analysis. We then utilised primer/probe kits for human GAPDH (Thermofisher 4333764F), *MX1* (Thermofisher Hs00895608_m1) and *OAS1* (Thermofisher Hs00973635_m1) to perform RT-qPCR. delta-delta cT analysis was undertaken, normalising ISG cT to GAPDH cT. Fold increase calculated relative to mock. We then normalised our data expression levels of D1 (D1 showing the highest levels of ISG response) to take in to account intra-experimental variation between replicates.

3. Results

3.1. Not All Cells are Equally Permissive to IAV Infection

3.1.1. Introduction

Madin-Darby Canine Kidney (MDCK) cells are an adherent, continuous cell line derived from a female adult Cocker Spaniel in 1958 by S.H Madin and N.B. Darby (ATCC). One of the earliest reports of MDCK susceptibility to Influenza virus was reported in 1962, whereby influenza B virus was serially propagated leading to significant cytopathic effects (CPE) (Green, 1962). Since then, MDCK cells have been routinely and widely used for influenza virus research (Gaush and Smith, 1968, Sidorenko and Reichl, 2004). Out-with of use in academic studies, MDCK cells have been routinely utilised for influenza vaccine propagation and characterisation (Audsley and Tannock, 2004, Doroshenko and Halperin, 2009, Genzel and Reichl, 2009, Youil et al., 2004). MDCK cells exhibit significant heterogeneity, with single cell isolates being used to culture different clonal cell lines that differ in their host cell-IAV interactions (Lugovtsev et al., 2013). As MDCK cells are of Canine origin, understanding how human influenza infection in MDCK cells poorly relates to infection in human airway cells. Previous studies have compared the relative infectivity of influenza in MDCK cells and 3D-differentiated normal Human bronchial epithelial cells (NHBE). These studies suggest that NHBE cells more effectively represent infection event in humans than MDCK cells (Ilyushina et al., 2012). Similarly, Charman M. et al. have shown that in 2D cell culture systems, A549 and HBEC3-KT cells were found to be restrictive to lab-adapted A/WSN/1933 infection relative to MDCK cells (Charman et al., 2021).

Such observations have ramifications for the use of MDCK cells during Flumist (AstraZeneca) quadrivalent influenza vaccine (QLAIV) potency assays (Hawksworth et al., 2020), where vaccine FFU/cell titres may reflect differently in alternative, more physiologically representative cell lines. We hypothesise that deeper understanding of host cell responses to IAV/LAIV infection will provide a rationale for the use of specific cell types depending on the intended study outputs.

We therefore set out to investigate how comparable influenza infection is in MDCK cells relative to laboratory adapted human airway epithelial cells. We use human lung adenocarcinoma (A549) (Giard et al., 1973) and hTERT/CDK4-immortalised Human bronchial epithelial (HBEC3-KT) cells (Ramirez et al., 2004). Similar to MDCK cells, A549 cells have been shown to be a heterogeneous cell line, comprising four major subpopulations, each exhibiting characteristics of adenocarcinoma (Croce et al., 1999). As an adenocarcinoma cell line, A549 cells have been found to exhibit variations in aneuploidy (Isaka et al., 2003), suggesting that changes to the cell's underlying genetics have taken place, what effect this may have on cell-virus interactions remains unclear.

Both A549 and HBEC3-KT cells have been used for the study of influenza infection (Ahmed and Husain, 2021). Here we investigated whether the previously reported restriction of multi-cycle IAV infection in A549, and HBEC3-KT cells extends to early restriction during single-cycle infection.

Looking at the relative ability of MDCK and human airway cells to establish influenza infection will enable us to infer how host-cell species and genetic status (spontaneously continuous such as MDCK and A549 or primary-like such as HBEC3-KT) differ in their anti-Influenza A Virus responses. An important contributing factor to consider is whether there are any differences in the ability of IAV to attach and subsequently enter specific cell types. IAV cell entry is mediated by the viral surface glycoprotein Haemagglutinin (HA) binding to cell surface sialic acid receptors. IAV-HA binds to cell surface sialic acids with human strains preferentially binding to α-(2,6) sialic acids as reviewed by Cross, K et al. (2001) (Cross et al., 2001). Humans predominantly express α-(2,6) sialic acids (Gagneux et al., 2003). In contrast, MDCK cells have been shown to have widely variable distribution of sialic acid subtypes depending somewhat on their origin and the media conditions they are cultured in (Nelson et al., 2019). To that end, MDCK-SIAT1 cells have been developed which over-express surface α-(2,6) sialic acids leading to increased IAV permissivity to infection (Oh et al., 2008). We hypothesise that human airway epithelial cells will have increased rates of viral entry compared to MDCK cells. To understand this, we will conduct multi-cycle plaque-assay type assays in MDCK, A549 and HBEC3-KT cells. Looking at plaque morphology (relative size) to draw conclusions on the ability of IAV to complete its full life cycle, inclusive of virus attachment/entry, replication and budding.

3.1.2. Results

3.1.2.1. MDCK Cells are Significantly More Permissive to Multicycle Infection of A/WSN/1933 and A/California/07/2009 than A549 and HBEC3-KT cells.

To determine whether IAV is restricted during single-cycle infection, we first corroborated findings by Charman et al (Charman et al., 2021), that demonstrated human airway epithelial cells to be restrictive to IAV multicycle infection relative to MDCK cells. Using a plaque-forming unit-style assay, we were able to determine the relative permissibility to IAV multi-cycle infection in MDCK, A549 and HBEC3-KT cells (Figure 6). MDCK, A549 and HBEC3-KT cells were infected with serially diluted A/WSN/1933 and A/California/07/2009 for 48hpi under a semi-solid overlay at 37 ^{o}C. IAV-NP Immunocytochemistry for Influenza NP enabled quantification and visualisation of plaque morphology. As seen by PFU/ml calculated from each cell type, A/WSN/1933 had significantly higher infectivity in MDCK cells relative to A549 and HBEC3-KT cells (Figure 6A, P = 0.0016 and 6B, P = 0.0181 respectively). Figure 6C shows that relative to MDCK cells, the level of restrictiveness to A/WSN/1933 in HBEC3-KT is significantly higher than that of A549 cells (P = 0.0036). Similarly, MDCK cells were significantly more permissive to A/California/07/2009 than A549 and HBEC3KT cells (Figure 6E, P = 0.0016 and Figure 6F, P= 0.0183 respectively). Again, when comparing A549 and HBEC3-KT restiveness relative to MDCK cells, HBEC3-KT cells show a significantly higher level of restriction (Figure 6F, P = 0.0127). Plaque morphology alters between cell type also. Figure 6D and 3H show that for both A/WSN/1933 and A/California/07/2009 respectively, plaque size is greatly reduced in A549 relative to MDCK, and similarly for HBEC3-KT relative to both A549 and MDCK cells.

Our data suggest that human airway epithelial cells are significantly more restrictive to IAV multi-cycle infection than MDCK cells. We hypothesise that this phenotype will extend to single cycle infection also. To test this, we optimised the input MOI (PFU/cell) that would be required for detecting viral NP antigen at 6hpi using immunofluorescence for viral NP.

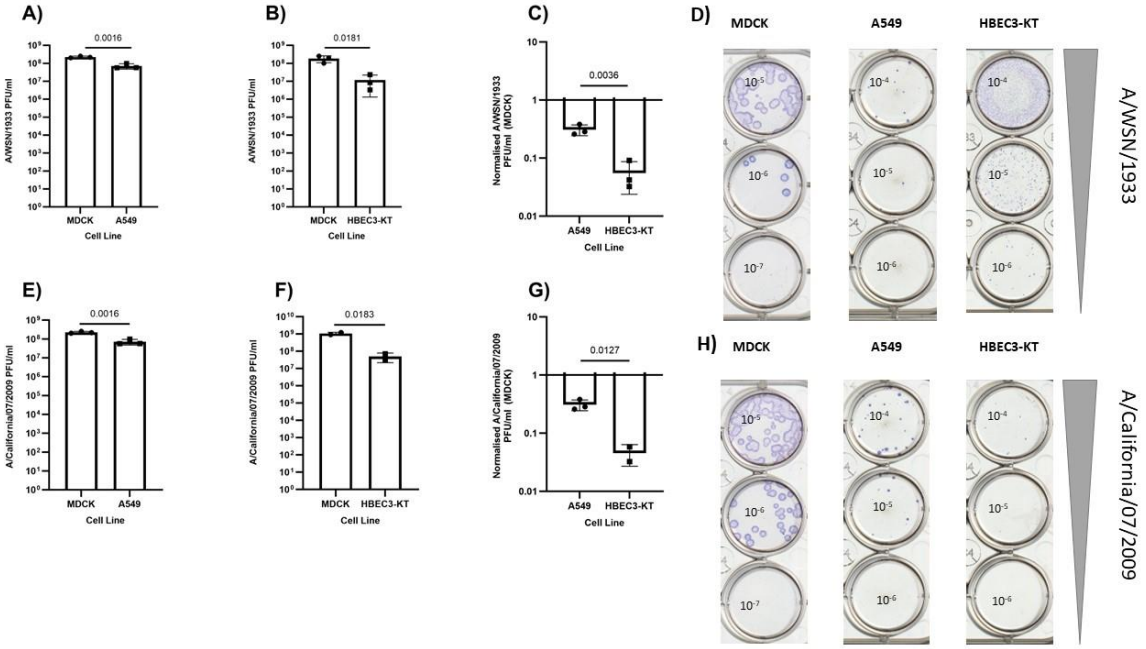

Figure 6. A/WSN/1933 and A/California/07/2009 are significantly restricted in A549 and HBEC3-KT cells relative to MDCK cells. A/WSN/1933 and A/California/07/2009 were used to infect MDCK, A549 and HBEC3-KT cells at a serially diluted inoculum (1 in 10 from stock) for 48 hours and plaques visualised by immunocytochemistry. A) A/WSN/1933 PFU/ml in MDCK cells and A549 cells. B) A/WSN/1933 PFU/ml in MDCK and HBEC3-KT cells. C) A/WSN/1933 PFU/ml normalised to MDCK in A549 and HBEC3-KT cells. D) Scanned plaques of A/WSN/1933 in MDCK, A549 and HBEC3-KT cells with decreasing inoculum concentrations, dilutions shown as inoculum dilution from stock. E) A/California/07/2009 PFU/ml in MDCK cells and A549 cells. F) A/California/07/2009 PFU/ml in MDCK and HBEC3-KT cells. G) A/California/07/2009 PFU/ml normalised to MDCK in A549 and HBEC3-KT cells. H) Scanned plaques of A/California/07/2009 in MDCK, A549 and HBEC3-KT cells with decreasing inoculum concentrations. Results derive from 3 independent repeats with A/California/07/2009 plaque forming assay in MDCK and HBEC3-KT cells deriving from 2 independent repeats. Statistical tests carried out using unpaired two-tailed t-test. Histogram bars denote mean PFU/ml +/- standard deviation. Infections conducted at 37°C + 5% CO_2.

3.1.2.2. Optimising input MOI to quantify viral antigen expression in cell monoculture.

To examine the relative permissibility of different cell types to IAV infection, we examined the optimal input MOI (PFU/cell) of A/WSN/1933 in MDCK cells to detect viral NP expression at 6 hpi.

MDCK cells were infected with a range of input MOI's (2.0, 1.0, 0.1, 0.01, 0.001 and 0.0001 PFU/cell). Figure 7A shows that at an input MOI of 0.001 PFU/cell, to have reached the limit of detection of this assay. At an MOI input of 2.0 PFU/cell, the assay shows signs of saturation where the majority of cells are antigen positive. Figure 7B shows the linear regression of antigen-positive cell percentage vs input MOI (1.0, 0.01 and 0.001 PFU/cell). These MOI's have a statistically linear correlation ($R^2 = 0.99$, P = <0.0001). Thus, we chose an input MOI of 1.0 PFU/cell for subsequent analysis.

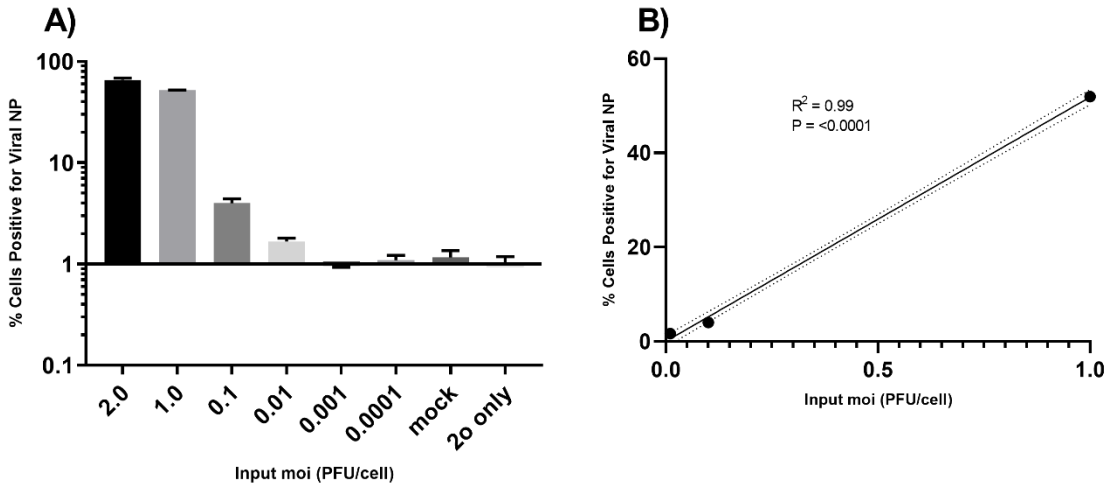

Figure 7. Quantification of viral antigen positive MDCK cells over a range of input MOIs. MDCK cells were infected with A/WSN/1933 using a range of input MOI's (2.0 – 0.0001 PFU/cell) for 6 hours at 37 ºC. Immunofluorescence for viral-NP was carried out. **A)** Percentage of cells showing positive viral-NP expression at 6 hpi. **B)** Linear regression analysis of percentage cells positive for viral-NP at input MOI 0.01, 0.1 and 1.0 PFU/cell. Results represent a single biological replicate. Histogram bars denote mean PFU/ml +/- standard deviation.

3.1.2.3. MDCK cells are significantly more permissive to A/WSN/1933 (H1N1) than A549 and HBEC3-KT cells at 6 hpi.

We infected MDCK, A549 and HBEC3-KT cells with lab-adapted A/WSN/1933 and A/California/07/2009 at 1.0 FFU/cell. We calculated this by performing cell counts using DAPI staining prior to infection and adjusting virus inoculums as required for each cell line. After 6 hours we fixed, permeabilised and stained cells for viral NP. The relative percentage of NP-positive cells enables a comparison between cell lines, of their permissibility to infection. We determine that the presence of antigen on a cell is an indicator of active infection within that cell. Thereby we hypothesise that cell lines that are differentially permissive to influenza, will have different proportions of their cells having active infection and thus differing in the number of NP-positive cells. This determination is an assumption that all cells associated with an NP signal have had active infection, and this should be validated with further testing.

To begin our analysis, MDCK, A549 and HBEC3KT cells were infected with A/WSN/1933 at input MOI of 1.0 PFU/cell for 6 hpi at 37 ^{o}C (6 hour time point was chosen to conform with established influenza infection protocols in the Boutell laboratory, data not shown). Using immunofluorescence to stain for influenza NP, we calculated the percentage of cells that were positive for NP and compared these levels across cell types. Figure 8A shows that MDCK cells had a significantly higher proportion of NP-positive cells relative to both A549 and HBEC3-KT cells ($P = 0.0009$ and $P = <0.0001$ respectively). A549 cells had significantly higher levels of antigen positive cells than HBEC3-KT cells ($P = 0.026$). Figure 8B shows the immunofluorescence for viral NP for each cell type, which clearly shows a decrease in the relative levels of IAV-NP antigen-positive cells between MDCK, A549 and HBEC3-KT cells. We see a small level of NP-positive cells in our mock infections, we hypothesis that this is autofluorescence background signal and therefore we subtracted the ‘background’ signal from our infection signal to account for this.

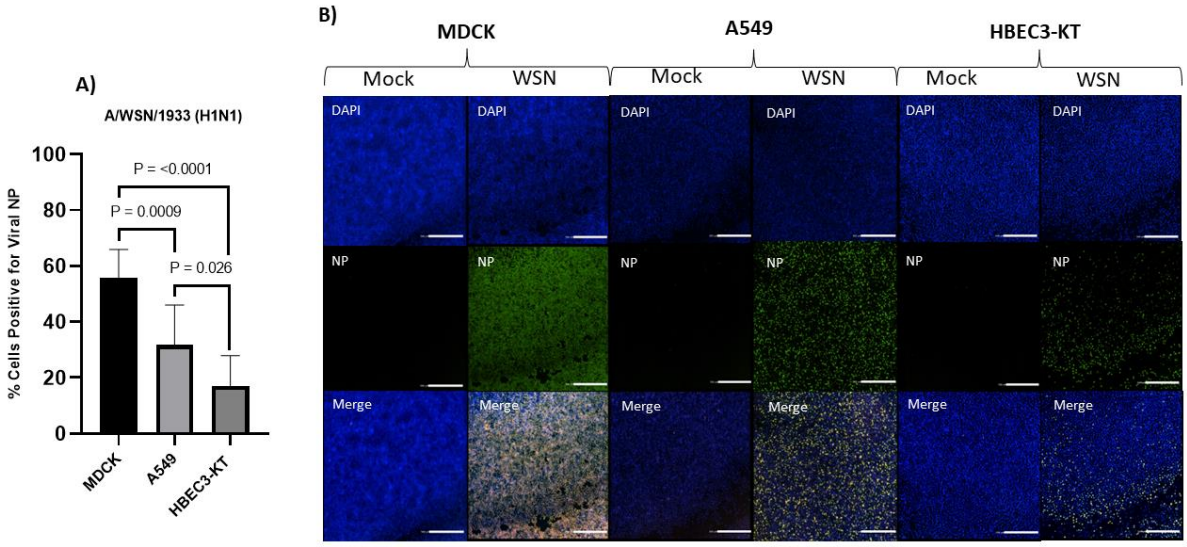

Figure 8. A549 and HBEC3-KT cells are significantly more restrictive to A/WSN/1933 infection at 6 hpi relative to MDCK cells. MDCK, A549 and HBEC3-KT cells were infected with A/WSN/1933 at 1.0 PFU/cell for 6 hours. Immunofluorescence was carried out for viral NP. A) Percent of MDCK, A549 and HBEC3-KT cells positive for viral-NP staining. Statistical test used: Unpaired two-tailed t-test. Results are from 3 independent biological replicates. Histogram bars denote mean % cells positive for viral NP +/- standard deviation. B) Immunofluorescence images of MDCK, A549 and HBEC3-KT, mock and A/WSN/1933 infected. DAPI (blue), NP (green) and Merged images shown as a representative of 3 independent biological repeats.

3.1.2.4. TrypLE does not sufficiently enable continued replication of WT A/Slovenia/2903/2015 in hAECn cells.

We have demonstrated that human airway (A549 and HBEC3-KT) cells are restrictive to lab-adapted influenza virus infection. LAIV infection is restricted to the upper airway tract as a result of the temperature attenuated Ann Arbor backbone. Therefore, to study LAIV infection in more physiologically representative monoculture systems, we utilised primary nasal epithelial (hAECn) cells. This presents challenges as influenza infection requires the addition of proteases to cleave viral HA and allow multi-cycle infection 6. Such proteases are used as cell detachment reagents (Trypsin) during routine passaging. Therefore, we determined measures by which we could utilise such reagents to enable multi-cycle infection whilst maintaining the cell monolayer.

hAECn cells are highly susceptible to trypsinisation and are highly prone to detachment with a Trypsin-TPCK overlay (data not shown). We therefore aimed to understand whether we could use TrypLE as a replacement. Figure 9A shows that high concentrations of TrypLE (1in25, 1in50, and 1in75 dilution from 1x stock) there is significantly fewer cells remaining adhered to the tissue culture plastic compared to no TrypLE after 72 hours incubation ($P = <0.0001$, $P = 0.0004$, $P = 0.0336$ respectively). At 1 in 100 dilutions of TrypLE, there was no significant difference in cell numbers compared to no TrypLE control. We next assessed whether TrypLE can enable multicycle IAV infection. We chose wild-type A/Slovenia/2903/2015 as our test strain as we would use this as a control/comparator for LAIV studies. Figure 9B shows virus release quantitation of WT A/Slovenia/2903/2015 up to 72hpi. A/California/07/2009 was chosen as a trypsin-independent control. These data suggest that at 1 in 50 dilution we are seeing continual virus production up until 48 hpi at a highly reduced number compared to A/California/07/2009. At 1 in 75 dilutions of TrypLE, we can see continual growth of virus numbers at 72 hpi. Figure 9C shows that the number of cells showing positive presentation WT A/Slovenia/2903/2015 haemagglutinin did not noticeably increase over time, indicating the absence of cell-to-cell spread.

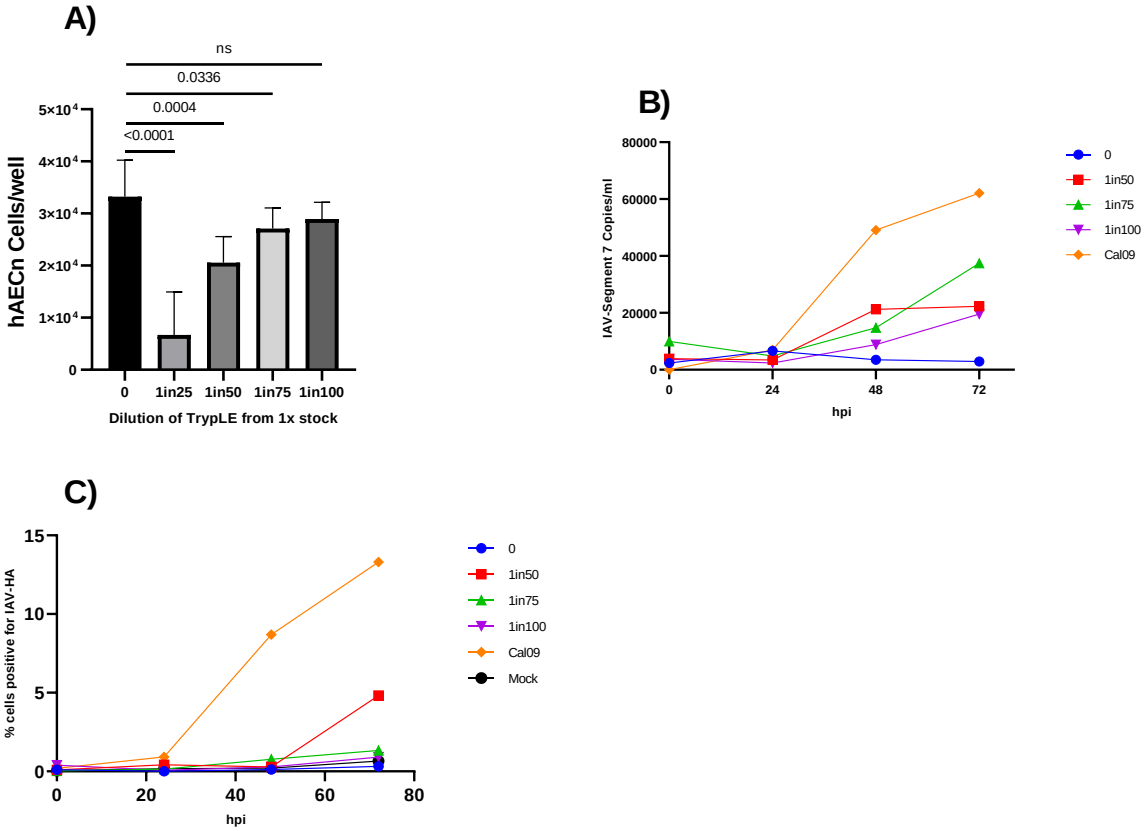

Figure 9. TrypLE will promote viral release of WT A/Slovenia/2903/2015 in hAECn cells but shows little to no signs of cell-to-cell spread by immunofluorescence. A) hAECn cells were cultured at 37 ºC with TrypLE at dilutions 1 in 25, 1 in 50, 1 in 75 and 1 in 100 from 1X stock. Cell numbers were obtained at 75 hpi using DAPI stain to count remaining adhered cells. Statistical test used: two-tailed unpaired t-test. Results are from 3 independent biological replicates. B) hAECn cells were infected with WT A/Slovenia/2903/2015 with overlay containing 1 in 50, 1 in 75 and 1 in 100 dilution of 1X TrypLE with a no TrypLE control and A/California/07/2009 as a trypsin-independent strain. Supernatants were collected at 24 hour intervals and released virions quantified using ddPCR for IAV segment 7. Results are from a single replicate. **C)** Once supernatant was collected, cells were fixed and stained for viral haemagglutinin. Cells were co-stained with DAPI to obtain both cell counts, and HA foci counts using Celigo apparatus. Results are from a single replicate.

3.1.3. Conclusions and Next Steps

Our data corroborates findings by Charman et al. showing A549 and HBEC3-KT cells to be restrictive to multicycle IAV infection relative to MDCK cells (Charman et al., 2021). The restrictive nature of A549 cells has been previously reported (Ujie et al., 2019) whereby long-term culture led to greater permissibility to some strains to influenza, particularly influenza A viruses. Here we show that the restrictive nature of human airway cells relative to MDCK cells is significantly greater in HBEC3-KT cells compared to A549 cells. We show that this restriction phenotype occurs not only during multicycle infection, but at single cycle too. This suggests that IAV is being restricted at an early phase of infection and the extent to which is cell-type dependent. Whether this is due to an immediate host cell innate immune response that is more prevalent in HBEC3-KT and A549 cells compared to MDCK cells is not understood.

Our data suggests two potentially cell tropism causes for differential levels of IAV permissibility: 1) cell type species origin. 2) Genetic status of cell types. In terms of cell type species origin, MDCK cells are derived from a canine kidney tissue, therefore we can hypothesise that anti-IAV responses, particularly to H1N1 influenza virus, may be lacking in MDCK cells relative to cells of human lung origin. With regards to the genetic status of cells, MDCK cells are an immortalised cell culture line that exhibit neoplastic properties. The tumorigenic potential of MDCK cells is not well understood, with conflicting data published as summarised by Omeir R. et al (Omeir et al., 2011). Indeed A549 cells are of adenocarcinoma origin (Isaka et al., 2003) whereby HBEC3-KT cells are primary-transformed cells with telomeric extensions used to prolong passage time in cell culture (Ramirez et al., 2004). We can therefore hypothesise that each of these cell types would have different constitutive expression profiles of anti-viral genes, indeed this has been shown in previous studies comparing A549 anti-IAV responses to human lung tissue cells showing that decreased viral burdens in A549 cells relative to primary human alveolar cells related to decreased host antiviral gene induction (Bertrams et al., 2022).

Together our data suggests that although MDCK cells are potential a good model system for high-yield propagation of IAV, they do not appear to be representative of the infection dynamics between IAV and human lung epithelial cells. More work would be required to discern the mechanisms behind this cell type-dependent differential permissibility to Influenza.

With human nasal epithelial cells being the primary target of LAIV infection (Hawksworth et al., 2020, Mohn et al., 2016a, Maassab, 1967), we aimed to understand whether primary nasal epithelial cells exhibit similar restriction phenotypes with LAIV strains. To do this, we first needed to optimise assays for multicycle growth of IAV in hAECn cells. Our data shows that establishing multicycle infection of wild-type A/Slovenia/2903/2015 in hAECn cells *in* vitro is not straight forward. We cannot utilise TPCK-Trypsin as this leads to cell detachment from tissue culture plates. The use of TrypLE in place of Trypsin-TPCK appears to lead to increased virion release, although cell-to-cell spread was not observed.

Promisingly, we observed that utilising mucus washes from 3D-differentiated Human bronchial epithelial cells leads to a significant increase in A/Puerto Rico/2008 plaque sizes relative to no protease addition, but these were still significantly smaller plaques than those grown in the presence of Trypsin-TPCK. The use of such mucus washes would require large amounts of optimisation to equalise the concentration of proteases used between assay replicates. Additionally, proteome analysis of mucosal washes would need to be carried out to understand the contents and how this may impact viral infection. Moreover, the presence of mucins in these washes would hinder IAV infection (McAuley et al., 2017). Mucins are heavily sialylated and require influenza neuraminidase activity to cleave through the mucins (Cohen et al., 2013), thus providing a competitive inhibitor for cell-surface sialic acids. To this end, Mucins would need to be removed from mucus washes to ensure this inhibition does not take place.

Given the difficulties in establishing an assay for IAV multicycle growth in MDCK cells, we chose to focus on single-cycle infections to understand hAECn relative permissibility to LAIV in chapters 4. We also use single-cycle infection understand how primary human nasal cell innate immune response changes dependent on the LAIV strain used for infection for chapter 3.2.

Chapter 3.2 will look to apply our understanding of relative influenza replication dynamics between human airway cells and MDCK cells to elucidate whether LAIV is similarly restricted in primary human nasal epithelial cells relative to MDCK cells. We will ask two key questions; 1) are primary hAECn cells restrictive to wild-type IAV and LAIV compared to MDCK cells? 2) are there differences in viral entry efficiencies in hAECn cells between two LAIV strains; LAIV A/Slovenia/2903/2015 and A/Bolivia/559/2013?

3.2. LAIV is Restricted in Primary hAECn Cells Relative to MDCK cells, and this is not a Result of Reduced Viral Entry

3.2.1. Introduction

In Chapter 3.1, we showed that human airway epithelial cells (A549 and HBEC3-KT) were significantly more restrictive to IAV than MDCK cells for both single and multicycle infection. In Chapter 3.2, we will investigate the relative infectivity of LAIV in MDCK cells, commonly used in LAIV effectiveness studies, to that of primary human nasal epithelial (hAECn) cells.

To establish a hAECn cell model for medium throughput *in vitro* assay's applicable to pharmacology studies, we immortalised cells by over-expressing hTERT and CDK4, an approach previously used to extend primary airway cell longevity through the inhibition of cellular senescence (Ramirez et al., 2004)

With LAIV H1N1 VE being sub-optimal for both the 2013-14, and 2015-2016 influenza season (Caspard et al., 2016, Caspard et al., 2017), efforts have been made to further understand the biology behind LAIV, and how VE can be improved. LAIV A/Bolivia/559/2013 was shown to have reduced VE during the 2015-2016 season (Caspard et al., 2017) with the exception of a single study finding a VE of 65% (Buchan et al., 2018). A recent study by Dibben O, et al. showed reduced replicative fitness of LAIV A/Bolivia/559/2013 compared to other strains in both a trivalent and quadrivalent formulation (Dibben et al., 2021). These data suggest a competitive disadvantage for LAIV A/Bolivia/559/2013 that could account for relatively low VE. Similarly, replication studies in 3D-differentiated human nasal cells show that there are inter-strain differences in both single-cycle and multicycle infection titres between two LAIV strains, showing LAIV A/Slovenia/2903/2015 to have a peak titre of 1.23 $\log_{10}$ higher than that of LAIV A/Bolivia/559/2013 (Hawksworth et al., 2020). We aim to further our understanding of LAIV infection in primary human nasal epithelial cells. These studies will increase our understanding of host cell responses to LAIV, elucidating the biology behind the use of primary hAECn cells for medium-throughput LAIV research and development assays.

Chapter 3.2 will determine the relative permissivity of MDCK and hAECn cells to LAIV infection. We will use LAIV A/Bolivia/559/2013 and LAIV A/Slovenia/2903/2015 as representatives of LAIV vaccine strains with known sub-optimal and high VE, respectively (Caspard et al., 2017).

To elucidate the infection phenotypes of LAIV in primary hAECn cells, we first aimed to determine whether hAECn cells are restrictive to LAIV relative to MDCK cells. With MDCK cells being used as a cell line of choice for LAIV potency assays such as with the focus-forming unit assay (i.e. peak titre obtained through single-cycle infection) (Hawksworth et al., 2020), understanding how hAECn cells compare will enable us to determine how representative or otherwise MDCK cells are for use in such assays that are commonly used in a pharmacology setting for investigating VE. The use of nasal epithelial cells has been chosen owing to the temperature attenuation of LAIV afforded to it by the use of the cold-adapted Ann Arbor backbone (Maassab, 1967). This cold adaptation restricts LAIV replication to the cooler upper airway tract (33^{o}C) whereby localised innate and humoral responses are established (Dibben et al., 2021).

We hypothesise that using hAECn will provide a more physiologically representative cell model system for IAV/LAIV *in vitro* studies that closer resemble the upper airway in which LAIV replication is restricted (Mohn et al., 2016a).

3.2.2. Results

3.2.2.1. hTERT/CDK4-immortalised hAECn cells reduce their proportion of epithelial cells on subsequent passaging.

In Chapter 3.1, we showed that human airway cells (A549 and HBEC3-KT) are significantly more restrictive to multi- and single-cycle IAV infections relative to MDCK cells. Having used laboratory adapted IAV strains (A/WSN/1933 and A/California/07/2009), we aimed to determine whether LAIV is similarly restricted in human airway cells in a cell type-dependent manner. With LAIV being restricted to the upper airway tract as a result of the cold-adaptation Ann Arbor backbone used in LAIV reverse genetics, we chose human nasal epithelial cells as our model. Primary human nasal epithelial cells have a short life span in vitro, being viable up to passage 12. This makes use of primary nasal epithelial cells for LAIV development and research costly and reduces continuity of cell culture integrity. In order to extend the life span beyond 12 passages, we undertook immortalisation via telomerase extension based on the methodology utilised with HBEC3-KT cells (Ramirez et al., 2004).

Post-immortalisation, we visually observed a change in cell morphology observed over subsequent passaging (figure 10). We hypothesised that we were seeing a reduction in the proportion of cells that were epithelial. To maintain consistency in infection conditions between experiments, continuity in the ratios of cell types between passages would be required. With epithelial cells being the primary target of influenza virus (Couceiro et al., 1993), and seeing their relative numbers reduce over subsequent passaging, we determined the need for selecting epithelial cells.

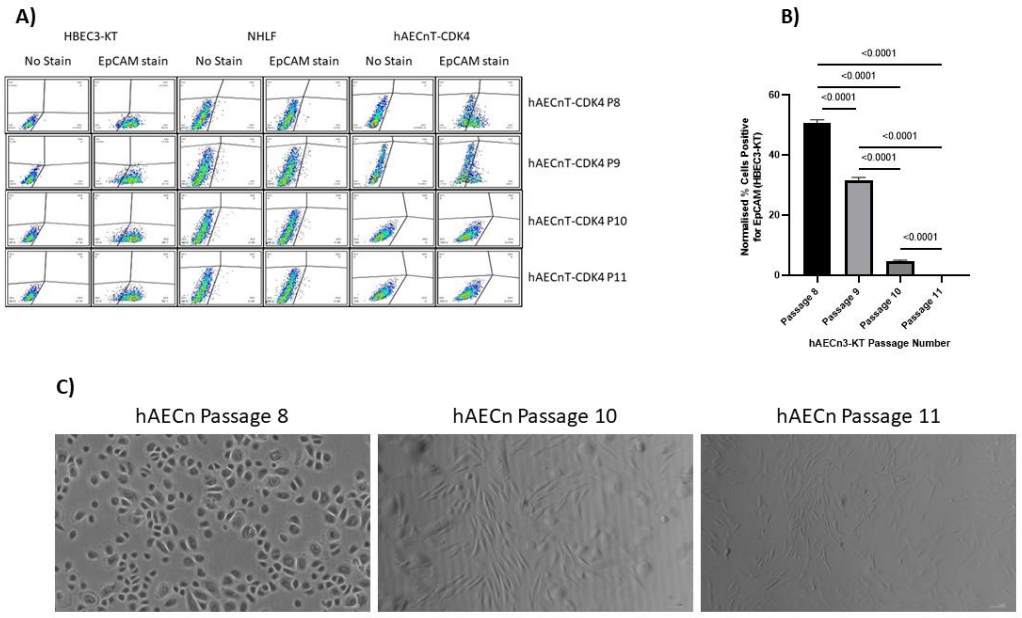

Figure 10. hTERT/CDK4-Immortalised hAECn cells have reduced epithelial cell populations over serial passaging. hAECN-KT cells were grown to 70-80% confluence and stained with anti-EpCAM primary antibody and anti-mouse secondary antibody for epithelial cell quantification by flow cytometry. A) Cell gating for hAECN3-KT with HBEC3-KT as a positive control and NHLF as a negative control for EpCAM expression. No stain indicates cells that have not been targeted with any antibody. B) Percentage of cells positive for EpCAM, normalised to HBEC3-KT. Histogram bars denote mean % EpCAM-positive cells +/- standard deviation. Statistical test used: two-tailed unpaired t-test. Results are from 3 independent replicates. C) Light field images were taken prior to flow cytometry.

Figure 10 shows the percentage of epithelial cells (EpCAM positive) reduced from passage 8 over subsequent passages to passage 11, (figure 10 A-B) at which no epithelial cells were detected (P = <0.0001). Figure 10C shows how the morphology of hAECN3-KT cells changed over time, in passage 8, the cells show cobblestone morphology consistent with epithelial cells, whereas at passage 11, the cells morphology changes to elongated fibroblast-like cells. These data suggest hTERT-immortalised hAECn cells cannot be used as a cell model system without further analysis and optimisation.

We determined the need to selecting of epithelial cells to remove fibroblast contaminants and maintain epithelial cell ratios over subsequent passaging. To do this we used fluorescence-associated cell sorting (FACS) to positively select for epithelial cells using EpCAM as an epithelial cell-specific marker as in Figure 9. Primary airway cells are highly susceptible to stress, we found that maintaining cell viability post-FACS was difficult, with cells not surviving past 2 passages post sorting (data not shown). Owing to time constraints imposed by COVID-19, we decided not to continue with the optimisation of hAECn-KT isolation and to focus instead on LAIV infection in non-immortalised primary human nasal cells would elucidate strain dependent host-cell responses.

3.2.2.2. Establishing a fluorescence-associated cell sorting (FACS) assay for the positive selection of epithelial cells using HBEC3-KT cells as a positive control

Having shown in figure 10 that we can use EPCAM as an epithelial cell marker to discern epithelial cells from fibroblast (IMR90) cells, we aimed to use EPCAM to select for, and collect epithelial cells from a mixed-cell population such as within immortalised hAECn cells. Figure 11 shows a proof-of-principle sorting experiment with HBEC3-KT cells. HBEC3-KT cells were strained with conjugated anti-EPCAM (488). For FACS analysis we require an unstained sample to gate for cells not stained with EPCAM, these scatter plots are shown in Figure 11A. 4′,6-diamidino-2-phenylindole (DAPI) is used as a live cell marker in this instance, staining nuclear DNA (Tawa et al., 2016). Figure 11B shows scatter plots of EpCAM-positive HBEC3-KT.

Having shown that epithelial cells can be detected and selected for using FACSaria^{TM} (figure 11), we next wanted to use this assay to stain immortalised hAECn epithelial cells and positively select for epithelial cells from a mixed hAECn culture.

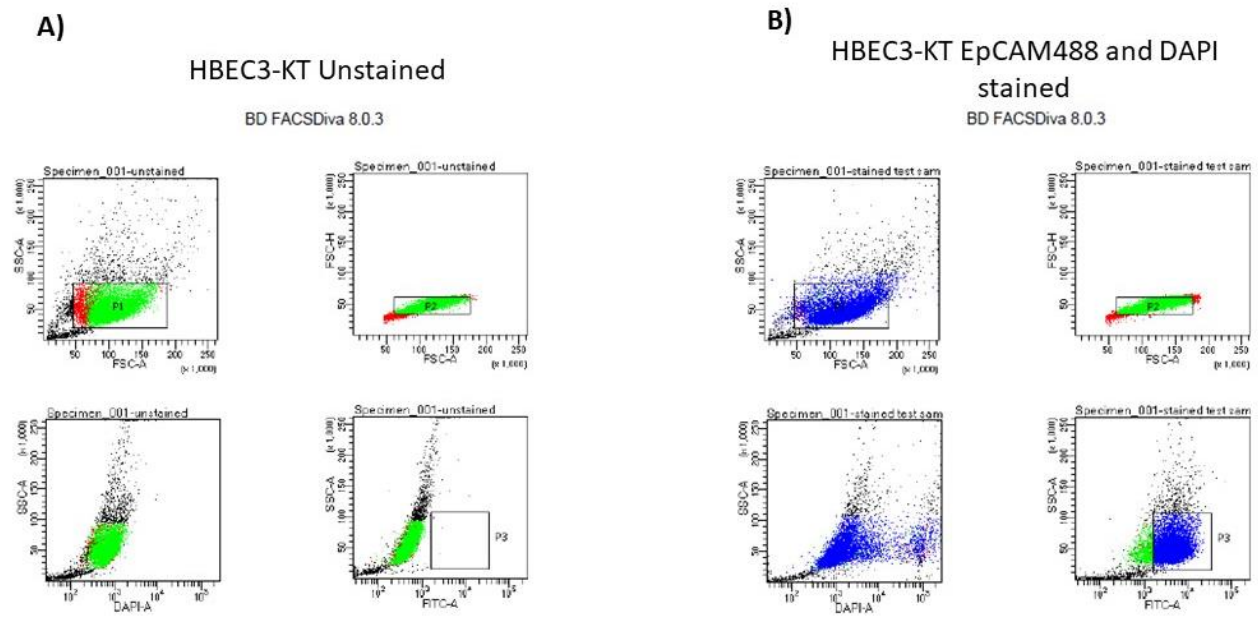

Figure 11. FACS can be used to select for epithelial cells. A) Unstained HBEC3-KT scatter plots for non-stained cells. B) Scatter plots for gating of EpCAM-stained EPCAM3-KT cells. FACS undertaken using 10,000 events. For both A and B, panels show upper left, forward vs side scatter. Upper right forward vs forward scatter to remove doubling events. Lower left, DAPI detection to remove dead/non-viable cells. Lower right; gating of EpCAM positive cells (Alexa fluor488 (FITC)).

3.2.2.3. Fluorescence-associated cell sorting (FACS) can successfully sort epithelial cells from a mixed-cell population.

Out of 10,000 immortalised hAECn cells, we were able to detect, isolate and collect epithelial cells that represented 54% of the total cell count analysed through FACS, shown through P4 – population of cells gated as being positive for Alexa-fluor 488 (FIT-C) (figure 12C and 12F). Immortalised hAECn cells selected for during FACS were collected and seeded on to tissue culture 66mm dish and allowed to propagate under standard conditions (37ºC + 5% CO_2). Cells grew to 70-80% confluence and passaged as per standard hAECn cell passaging protocol. Cells were seeded in to a small T25 tissue culture flask and allowed to propagate under standard conditions. Cells ceased to grow after this single post-FACS passage and cell death followed (data not shown). We tried optimising the assay to increase cell numbers retrieved through FACS and reduce FACS-associated stresses such as time spent out of maintenance media. However, we were unable to maintain cell health and undertake continual cell passaging post-sorting.

Being unable to maintain cell health post-FACS sorting, we chose to focus on primary non-immortalised hAECn host-cell responses to LAIV infection. Doing this will allow us to assess how these cells may be used in 2D culture systems for high-throughput assays commonly used in IAV infection studies and LAIV development such as TCID50 and FFU assays. We will be able to characterise innate responses to LAIV in these 2D hAECn cultures, ultimately aiming to determine the biology of, and feasibility of hAECn cells for such assays as a more physiologically representative cell line than those currently used such as MDCK cells.

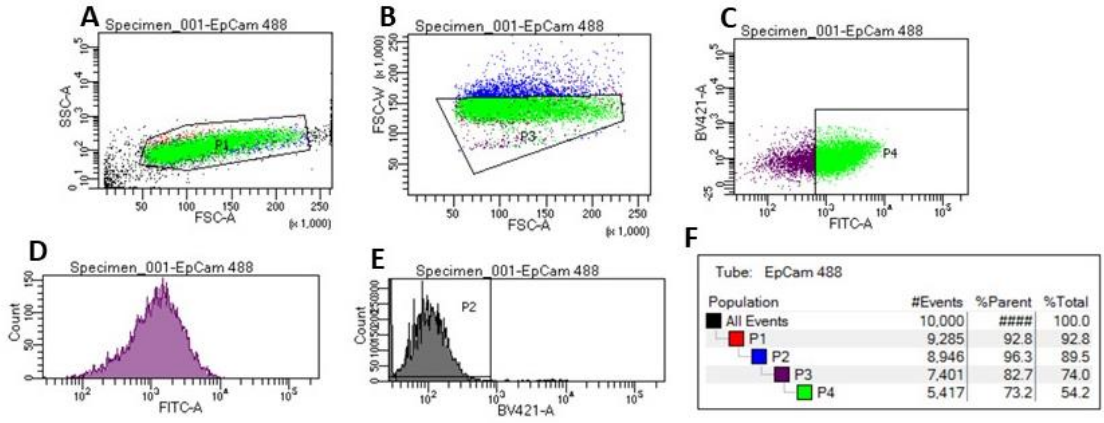

Figure 12. hAECn-KT epithelial cells can be selected for by FACS. Scatter plots for gating of EpCAM-stained EPCAM3-KT cells. Staining hAECn-KT cells with a conjugated EPCAM antibody can be used for detection and selection of epithelial cells. A1) side scatter vs forward scatter. B) Forward scatter-W vs Forward Scatter-A. C) EpCAM positive cell gating (FITC-A). D) frequency of EpCAM-positive hAECn-KT cells. E) DAPI positive population of cells, DAPI-positive indicates dead/non-viable cells, these were gated and removed from further selection. F) Event number, P4 indicates EpCAM-positive cell number.

3.2.2.4. Relationship between PFU/ml, FFU/ml and Copies/ml Titres for Quantifying LAIV/IAV stocks

With being unable to obtain plaque assay titres for WT and LAIV IAV strains in the IAV-permissive MDCK cell line, we chose to utilise focus forming unit assays and gene copy quantitation assays to obtain FFU/ml and copies/ml respectively. Performing plaque assays (where possible) for A/WSN/1933 and A/California/07/2009, as well as focus forming assays and virion gene copy number quantitation for all strains, enabled us to compare ratios between these titres. Table 10 shows the raw titres for all strains (all results derived from MDCK cell infections). PFU/ml was not available for WT A/Slovenia/2903/2015, LAIV A/Slovenia/2903/2015, WT A/Bolivia/559/2013 and LAIV A/Bolivia/2903/2013.

Table 11 shows the titre ratios. Our lab adapted IAVs, A/WSN/1933 and A/California/07/2009 had comparable copy:FFU ratios of 2.89 and 5.57 respectively. However, there was a large difference in copy:PFU ratios where A/WSN/1933 had a copy:PFU ratio of 7.66 but A/California/07/2009 was 13-times higher at 97.09. This trend was similar for FFU:PFU ratios with A/WSN/1933 at 2.65 and A/California/07/2009 at 17.44. WT and LAIV strains had comparable copy:FFU to both A/WSN/1933 and A/California/07/2009. WT A/Bolivia/559/2013 had the greatest copy:FFU of 14.94, 5 times greater than A/WSN/1933 and 3 times greater than A/California/07/2009 (2.89 and 5.57, respectively). LAIV A/Slovenia/2903/2015 had a copy:FFU ratio 3 times that of LAIV A/Bolivia/559/2013 (10.15 and 3.42 respectively). Whilst WT A/Slovenia/2903/2015 had a copy:FFU ratio 3 times lower than WT A/Bolivia/559/2013 (4.78 and 14.94 respectively). We were confident that there were no major differences in copy:FFU ratio between our WT and LAIV strains. Equally there was no major difference in copy:FFU ratio between our LAIV strains (LAIV A/Slovenia/2903/2015 and LAIV A/Bolivia/559/2013). This led us to use both FFU/ml and copy/ml as a basis for inoculum calculations in future studies.

Table 10. Copies/ml (IAV M-gene absolute quantification by ddPCR), FFU/ml, and PFU/ml Titres for IAV and LAIV Stocks used in this Study. For each strain, copies/ml titres were calculated using digital-droplet PCR - against IAV genome segment 7, for absolute quantification of virion numbers. FFU/ml was carried out for A/WSN/1933 and A/California/07/2009 in MDCK cells at 37ºC for 6 hours, staining for IAV-NP, for LAIV A/Slovenia/2903/2015, LAIV A/Bolivia/559/2013 and their matched wild-type strains, FFU/ml was determined based on infection of MDCK cells at 33ºC for 20 hours. PFU/ml was only determined for A/WSN/1933 and A/California/07/2009. MDCK cells were infected for 48 hours at 37ºC and plaques stained for viral NP. Plaque assay was not possible for LAIV and matched wild-type strains (data not shown). Results are mean average of two independent experiments for each titre methodology. 'N/A' denotes samples for which obtaining PFU/ml was not available.

Strain	Copies/ml (IAV M-gene absolute quantification by ddPCR)	FFU/ml	PFU/ml
A/WSN/1933	1.19E+09	4.11E+08	1.55E+08
A/California/07/2009	1.75E+09	3.14E+08	1.80E+07
WT A/Slovenia/2903/2015	9.55E+07	2.00E+07	N/A
LAIV A/Slovenia/2903/2015	5.93E+08	5.84E+07	N/A
WT A/Bolivia/559/2013	3.53E+08	2.36E+07	N/A
LAIV A/Bolivia/559/2013	3.06E+08	8.97E+07	N/A

Table 11. Titre Ratios for Copies/ml (IAV M-gene absolute quantification by ddPCR), PFU/ml, and FFU/ml for LAIV and IAV. Titres obtained for each strain (Table 1) were used to calculate their respective ratios. 'N/A' denotes samples for which obtaining PFU/ml was not available.

Strain	Copy:FFU	Copy:PFU	FFU: PFU
A/WSN/1933	2.89	7.66	2.65
A/California/07/2009	5.57	97.09	17.44
WT A/Slovenia/2903/2015	4.78	N/A	N/A
LAIV A/Slovenia/2903/2015	10.15	N/A	N/A
WT A/Bolivia/559/2013	14.94	N/A	N/A
LAIV A/Bolivia/559/2013	3.42	N/A	N/A

3.2.2.5. FFU Assay Shows NA and HA Antigens are Expressed at Equivalent Levels

To assess whether LAIV and wild-type IAV are restricted in primary nasal epithelial cells, we aimed to conduct an antigen-expression assay under the following conditions: 33 ºC for 20 hours. As the sheep anti-HA (TGA, IVR180) had been qualified by AstraZeneca for quantification of LAIV, we aimed to determine whether viral NP and HA antigens are presented at equivalent levels. To do this, we first tested our sheep anti-HA primary antibody (TGA, IVR-180) to elucidate any differences in antigen presentation between NP and HA.

To do this, we conducted an FFU assay with WT A/Slovenia/2903/2015, LAIV A/Slovenia/2903/2015, WT A/Bolivia/559/2013 and LAIV A/Bolivia/559/2013. We counted foci using NP and HA as target antigens and compared the FFU/ml titre using each. There was no significant difference in FFU/ml using either NP or HA for all IAV/LAIV strains (figure 13). We therefore chose to use sheep anti-HA (TGA, IVR180) antibody for immunofluorescence studies with LAIV moving forward.

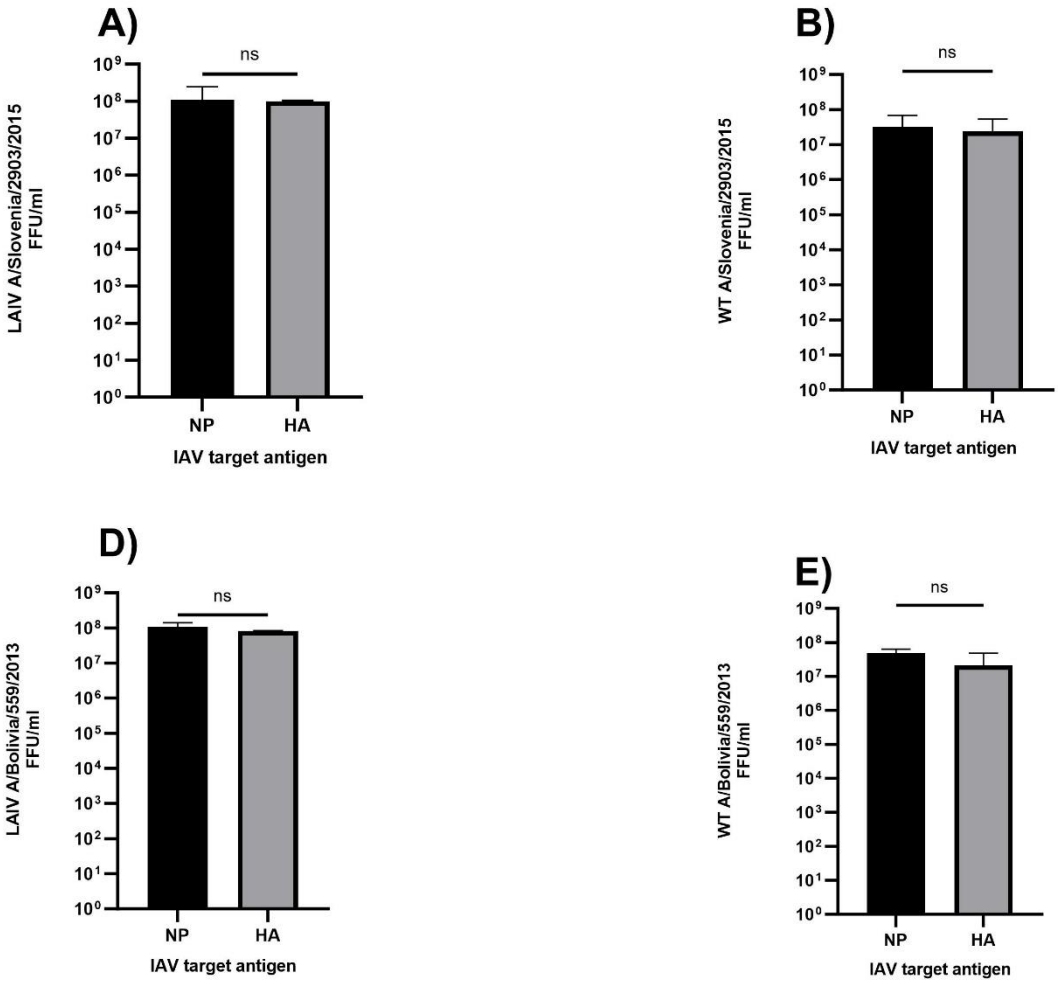

Figure 13. Using both NA and HA as targets for immunofluorescence shows comparable titres with each viral antigen. MDCK cells were infected with each strain at 1 in 10 serial dilution for 20 hours at 33ºC. Cells were co-stained with mouse-anti NP and sheep-anti HA primary antibodies. DAPI was used to quantify cell numbers. FFU/ml was calculated using each antigen and resulting titres compared. A) LAIV A/Slovenia/2903/2015, B) WT A/Slovenia/2903/2015, C) LAIV A/Bolivia/559/2013 and D) WT A/Bolivia/559/2013. Test used: two-tailed unpaired t-test. Results are form two independent experiments. Histogram bars denote mean FFU/ml +/- standard deviation.

3.2.2.6. LAIV/IAV is Restricted in hAECn cells Compared to MDCK Cells during Single-Cycle Infection

In chapter 3.1, we showed that A/WSN/1933 is restricted human airway epithelial cells (A549 and HBEC3-KT) relative to MDCK cells. Here we aimed to test whether the trend holds true for LAIV and their matched wild-type strains in primary hAECn cells relative to MDCK cells in a donor independent manner. For this we used primary hAECn cells derived from two donors, D1 (donor 1, AB0608.01. 50y/o, M, Caucasian) and D2 (donor 2, AB0541.01. 57y/o, Female, African). Our data suggests that primary hAECn cells are restrictive to LAIV and WT-IAV relative to MDCK cells. We also suggest that there are differences in relative antigen expression levels between LAIV and WT-IAV strains in MDCK cells and in primary hAECn cells.

Figure 14A shows that in MDCK, LAIV A/Slovenia/2903/2015 led to significantly higher proportion of cells positive for viral-HA than LAIV A/Bolivia/559/2013 ($P = 0.0271$). WT A/Slovenia/2903/2015 had a significantly smaller proportion of antigen-positive cells compared to its matched LAIV strain ($P = <0.0001$) whereas for A/Bolivia/559/2013, the trend is reversed; WT A/Bolivia/559/2013 had a significantly higher proportion of antigen positive MDCK cells compared to its matched LAIV strain ($P = 0.0014$). WT A/Bolivia/559/2013 also had a significantly higher proportion of antigen positive MDCK cells than WT A/Slovenia/2903/2015 ($P = <0.0001$).

For D1 (figure 14B), similar trends emerged to that seen in MDCK cells. LAIV A/Slovenia/2903/2015 led to significantly higher proportion of antigen positive cells that LAIV A/Bolivia/559/2013 ($P = 0.0051$). Although there was no significant difference between WT and LAIV A/Bolivia/2903/2015, this was not the case for A/Slovenia/2903/2015, whereby LAIV led to significantly higher proportion of antigen positive cells than its matched WT strain ($P = 0.00313$).

As with D1, D2 showed strain-specific levels of antigen positivity (figure 14C). LAIV A/Slovenia/2903/2015 had significantly higher proportion of antigen-positive cells tan LAIV A/Bolivia/559/2013 ($P = 0.0069$). Again, like D1, there was no significant difference between WT and LAIV A/Bolivia/559/2013, but there were significantly higher levels of antigen positivity for LAIV A/Slovenia/2903/2015 than its WT matched strain ($P = 0.0032$).

When comparing hAECn permissibility to LAIV to that of MDCK cells (figure 14D), WT A/Slovenia/2903/2015 was significantly restricted in hAECn cells, both D1 and D2 ($P = 0.0018$ and $P = 0.0154$ respectively). This was true also for WT A/Bolivia/559/2013 ($P = <0.0001$ and $P = <0.0001$ respectively). The trend held true for LAIV strains also, with LAIV A/Slovenia/2903/2015 leading to significantly fewer antigen positive hAECn cells (in D1 and D2) compared to MDCK cells ($P = 0.0006$ and $P = 0.0004$ respectively). LAIV A/Bolivia/559/2013 was restricted in hAECn D1 and D2 compared to MDCK cells also ($P = <0.0001$ and $P = <0.0001$ respectively). With the exception of WT A/Bolivia/559/2013 ($P = 0.0205$), there was no significant difference in the proportion of antigen positive hAECn cells between D1 and D2.

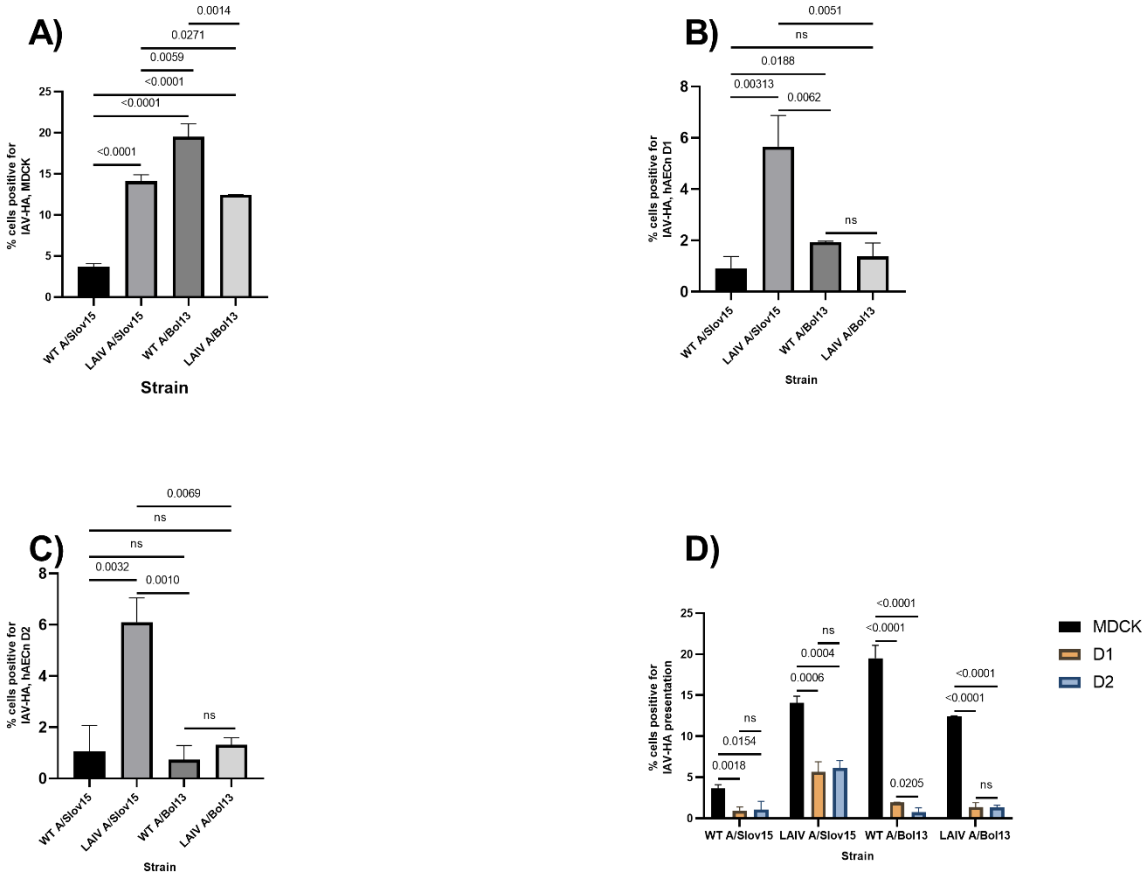

Figure 14. LAIV A/Bolivia/559/2013 leads to few antigen-positive cells than LAIV A/Slovenia/2903/2015 in both MDCK cells and primary hAECn cells. MDCK and hAECn cells were infected with LAIV and IAV strains at 0.5FFU/cell for 20hours at 33ºC. Cells were fixed, permeabilised and stained for HA (TGA IVR180). Number of cells presenting HA antigen as a percentage of total cells (DAPI positive) was calculated. A) Percentage of MDCK cells positive for IAV/LAIV HA. B) Percentage of hAECn D1 cells (donor 1, AB0608.01. 50y/o, M, Caucasian) positive for IAV/LAIV HA. C) Percentage of hAECn D2 (donor 2, AB0541.01. 57y/o, Female, African) positive to IAV/LAIV HA. D) differences in the proportion of cells positive for IAV/LAIV HA for each WT and LAIV IAV strain. Statistical test used: two-tailed unpaired t-test. Results are from 3 independent experiments (D2 WT A/Bolivia/559/2013 results from two independent experiments). Histogram bars denote mean normalised percentage cells positive for viral antigen (HA) +/- standard deviation.

3.2.2.7. LAIV A/Slovenia/2903/2015 Enters hAECn Cells to Greater Extent than MDCK Cells, Where LAIV A/Bolivia/559/2013 Enters hAECn Cells at an Equal Efficiency to MDCK Cells

We have shown that LAIV and WT-IAV are restricted in primary hAECn cells relative to MDCK cells, and that even within specific cell types, there are differences in permissibility to single-cycle infection between strains and donors (figure 14). We aimed to understand whether this restrictive phenomenon is a result of differential levels of virus virion entry between hAECn and MDCK cells. To do this, we infected MDCK and hAECn cells with LAIV A/Slovenia/2903/2015 and LAIV A/Bolivia/559/2013 at an MOI of 0.5 copies/cell for 2 hours at 33ºC in the presence of CHX. Cells were harvested by trypsinisation to remove surface virions and genomes copy numbers were measured by ddPCR to IAV segment 7.

Figure 15A shows that for LAIV A/Slovenia/2903/2015, there was significantly higher levels of intracellular virions in both D1 and D2 hAECn than in MDCK cells ($P = 0.0022$ and $P = 0.0455$ respectively). For LAIV A/Bolivia/559/2013, there was no significant difference between hAECn and MDCK intracellular virion copy numbers, and this was true of both hAECn donors (figure 15B).

As well as comparing intracellular copy numbers (IAV segment 7) between cell types, we compared intracellular virion numbers between both LAIV strains within each cell type (figure 15C). Although there no difference observed between strains in MDCK cells and hAECn D2, we saw significantly higher number of intracellular LAIV A/Slovenia/2903/2015 virions compared to LAIV A/Bolivia/559/2013 in hAECn D1 ($P = 0.00479$).

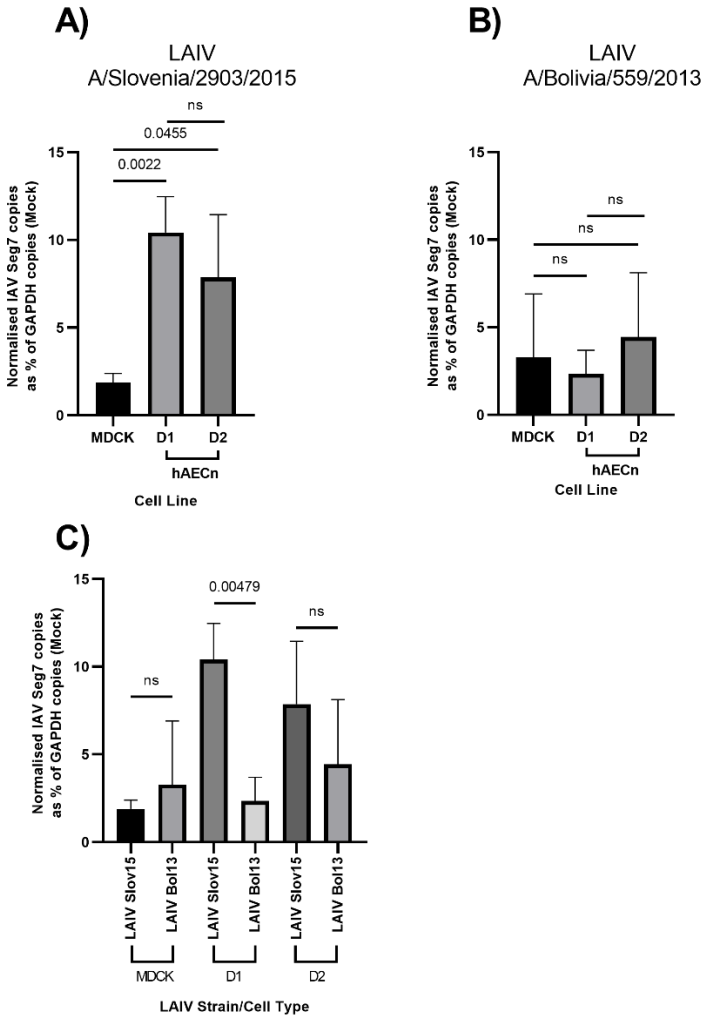

Figure 15. LAIV has higher entry efficiency in hAECn cells than MDCK cells. MDCK and two hAECn donors were infected with LAIV A/Slovenia/2903/2015 and LAIV A/Bolivia/559/2013 at an input MOI of 0.5 copies/cell for 2 hours at 33ºC. Total RNA was extracted and copy numbers for cellular GAPDH, and viral Segment 7 were determined using ddPCR. D1 (hAECn donor 1, AB0608.01. 50y/o, M, Caucasian). D2 (hAECn donor 2, AB0541.01. 57y/o, Female, African). Statistical test used: two-tailed unpaired t-test. Results are from 3 independent experiments. Histogram bars denote mean IAV-Segment 7 gene copies expressed as a percentage of cell number (GAPDH) +/- standard deviation.

Together, these data show that LAIV A/Slovenia/559/2015 enters primary hAECn cells with greater efficiency than MDCK cells. This implies that the single-cycle relative restriction we see by antigen-expression assays (figure 14) in hAECn cells is a result intracellular anti-viral host responses in hAECn cells that may not be present, or may be reduced, in MDCK cells.

3.2.3. Conclusions and Next Steps

In Chapter 3.1, we showed that human airway cells (A549 and HBEC3-KT) are significantly more restrictive to IAV than MDCK cells during both single-cycle and multi-cycle infections. In Chapter 3.2, we look to expand this finding to determine whether LAIV is similarly restricted in human airway epithelia compared to MDCK cells. As LAIV is restricted in the upper airway, we utilised primary human nasal epithelial (hAECn) cells.

As shown in Chapter 3, we encountered difficulties in optimising multi-cycle replication of WT/LAIV IAV strains in both MDCK and particularly in hAECn cells. As such we were unable to establish a plaque assay for WT/LAIV IAV. We therefore utilised the focus-forming unit assay to obtain FFU/ml titres and absolute quantification using ddPCR to determine genome copies/ml titres. By comparing these ratios, including PFU/ml for A/WSN/1933 and A/California/07/2009, we were able to determine the relative proportions of infectious virus within the stock samples. In comparing LAIV/WT IAV titre ratios to lab adapted WSN and Cal09, we must note that WT and LAIV strains are propagated in chicken eggs, whereas WSN and Cal09 are propagated in MDCK cells, therefore potential cell culture adaptations may be present in WSN and Cal09 that may increase their infection potential relative to WT and LAIV strains.

LAIV A/Slovenia/2903/2015 elicited a significantly greater proportion of antigen positive cells than its wild-type matched strain in both MDCK cells and hAECn D1 and D2. Interestingly, LAIV A/Bolivia/559/2013 showed no significant difference in the proportion of antigen positive cells than its matched wild-type strain in both hAECn donors. In MDCK cells, there is a greater proportion of WT A/Bolivia/559/2013 antigen positive cells than seen with its matched LAIV strain. When comparing the relative proportion of antigen positive cells between the two LAIV strains, we see that LAIV A/Slovenia/2903/2015 leads to a greater proportion of antigen positive cells than LAIV A/Bolivia/559/2013. These data may confirm previous studies finding that replication of LAIV A/Bolivia/559/2013 is low relative to other LAIV strains (Dibben et al., 2021).

When looking at the relative permissibility of MDCK cells to hAECn cells, we saw a clear phenotype that matched our findings in Chapter 3. Both LAIV A/Slovenia/2903/2015, LAIV A/Bolivia/559/2013 and their matched WT strains showed significantly higher proportions of antigen-positivity in MDCK cells compared to human nasal epithelial cells, although there was no significant difference seen between the two hAECn donors for any LAIV/IAV strain. These data suggest that the use of MDCK cells for determining LAIV potency by AstraZeneca may skew the understanding of LAIV infection potential in the human airway epithelia.

In order to further understand the relative permissibility of MDCK cells to LAIV (A/Slovenia/2903/2015 and A/Bolivia/559/2013), we determined the comparative entry efficiency of LAIV in to both MDCK cells and hAECn cells. Although LAIV A/Slovenia/2903/2015 was restricted in hAECn cells relative to MDCK cells, our data show that there is an increased ability of LAIV A/Slovenia/2903/2015 to enter hAECn cells than MDCK cells. These data suggest that restriction is not occurring as a result of an entry defect relating to hAECn cells, but rather we hypothesise that the host innate immune response is greater in hAECn cells compared to MDCK cells. This raises the question as to why there may be differences between LAIV strains that differ only in their surface glycoproteins (HA and NA). This suggests that restriction may take place at HA-mediated viral movement across cellular membranes, or NA-mediated cleavage of new virions. As we are only looking at single cycle infections, we hypothesise that HA-mediated attachment and entry, or endosomal release, may be the targets for host cell responses that are dependent on strain-specific HA glycoproteins. For LAIV A/Bolivia/559/2013, we saw no significant difference in the entry efficiencies between MDCK and hAECn cells, again this supports our hypothesis that restriction of LAIV in hAECn cells is a result of host responses rather than any entry defect. When comparing the entry efficiency of LAIV A/Slovenia/2903/2015 to LAIV A/Bolivia/559/2013, we see that there is no significant difference in intracellular virion counts in between hAECn and MDCK cells. However, we see a greater number of intracellular A/Slovenia/2903/2015 in both hAECn donors, although this was only statistically significant in donor 1 (D1).

Taken together, our data shows that MDCK cells are significantly more permissive to LAIV than hAECn cells, but that this is not a result of differential entry efficiencies between cell types. The reduced entry efficiency of LAIV A/Bolivia/559/2013 relative to A/Slovenia/2903/2015 may account for its previously reported reduced VE relative to other vaccine strains (Caspard et al., 2017).

In Chapter 3.3, we will determine potential causes of reduced LAIV infectivity in primary hAECn cells, and how host-cell responses differ for different LAIV strains. To do this, we will utilise RT-qPCR methodologies to determine relative expression levels of ISG between LAIV-infected hAECn cells and non-infected cells.

3.3. Innate Immune Responses to LAIV Suggest Strain- and Donor- Dependent Differences in Innate Immune Gene Expression

3.3.1. Introduction

In Chapter 3.2, we showed that 2D primary hAECn cells are restrictive to LAIV/WT-IAV relative to MDCK cells (figure 14). We show that this is not a result of a reduced ability of LAIV/WT-IAV to enter primary hAECn cells (figure 13). Therefore, we hypothesise that the restriction to LAIV/WT-IAV infection we see is a result of host cell responses. In Chapter 3.3, we will determine relative expression of *MX1* between LAIV A/Slovenia/2903/2015 and LAIV A/Bolivia/559/2013. We will study the differences in ISG expression (*MX1* and *OAS1*) in response to LAIV A/Slovenia/2903/2015 between three distinct hAECn cell donors. During the process of LAIV development, primary 3D-differentiated hAECn cells from mixed pool of donors are used to determine and validate LAIV strain potency. We aim to determine the effect on ISG response to LAIV infection of pooling donors relative to that of the constitutive independent donors.

LAIV works on the principle of 'infect to protect', whereby reverse genetics systems incorporate influenza virus surface glycoproteins (HA and NA) into the backbone containing genes/proteins from temperature sensitive Ann Arbor IAV and IBV strains (Jin et al., 2003, Hoffmann et al., 2005). This cold adaptation restricts replication to the upper respiratory tract, preventing serious disease and pathology associated with lower respiratory infection (Herold et al., 2015). Active infection in the upper respiratory airway leads to the induction of a specific and long lasting adaptive immune response to challenge by circulating influenza virus strains (Zens et al., 2016, Cherukuri et al., 2012). Adaptive immune responses to LAIV have been widely studied, with studies showing robust protection in both children and adults (Coelingh et al., 2015, Carter and Curran, 2011, Overton et al., 2014, Block et al., 2007, Shannon et al., 2020, Barría et al., 2013, Zens et al., 2016, Li et al., 2014, Wang et al., 2016, Mohn et al., 2015, Cherukuri et al., 2012, Mohn et al., 2016b, Sasaki et al., 2007). In addition to a strong Type 1 response resulting from IFNγ production and subsequent T-cell responses, LAIV has been shown to modulate innate immunity (Lanthier et al., 2011), thus suggesting LAIV induces a heterosubtypic innate immune response. Interestingly, LAIV has been shown to induce a greater innate immune response than wild-type IAV in 3D-differentiated airway epithelial cells (Forero et al., 2017, Fischer et al., 2014, Fischer et al., 2015). Where innate immunity to influenza virus has been widely studied as reviewed by Iwasaki and Pilai (Iwasaki and Pillai, 2014), who describe a number of ISGs that are well characterised in their anti-influenza virus activity, less is known about the specific innate immune response to LAIV, and how these innate immune responses may differ between LAIV strains.

With the establishment of a robust adaptive immune response requiring the activation of persistent and effective innate immunity (Medzhitov and Janeway, 1997), we aim to provide preliminary understandings of the innate immune response to LAIV, providing more information on the feasibility and underlying biology that would be indicated in using hAECn cells as a 2D culture model system for the study of IAV/LAIV.

We will use *MX1* and *OAS1* as our ISG targets to determine strain- and donor-dependent innate immune responses to LAIV. Human *MX1* is a GTPase located in the cytoplasm (Sehgal et al., 2020). MX proteins work by recognising viral NP, both incoming and newly transcribed. Attachment of *MX1* to viral NP inhibits viral entry into the nucleus, thereby halting early phases of viral replication (Haller and Kochs, 2020). *OAS1* belongs to the gene family Oligoadenylate synthases, these contain *OAS1, OAS2, OAS3* and *OASL* (Hovanessian, 2007). *OAS1* has been shown to be up-regulated in response to IAV (WSN) infection (Çağlayan and Turan, 2022). *OAS* enzymes act to degrade RNA molecules, both cellular and viral (Castelli et al., 1997, Chakrabarti et al., 2012, Zhou et al., 1997). Using these anti-influenza virus ISGs, we will use two-step RT-qPCR to determine relative levels of innate immune activation between LAIV strains, we will also use these genes to determine relative innate immune responses to LAIV between individual donor hAECn cells and a hAECn culture of pooled donors.

Few studies have been conducted looking at the relative innate immune response of cultures from different donors to IAV infection. Where we here are interested in understanding the feasibility of 2D airway cultures for use in high-throughput assays such as during LAIV development and research, other studies focus on differentiated airway epithelia. Indeed, a study by Ilyushina N. et al. 2019 used differentiated airway epithelia (NHBE cells) from two distinct donors to measure their immune responses to influenza virus infection. They found significant differences in both interferon expression levels, and ISG expression including *MX1*, and *OAS1* (Ilyushina et al., 2019). Although these studies were longitudinal, we will look to corroborate these findings in our 2D culture systems to hypothesise whether differences in infection phenotypes seen in chapter 3.2 may be explained by differential host responses.

In chapter 3.3, we aim to provide preliminary data to begin to determine host cell innate immune responses to LAIV. Understanding how hAECn cells respond to LAIV infection in 2D culture settings will allow us to further understand the complexities surrounding the potential use of 2D hAECn models for LAIV/IAV immunobiological and potency assays.

3.3.2. Results

3.3.2.1. Optimising Input MOI for Quantifying MX1 And OAS1 Responses to LAIV/IAV in hAECn Cells

In order to study the differences in innate immune activation between LAIV A/Slovenia/2903/2015 and LAIV A/Bolivia/559/2013, we first ran a pilot experiment to determine the input MOI we will use in further experiments. Using RT-qPCR to quantify *MX1* and *OAS1* expression levels in response to different input MOIs of LAIV A/Slovenia/2903/2015, we show that there is increasing *MX1* (Figure 16A) and *OAS1* (figure 16B) responses that begin to plateau at input MOI 5 copies/cell. There is a strong linear correlation ($R^2 = 0.99$) from input MOIs ranging from 0.01 to 5 copies/cell for both *MX1* and *OAS1* responses (figure 16C and 16D). using these data, we determined that MOI 5.0 copies/cell would be optimal for our assays.

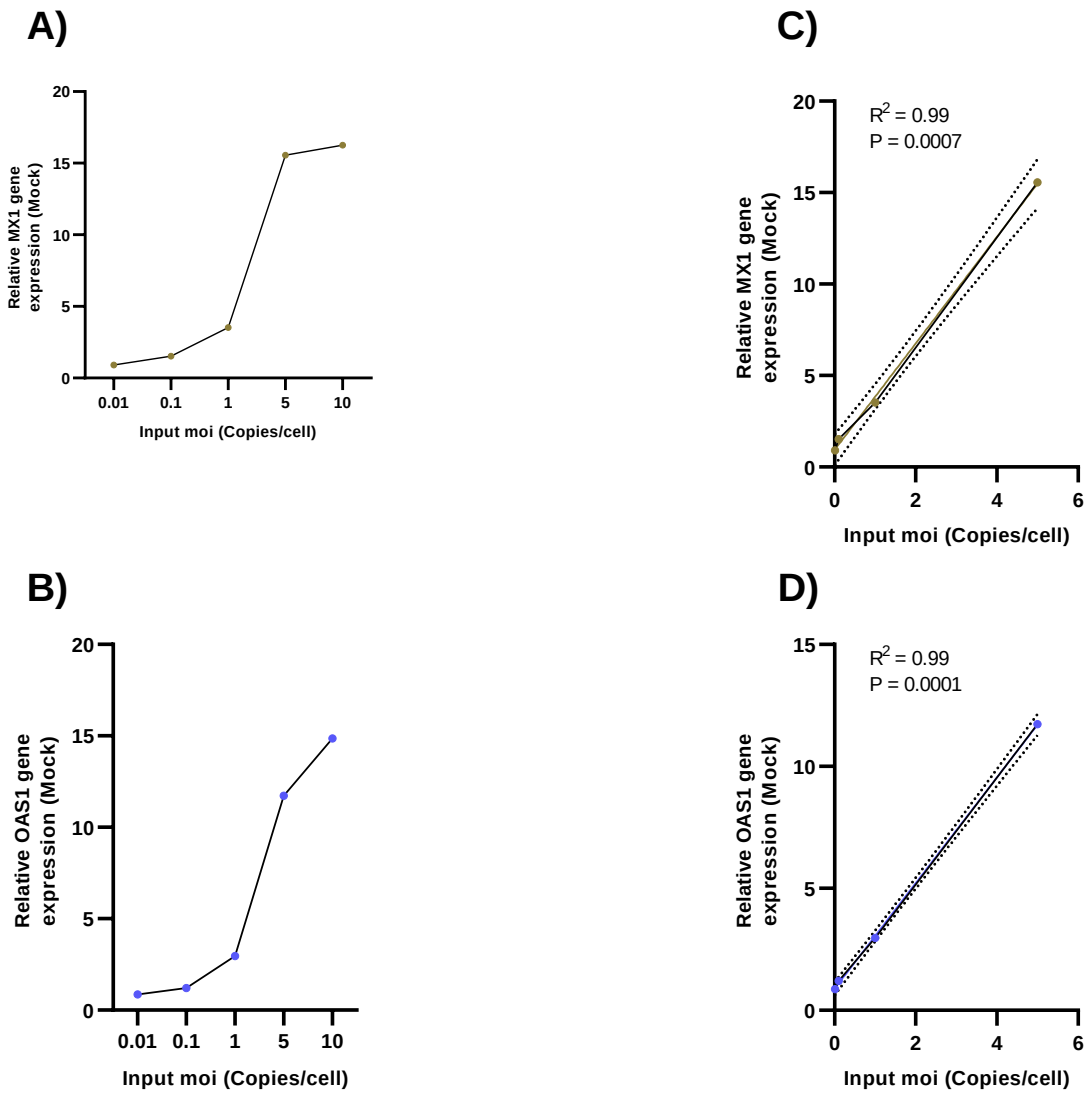

Figure 16. hAECn ISG response to LAIV A/Slovenia/2903/2015 is positively correlated to input viral load. hAECn cells were infected with LAIV A/Slovenia/2903/2015 over a range of MOI 0.01, 0.1, 10, 1, 5 and 10 genome copies/cell (copies/cell based on ddPCR absolute quantification of virions in viral stocks) for 12 hours at 33ºC. RT-qPCR was carried out to quantify the relative expression levels of *MX1* and *OAS1* relative to mock infection. A) Dose-response curve of *MX1* expression. B) Dose-response curve of *OAS1*. C) *MX1* regression analysis. D) *OAS1* regression analysis. Statistical test used: standard linear regression analysis. Results are from a single biological experiment.

3.3.2.2. LAIV A/Slovenia/2903/2015 Induces a Higher MX1 Response in Primary hAECn Cells than LAIV A/Bolivia/559/2013

We used two-step RT-qPCR to quantify ISG (*MX1*) expression of primary hAECn cells of LAIV A/Slovenia/2903/2015, LAIV A/Bolivia/559/2013 and their matched strains. We ran three independent experiments with three independent hAECn donors, D1 (M, 50, Caucasian), D2 (F, 57, African) and D3 (M, 35, Caucasian) in order to discern any donor-dependent phenotypes. For all three donors, we found negligible *MX1* induction from both WT A/Slovenia/2903/2015 and WT A/Bolivia/559/2013. We see a trend across D1, D2 and D3 (Figure 17), showing LAIV A/Slovenia/559/2015 induces a higher *MX1* response than LAIV A/Bolivia/559/2013 (Figure 17), though this was only statistically significant in D1 and D2 ($P = 0.00264$ and $P = 0.0075$ respectively).

When we compared LAIV strains to their matched WT strains, we found that for D1 and D3, LAIV A/Slovenia/2903/2015 induced a higher *MX1* response than WT A/Slovenia/2903/2015 ($P = 0.0423$ and $P = 0.0081$ respectively). For D2 LAIV A/Slovenia/2903/2015 induced higher *MX1* expression than its matched WT strain although this was not statistically significant (Figure 17). LAIV A/Bolivia/559/2013 did not lead to a statistically significant difference in *MX1* expression relative to its matched WT strain in all three donors (D1, D2 and D3) (figure 17). For D1 and D2, LAIV A/Bolivia/559/2013 showed a decrease in *MX1* expression relative to mock (figure 17).

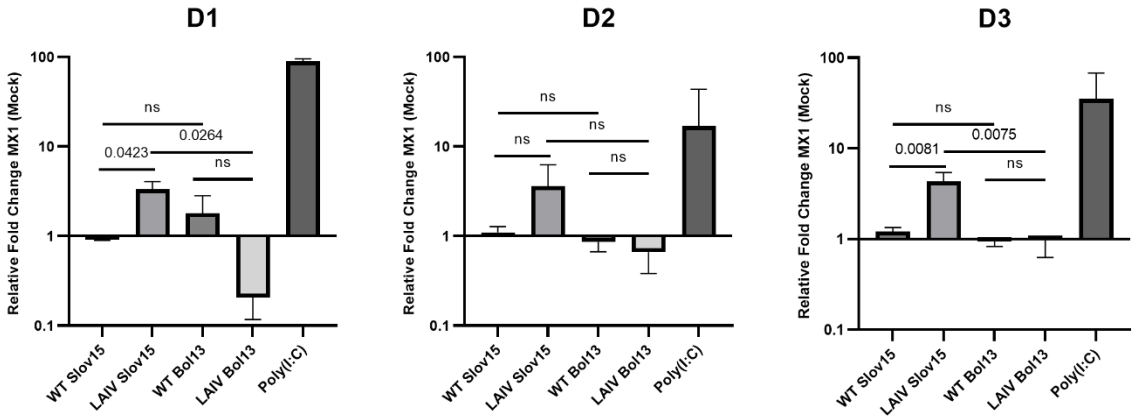

Figure 17. LAIV A/Slovenia/2903/2015 induces a greater *MX1* response than LAIV A/Bolivia/559/2013 in primary hAECn cells. Primary hAECn cells were infected with LAIV A/Slovenia/559/2015, LAIV A/Bolivia/559/2013 and their matched wild-type strains at an MOI of 5.0 copies/cell (based on ddPCR absolute quantification of virions in viral stocks) for 12 hours at 33ºC. A) MX1 expression levels in primary hAECn cells from donor 1 (D1, M, 50 yrs, Caucasian). Results are from 2 biological experiments. B) MX1 expression levels in primary hAECn cells from donor 2 (D2, F, 57 yrs, African). Results are from 3 biological experiments MX1 expression levels in primary hAECn cells from donor 3 (D3, M, 35 yrs, Caucasian). Results are from 3 biological experiments. Statistical test used: unpaired parametric t-test. Histogram bars indicate mean relative *MX1* expression +/- standard deviation.

3.3.2.3. LAIV A/Slovenia/2903/2015 Does Not Induce a Significantly Higher *OAS1* Response in Primary hAECn Cells than LAIV A/Bolivia/559/2013

We next quantified the expression levels of *OAS1*, another ISG well characterised as having anti-IAV properties (Çağlayan and Turan, 2022). For all three donors (D1, D2 and D3), we found there to be no significant difference in *OAS1* expression between LAIV A/Slovenia/2903/2015 and LAIV A/Bolivia/559/2013 (figure 18). Additionally, we found that in all three donors, there was also no statistically significant difference in *OAS1* expression between LAIV and their matched WT strains (figure 18).

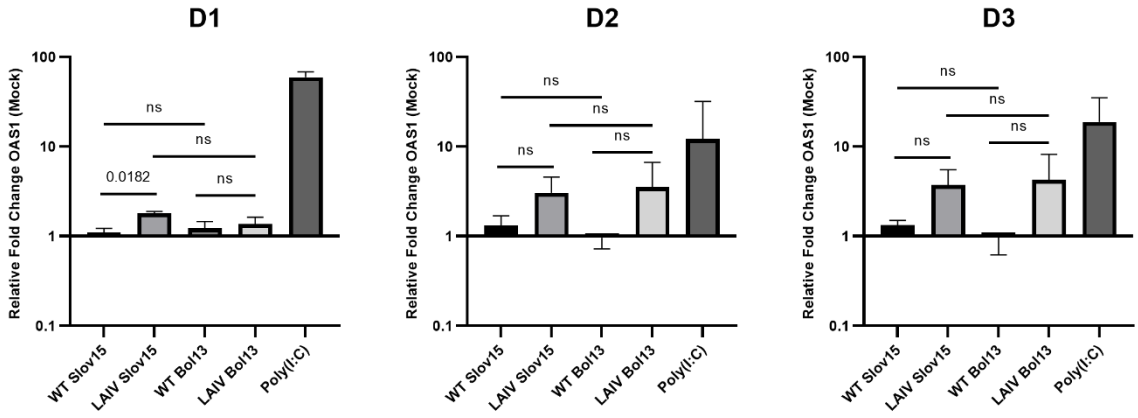

Figure 18. LAIV A/Slovenia/2903/2015 induces a greater *OAS1* response than LAIV A/Bolivia/559/2013 in primary hAECn cells. Primary hAECn cells were infected with LAIV A/Slovenia/559/2015, LAIV A/Bolivia/559/2013 and their matched wild-type strains at an MOI of 5.0 copies/cell (based on ddPCR absolute quantification in viral stocks) for 12 hours at 33ºC. A) OAS1 expression levels in primary hAECn cells from donor 1 (D1, M, 50 yrs, Caucasian). Results are from 2 biological experiments. B) *OAS1* expression levels in primary hAECn cells from donor 2 (D2, F, 57 yrs, African). Results are from 3 biological experiments. *OAS1* expression levels in primary hAECn cells from donor 3 (D3, M, 35 yrs, Caucasian). Results are from 3 biological experiments. Statistical test used: unpaired parametric t-test. Histogram bars indicate mean relative *OAS1* expression +/- standard deviation.

These data shows that *MX1* responses are different between individual LAIV strains. Our data also indicates that there may be differences in innate immune responses to LAIV between individuals. To study this, we next ran concurrent infections of all three donors, including a mixed-donor pool of equal ratios of total cell numbers with LAIV A/Slovenia/559/2015, using RT-qPCR to determine whether ISG (*MX1* and *OAS1*) expression levels vary in a donor dependent manner by RT-qPCR.

3.3.2.4. Pooling Primary hAECn Cells from Multiple Donors Elicits a Response Within the Range Elicited by the Individual Constituent Donors

Having shown a strain dependent ISG (*MX1*) response to LAIV infection (figure 15). We aimed to determine whether hAECn from different donor or a pooled donor cells; would differ in their respective innate immune responses to LAIV A/Slovenia/2903/2015 infection. *MX1* expression levels were significantly lower in hAECn D2 and D3 relative to D1 (P = 0.0211 and P = 0.0197 respectively) (figure 19). Pooled donor cultures showed no significant difference relative to D1, the donor with the highest level of *MX1* expression. *OAS1* expression levels followed similar trends to *MX1*, however there was no significant difference observed between any hAECn donor. Similarly pooled donor culture did not show a significant difference in *OAS1* expression between any individual donor.

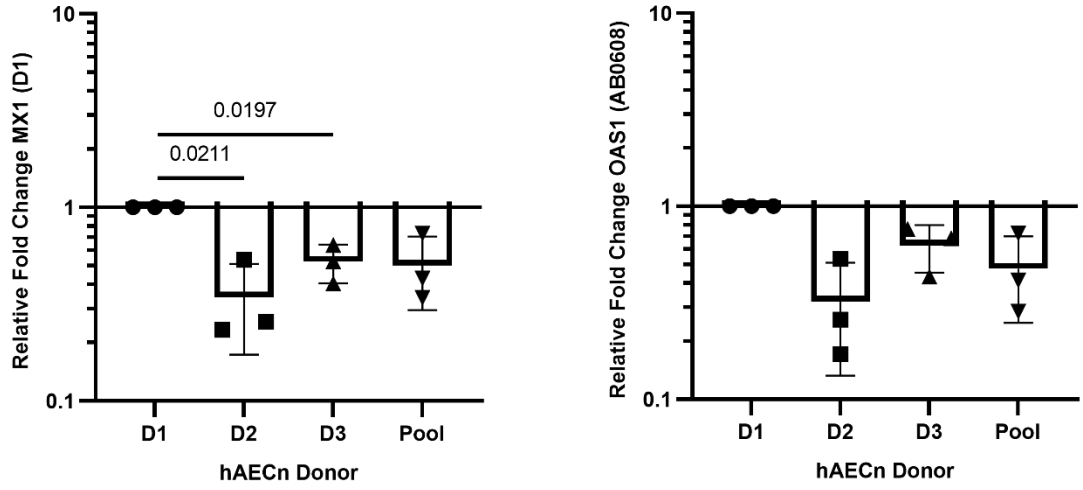

Figure 19. Innate gene expression (*MX1*) levels differ between hAECn cells from different donors. Primary hAECn cells from three distinct donors (D1 – M, 50, Caucasian, D2 – F, 57, African and D3 – M, 35, Caucasian) and pooled donor cells were infected with LAIV A/Slovenia/2903/2015 at MOI 5.0 copies/cell (based on copies/ml determined by ddPCR absolute quantification of viral stocks). Infections were carried out at 33ºC for 12 hours. A) *MX1* expression levels in D1, D2, D3 and pooled normalised to D1 *MX1* expression. B) *OAS1* expression levels in D1, D2, D3 and pooled donor cells. Values are normalised to D1 *MX1* expression. Results are from 3 independent biological experiments. Statistical test used: one-sample t-test. Histograms denote mean relative ISG expression +/- standard deviation. Only significant P values shown.

3.3.3. Conclusions and Next Steps

Our data show that LAIV induces greater induction of ISG (*MX1*) expression than matched wild-type strains (Figure 14). These data are in line with previous findings which have shown LAIV to induce greater innate immune activation than WT IAV (Fischer et al., 2014). Our studies were carried out at 33ºC in line with the replication conditions conferred on LAIV as a result of the attenuated Ann Arbor backbone (Jin et al., 2003, Hoffmann et al., 2005). IAV replication is optimal at 37ºC, with studies showing that the viral polymerase subunit PA shows distinct temperature sensitivity, specifically leading to reduced viral growth at 33ºC relative to 37ºC (Martínez-Sobrido et al., 2018). Additional to this, differences in ISG activation between LAIV and WT strains may be due to the difference in NS1 between WT strains and the Ann Arbor strains incorporated in to LAIV. Influenza virus NS1 is a well know immune antagonist. NS1 has a number of mechanisms to modulate host innate immune responses, including the inhibition of the PRR RIG-I through direct sequestering (Mibayashi et al., 2007), or interaction with TRIM25 to prevent ubiquitination and subsequent downstream signalling (Gack et al., 2009). Other examples of NS1 mechanisms of innate immune gene modulation include suppression of the inflammasome by direct inhibition of NLRP3, preventing the formation of NLRP3-ASC speck formation and subsequent production of IL-1β and the inflammasome response (Moriyama et al., 2016). Other methods by which NS1 modulates innate immune responses are reviewed by Nogales A, et. al. 2018 (Nogales et al., 2018). The comparatively low levels of *MX1* expression in LAIV A/Bolivia/559/2013 (figure 17) suggest that Ann Arbor NS1 is not significantly less immunomodulatory compared to WT NS1. It seems more likely that the low ISG expression levels in WT IAV compared to LAIV is due to the low 33ºC conditions of this assay. A counter hypothesis to this is that the reduced replication of WT strains at 33ºC relative to LAIV may lead to reduced levels of DVGs that are known to induce innate immune responses (Penn et al., 2022).

Our data shows a comparable trend in all three hAECn donors of differential *MX1* expression between LAIV A/Slovenia/2903/2015 and LAIV A/Bolivia/559/2013 (Figure 17). We show that LAIV A/Slovenia/2903/2015 induces greater *MX1* expression, although this was statistically significant in only in D3. We see variability in *MX1* expression between experimental replicates which we hypothesise is a result of external stresses placed on the cells from the cytology process, such as differences in cellular confluences between replicates. Greater number of replicates may narrow the standard deviations and show statistical significance to the trend we see.

With LAIV A/Bolivia/559/2013 showing reduced VE relative to LAIV A/Slovenia/2903/2015 within the human population in some previous seasons (Caspard et al., 2017), studies have been undertaken to understand the root cause(s). Dibben et al. (2021), reported that LAIV A/Bolivia/559/2013 had reduced replicative fitness than LAIV A/Slovenia/2903/2015 in airway epithelial cells (Dibben et al., 2021). Innate immunity to IAV infection is dependent on viral replication (Mifsud et al., 2021), we hypothesise that the lower replication rates of A/Bolivia/559/2013 seen by Dibben et al. (2021), may lead to reduced ISG (*MX1*) induction seen in our study (Figure 17). Together, these data suggest that not all LAIV strains are able to induce a comparative innate immune response. With LAIV being delivered in a quadrivalent formulation, we hypothesise that a strong innate response to a single LAIV strain may lead to viral clearance of all strains, preventing downstream activation of specific adaptive immune responses.

Interestingly, when looking at *OAS1* expression levels between LAIV A/Slovenia/2903/2015 and LAIV A/Bolivia/559/2013, there was no significant difference in expression levels. These data suggest that either 1) MX1 is an outlier and not representative of the ISGome response to differential LAIV strains, or 2) differential responses to LAIV infection are specific to certain ISGs. To answer these questions, bulk RNA sequencing would be required to quantify whole gene expression levels in hAECn cells infected with LAIV A/Slovenia/2903/2015 and LAIV A/Bolivia/559/2013. Our data provides a basis for such experimentation.

As well as a strain-dependent innate immune response, our data suggests that there is a donor-dependent response to LAIV (Figure 19). We show that when infected with LAIV A/Slovenia/2903/2015, there is a significant difference in *MX1* expression levels between hAECn from 3 donors (Figure 19A). We show a similar trend is true of *OAS1*, although this was not statistically significant (Figure 19B). This variance is considered in the development and manufacture of LAIV, whereby pooled-donor 3D-differentiated nasal epithelial cells are used to determine LAIV strain potency. The pooling of donors is used in an effort to obtain a cell culture system simulating a population, leading to averaged responses. We tested this by comparing innate immune activation between a pooled-donor culture and individual constituent donors. Figure 19 shows that for both *MX1* and *OAS1*, there is no significant difference in gene expression between pooled-donor cells and individual donor cells, confirming that pooling of cells leads to a response within the range of constituent donors.

Having shown data that suggests there may be a donor-dependent response to LAIV A/Slovenia/2903/2015 (Figure 19) we would recommend a bulk RNA-sequencing experimentation with a wider pool of donors in order to assess the relative expression levels of total ISGs in response to LAIV. Collectively with our findings from Chapter 3.1, show the complexities involved in producing a 2D human nasal airway cell model system for the medium-throughput assays involved in LAIV/IAV. A 2D immortalised nasal cell culture system would provide a cell culture model system that would be more cost-effective than established 3D-differentiated cells. However, immortalisation is challenging due to cell population heterogeneity and fibroblast outgrowth, and the requirement for epithelial cell sorting in a manner conducive to cell survival. Here in Chapter 3.3, we show preliminary data that suggests there may be differences in host cell responses to LAIV between nasal epithelial cell donors would also need to be considered when using primary human nasal cells in a 2D culture for the study of LAIV/IAV. Particularly, whether or not pooled donor cultures are the optimal system to gain an average response of all incorporated donors, or whether this would mask host cell responses of particular individuals that may represent significant phenotypes present in the population.

Collectively, these data suggest that there is both a strain dependent (figure 17) and a donor dependent (figure 19) innate immune response phenotype to LAIV infection. We hypothesise that variations in donor response to vaccination may be dependent on donor dependent responses to infection and/or particular demographics and corresponding constituent levels of immune gene expression that may influence the initiation of LAIV infection required to induce a type I IFN response to infection. In order to study this, we investigated open-access transcriptomic data to understand the effect of sex and age on the relative constitutive expression of lung ISGs.

In order to begin to understand how the genetic heterogeneity of individuals may influence LAIV VE within the population, we next aimed to understand how lung ISG constitutive expression is affected by both sex and age. Using open access data for the Human Protein Atlas/GTEX study, we will begin to elucidate natural variance in innate immune gene expression that has been shown to influence the initiation and outcome of IAV infection (Charman et al., 2021).

3.4. Constitutive Levels of Lung ISG Expression are Affected by Sex and Age

3.4.1. Introduction

Our original aim was to understand the feasibility of using immortalised primary nasal epithelial cells as a replacement for MDCK cells in LAIV/IAV medium-throughput assays that utilise 2D cell culture systems e.g., FFU and TCID50 assays to characterise vaccine strain replication efficiency. We have shown in chapter 3 and 5 that human airway cells are more restrictive to IAV in both multi- and single-cycle infection assays relative to MDCK cells. We show this restriction is not a result of viral attachment and entry efficiencies, and we suggest that this restriction is likely a result of intrinsic or innate host cell immune responses to infection. Our data suggest that innate immune activation (particularly *MX1*) differs between donors. To begin to elucidate if this donor-dependent effect could relate to intrinsic differences in the basal levels of constitutive ISG expression on a population level. We hypothesised that the host specific levels of constitutive ISG expression may account for the variance in VE observed in the human population.

Constitutive expression of ISGs (e.g., *TRIM22*) in human airway-derived cells have been previously shown to be a determinant of IAV infection outcomes independent of the induction of IFN-mediated innate immune defences (Charman et al., 2021). Utilising open access transcriptomic data (https://gtexportal.org/home/), this study identified lung airway to be enriched for constitutive ISG expression relative to other non-mucosal tissues (Charman et al., 2021) . These data show the potential importance of pre-existing levels of ISGs. We will expand this to understand how the constitutive expression of several ISGs in the lung varies amongst individuals.

In Chapter 3.4, we aim to understand the variation in host-cell constitutive lung ISG expression levels in the population. Our *in vitro* studies utilise cells from 3 independent donors. This is underpowered, making drawing conclusions and inferences on population variance difficult. To begin to understand how individuals differ in their innate immune responses, we utilise open access data from the GTEx Portal/Human Protein Atlas (Pontén et al., 2008, Carithers et al., 2015). The Human Protein Atlas is a program that began in 2003, using several omics approaches to map human proteins in cells, tissues, and organs. Using transcriptomics data from 578 individuals, we isolated expression data as normalised transcripts per million (nTPM) for 100 ISGs present in the lung. nTPM denotes estimated gene expression for each gene, normalisation steps have been undertaken to take in to account non-coding transcripts. Additional normalisation steps were undertaken enable between-sample mean comparisons (trimmed mean of M values methodology) (Robinson and Oshlack, 2010)

We obtained a list of ISGs that were upregulated ≥ $1.5\log_2$ in the presence of interferon from Shaw et al. 2017 (Shaw et al., 2017). We identified the top 100 most differentially expressed ISGs. Using these, we aimed to elucidate their levels of constitutive expression in the lung and how sex and age may impact upon their relative expression levels by categorising samples by demographics (sex and age).

3.4.2. Results

3.4.2.1. Breakdown of Sample Demographics in GTEX Portal Transcriptomic Study

We used GTEX portal transcriptomic data available through the GTEx-Portal/Human Protein Atlas (Pontén et al., 2008, Carithers et al., 2015) (proteinatlas.org). We chose to focus on transcriptome analysis of the lung tissue to elucidate differences in basal state of the physiological environment associated with respiratory disease. Ideally, we would use upper respiratory/nasal tract samples as the majority of influenza virus infection is limited to the mid/upper respiratory tract, with LAIV particularly being limited to these areas, however these data are unavailable with the GTEX Portal study.

The data set had a sample size totalling 578 donors. Figure 20 shows the sample number breakdowns in each demographic category available (sex and age). The dataset encompasses 183 females and 395 males (figure 20A). By age, the data set had at 20-29, 13 females and 20 males. For 30-39 the dataset had 10 females and 30 males. For 40-49 the dataset had 33 Females and 60 males. At 50-59 the dataset had 55 females and 145 males. At 60-69 the dataset had 68 females and 122 Males. 70-79 the dataset has 4 females and 18 males. In the age group of 70-79 there were very only 4 females (figure 20B). This was underpowered relative to the other age cohorts, therefore we grouped the final two age cohorts of 60-69 and 70-79 to create a combined group of 60–79-year-olds. This gave a dataset of 72 females and 140 males at 60-79 years old (figure 20C).

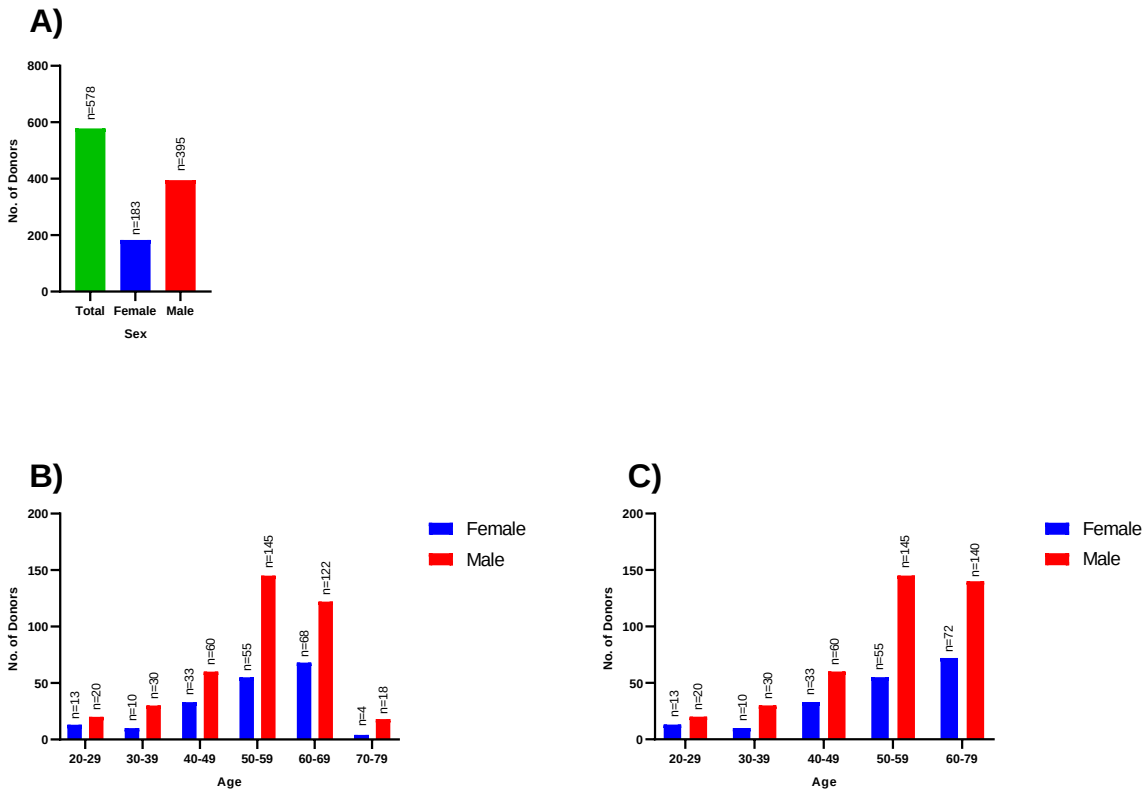

Figure 20. Breakdown of Transcriptome Sampling in GTEX Study by Sex and Age. A) Breakdown of lung GTEx transcriptome dataset by sex. B) Breakdown of lung GTEx transcriptome dataset by sex and age. C) Breakdown of lung GTEx transcriptome dataset by sex and age used for data sampling.

3.4.2.2. Constitutive expression of lung MX1 is not affected by age but shows a significant decrease in males between the ages of 40-49 and 50-59.

In Chapter 3.3 we present data suggesting that *MX1 and OAS1* expression may be different between donors in response to LAIV A/Slovenia/2903/2015 infection, though this trend was only statistically significant with *MX1*. To expand our understanding of where this potential donor-dependent differential expression comes from, we will elucidate whether *MX1* and *OAS1* constitutive expression levels differ between females and males, and whether these ISGs are significantly differentially expressed between age groups.

MX1 constitutive expression levels in the lung are not significantly different (P = 0.2548) between females and males (figure 21A). Equally when we combine expression levels (nTPM) of females and males for each age cohort, using multiple-comparison ANOVA, we found no instance of differential *MX1* expression between any age cohort (figure 21B). We next split the age cohorts into females and males and ran multiple comparison ANOVA testing to understand whether age may be a factor for a particular sex. Figure 21C indicates no significant effect of age on the constitutive expression levels of *MX1* in females (P = 0.8435). Although in females, there was no significant effect of age on constitutive expression of *MX1* (P = 0.8435), for males, there was a single instance of statistically significant change in *MX1* expression, between the age cohorts 40-49 and 50-59 (P = 0.0102) (figure 21D).

Having shown that *MX1* constitutive expression is comparable between females and males and increasing age (except for males between 40-49 and 50-59), we next used the above pipeline to determine the effect of sex and age on the constitutive expression levels of *OAS1* in the lung.

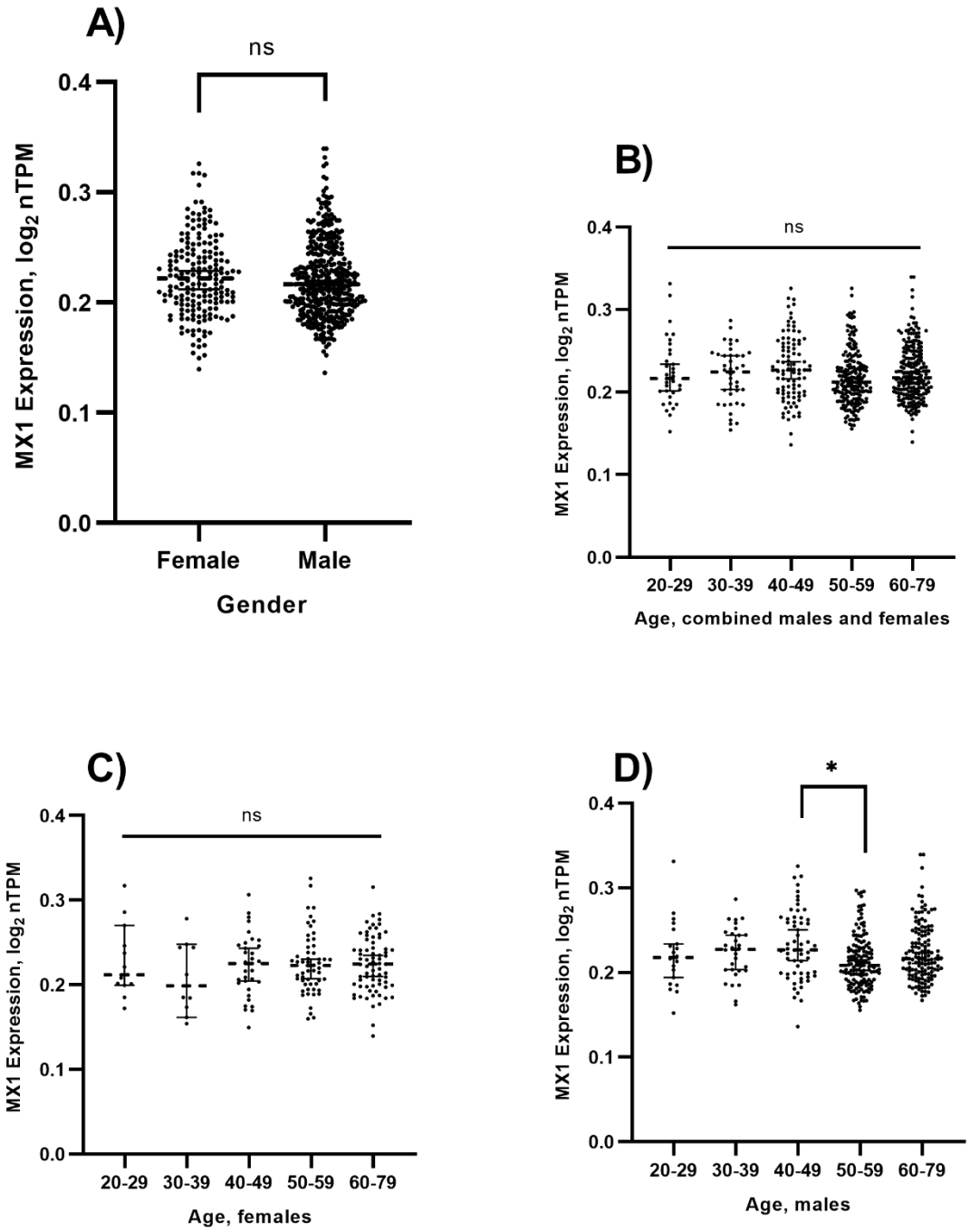

Figure 21. *MX1* constitutive expression in the lung is not dependent on sex or age. A) Effect of sex on *MX1* constitutive expression in the lung. Statistical test used: Two-tailed Mann-Whitney. B) Effect of age on constitutive expression of *MX1* in the lung. nTPMs for females and males were combined for each age cohort. C) Effect of age on constitutive expression of MX1 in the lung of females. D) Effect of age on constitutive expression of *MX1* in the lung of males. (B-D) one-way ANOVA Kruskal-Wallis multiple comparison test shown.

3.4.2.3. Constitutive expression of lung OAS1 is not affected by age but shows a significant change in males between the ages of 40-49 and 60-79

Like *MX1*, *OAS1* showed no statistically different levels of constitutive expression in the lung between females and males (P = 0.6913) (figure 22A). When female and male nTPM values were combined for each age cohort, only a single point of statistical significance was observed, between 50-59 and 60-79 (P = 0.0037) (figure 22B). Again, as with *MX1*, *OAS1* does not alter significantly in response to changing age between any age cohort (figure 22C). Males, however, show an age-dependent effect on constitutive expression. Between cohorts 40-49 and 50-59, there was a significant decrease in expression levels (P = 0.0013), conversely, between cohorts 50-59 and 60-79, there is a significant increase in *OAS1* constitutive expression (P = 0.0013) (figure 22D).

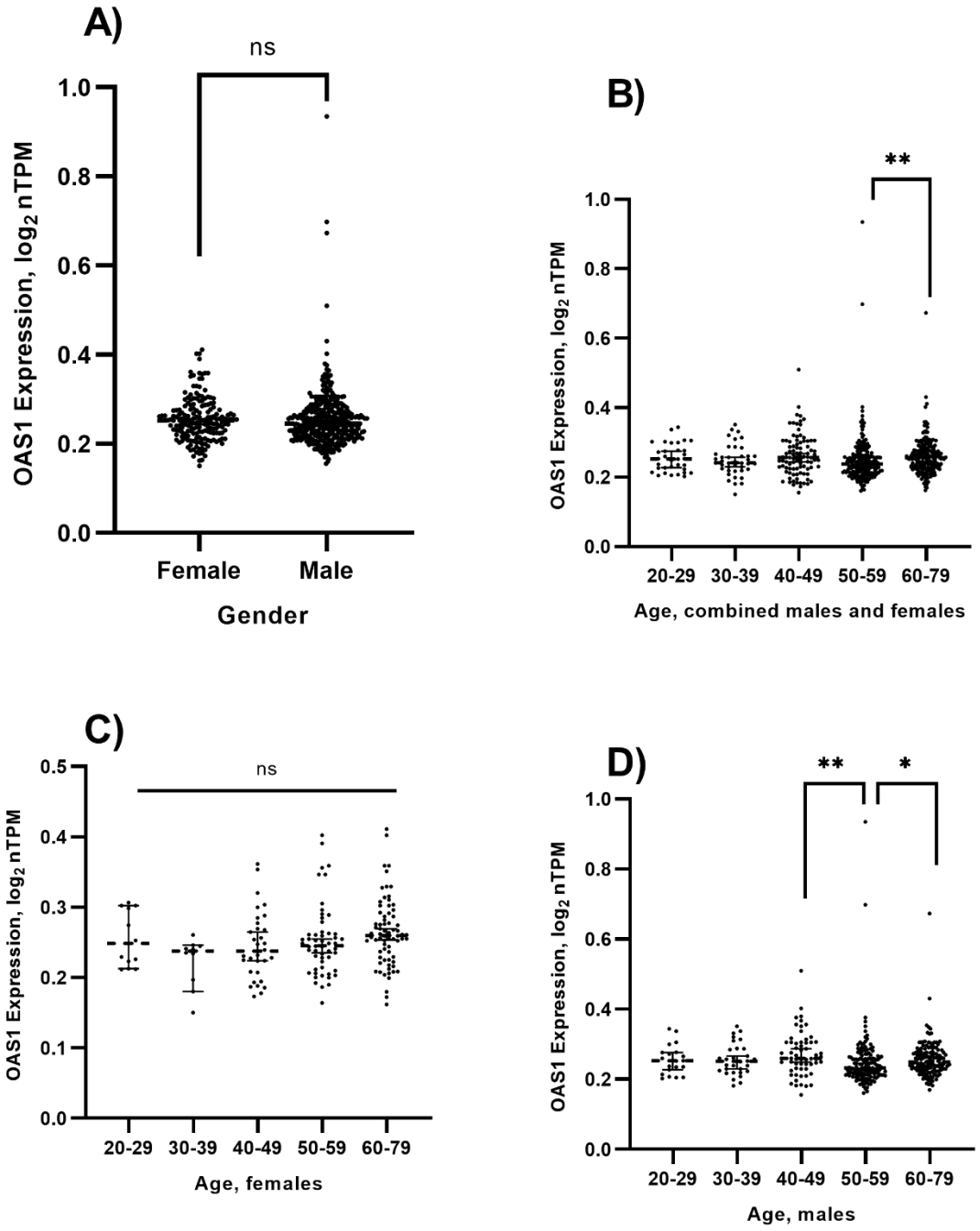

Figure 22. *OAS1* constitutive expression in the lung is not dependent on sex. A) Effect of sex on *OAS1* constitutive expression in the lung. Statistical test used: Two-tailed Mann-Whitney. B) Effect of age on constitutive expression of OAS1 in the lung. nTPMs for females and males were combined for each age cohort and multiple comparison ANOVA test conducted. C) Effect of age on constitutive expression of OAS1 in the lung of females. D) Effect of age on constitutive expression of *OAS1* in the lung of males. (B-D) one-way ANOVA Kruskal-Wallis multiple comparison test shown.

3.4.2.4. Of 100 lung ISGs tested, none show significant difference in baseline expression between females and males

To determine the differences in the constitutive expression of lung innate immune gene expression within the wider population, we selected 100 ISGs showing the greatest level of expression in response to interferon challenge in homo sapiens from a study by Shaw et al. 2017 (Shaw et al., 2017). Using these genes, we obtained constitutive expression levels (nTPM) in lung samples from GTEX Portal/Human Protein Atlas. The Human Protein Atlas was a Swedish study conducted in 2003 that used various technologies to map the proteomic, genomic, and transcriptomic data of a vast array of human tissues . We used the normalised transcripts per million (nTPM) provided by GTEX with no additional normalisation steps conducted to avoid potential bias based on the normalisation procedure. We used the Bonferroni multiple test correction to account for the high number of statistical tests undertaken (100).

We first determined any differences in constitutive level of lung ISGs between females and males. Figure 23A shows that there is no significant difference between females and males in expression levels of combined 100 lung ISGs. We next aimed to determine whether individual ISGs are differentially expressed between females and males. Of the 100 lung ISGs analysed, 7 were trended towards a difference, but showed no statistical significance regarding differential expression between females and males. Of these, promyelocytic leukaemia protein (*PML*) was the most differentially expressed (P = 0.0132), followed by Desmin (*DES*) and GTP-Binding Protein 2 (*GTPBP2*) (P = 0.0183, P = 0.0186 respectively). Opioid Growth Factor Receptor (*OGFR*), Patellin 1 (*PATL1*) showed similarly significant differences in constitutive expression between females and males (P = 0.044 and 0.045 respectively). Jagged Canonical Notch Ligand 1 (*JAG1*) and Solute Carrier Family 25 Member 28 (*SLC25A28*) were also differentially expressed between females and males (P = 0.046 and P = 0.047 respectively).

We next determined whether the lung ISGs that showed significant difference in expression level between females and males, were expressed to a higher level in either sex or whether this was a consistent phenotype between the ISGs. Of the 7 genes that showed the highest difference in expression level between females and males (figure 23B), all 7 showed that there was a trend to a higher level of expression in males than in females (figure 23C). PML showed the greatest degree of significance (P = 0.0312) with *SLC25A28* showing the least significant difference in expression level (P = 0.0465). Table 12 summarises known function of these 7 genes.

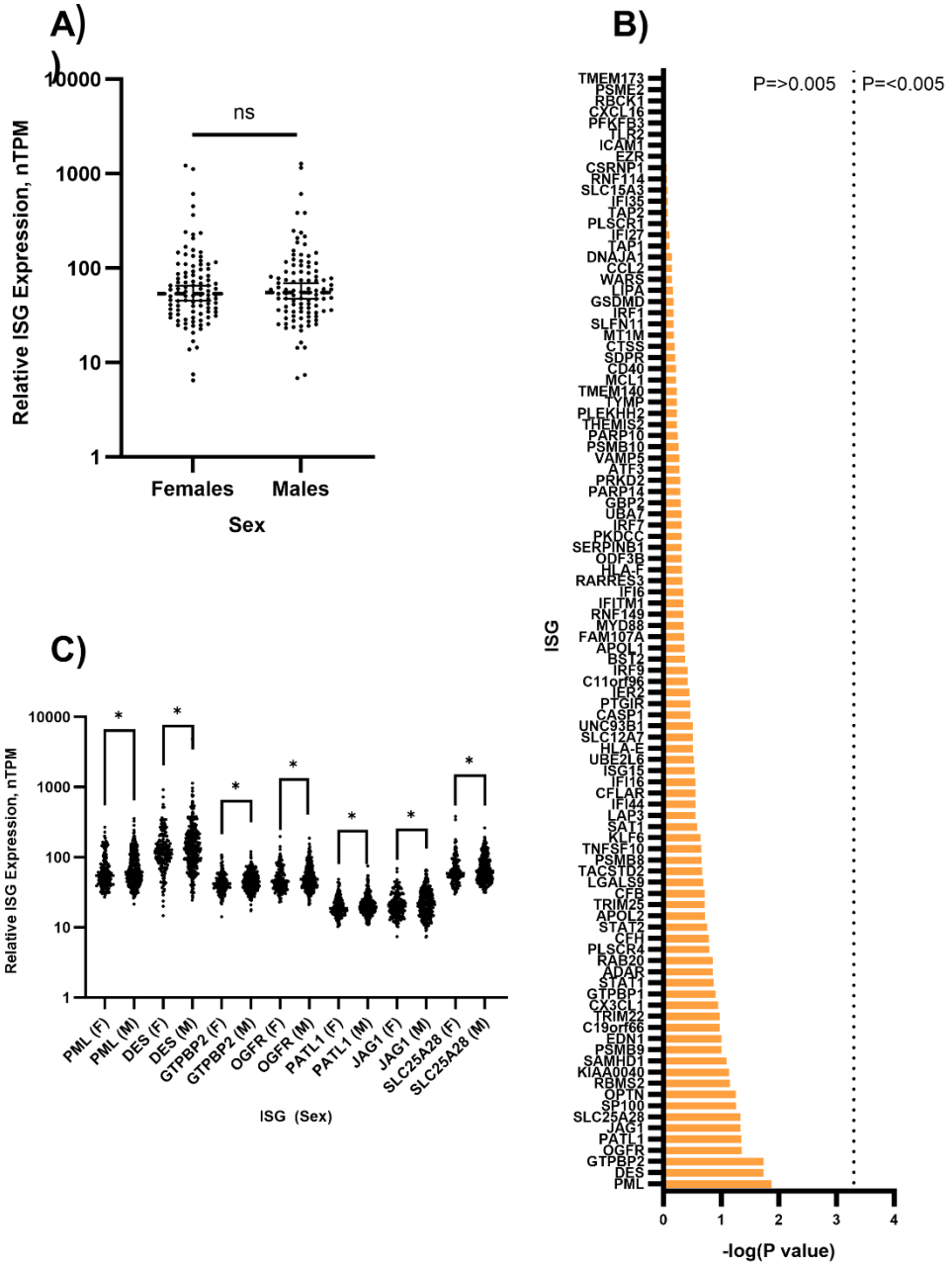

Figure 23. 0 out of 100 lung ISGs show a significant difference in constitutive expression levels between females and males. Constitutive expression profile of 100 ISGs (Shaw et al., 2017) in lung tissue. Data derived from GTEX Portal (Pontén et al., 2008) A) Constitutive expression profile (nTPM) of 100 ISGs characterised by sex. Statistical test used: two-tailed, unpaired Mann Whitney-U. B) Constitutive expression level of individual lung ISGs between females and males. Histogram bars indicate P value for each ISG. Dotted line indicates P value significance threshold of 0.05. C) Lung ISGs showing significant difference in expression level between females and males (identified in B). Histograms denote median nTPM +/- 95% CI. two-tailed, Mann-Whitney statistical test. N = 183 females and 395 males. Bonferroni multiple test undertaken to get a new P value of 0.005 for significance threshold.

Table 12. Details of Lung ISGs that Show Significant Differential Expression Between Females and Males

Lung ISG Abbreviation	Lung ISG Name	Function	Reference(s)
PML	Promyelocytic leukaemia protein	Cell cycle regulation, survival, and apoptosis and immune regulation	(Guan and Kao, 2015)
DES	Desmin	Skeletal muscle homeostasis	(Agnetti et al., 2022, Paulin and Li, 2004)
GTPBP2	GTP-binding protein 2	mRNA surveillance and ribosome-associated quality control, exosomal degradation of mRNAs	(Zinoviev et al., 2018)
OGFR	Opioid growth factor	Inhibition of cell proliferation, tissue organization	(Cheng et al., 2009)
PATL1	N/A	Modulates mRNA translation and degradation	(Scheller et al., 2007)
JAG1	Jagged 1	Regulation of cell fate specification	(Reynolds et al., 2022)
SLC25A28	Solute carrier family 25-member 28	Ferroptosis/Apoptosis	(Zhang et al., 2020)

3.4.2.5. 32 of 100 of Lung ISGs Studies Show Significant Changes in Constitutive expression as a Result of Changing Age

Having shown in figure 18 that there is no significant difference in constitutive expression levels of the combined expression levels of the 100 ISGs chosen for this study between females and males, and that of the 100 genes tested, none were found to have statistically significant differential expression between males and females. We next investigated whether age influenced the constitutive levels of ISG expression in the lung.

Our data show that 32 out of the 100 lung ISGs studied show some significant effect of age on expression levels (figure 24A). To determine whether there are differences in ISG expression levels between females and males at each age cohort for all 100 ISGs combined, we separated our samples based on sex and age and ran Mann-Whitney statistical testing between the sexes for each age cohort. For every age cohort, we show that there is no significant difference in the expression levels of ISGs (figure 24B).

Having shown that 32 out of 100 lung ISGs have statistically significant differential expression between age cohorts, we next aim to understand whether this trend is equal for both females and males. We aim to understand which of these age-dependent differentially expressed ISGs are common to both sexes, and which are unique to each.

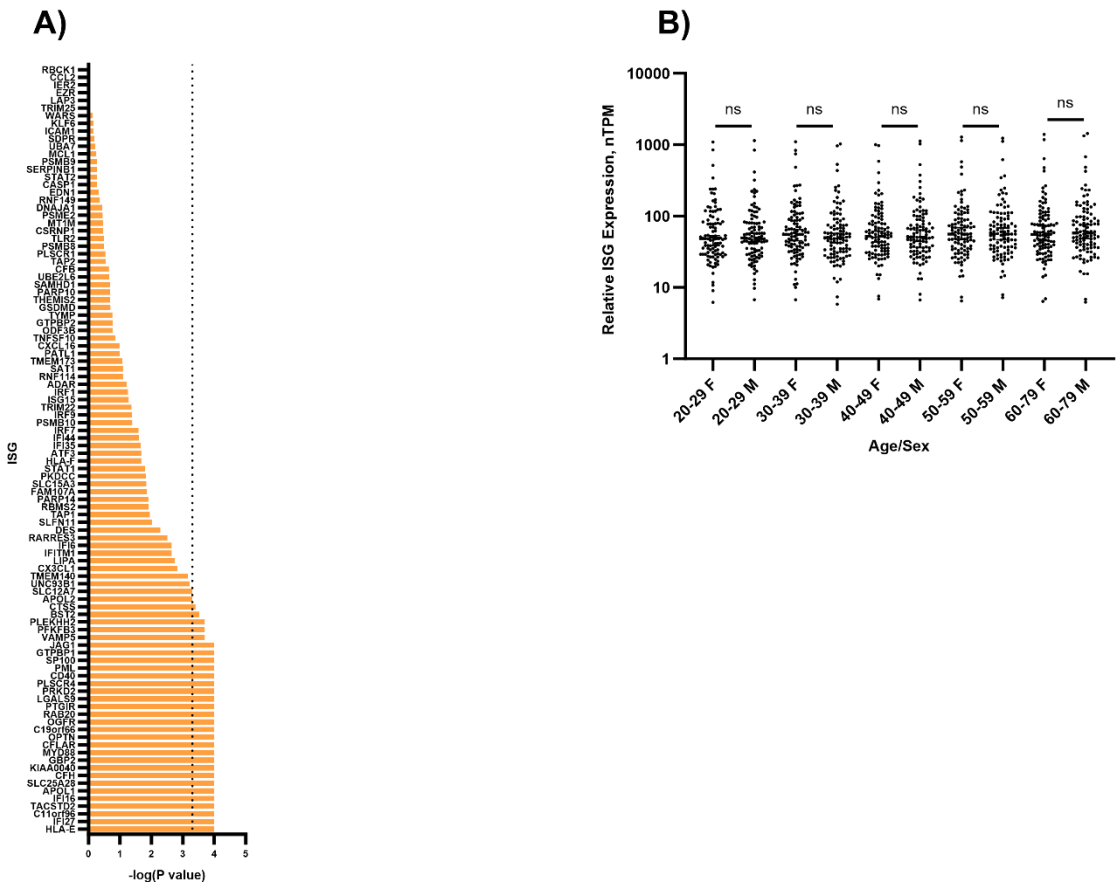

Figure 24. 32% of Lung ISGs constitutive expression is significantly affected by changing age. A) 32% of lung ISGs show significant change in constitutive expression because of changing age. nTPM values for each lung ISG were collected and sorted based on age (combined female and male samples). Histogram bars indicate P value for each ISG derived from unpaired multiple comparison Kruskal-Wallis ANOVA. Dotted line indicates significant threshold of P = 0.05. B) within each age group, there is no significant difference in ISG constitutive expression in the lung. Test used: unpaired Mann Whitney-U. Data shown as median nTPM +/- 95% CI.

3.4.2.6. Age-Associated Changes in Constitutive lung ISG Expression are Present in Both Females and Males

Having shown that 56% of ISGs studied showed differential expression because of changing age, we next wanted to understand whether females and males exhibit equal or different differential expression as it relates to age. To do this we separated our samples by sex and ran multiple comparison ANOVA (Kruskal-Wallis) for each ISG across all age cohorts. We used the Bonferroni test to correct the P value threshold of significance to account for the high number of statistical tests performed (100)

Of the 100 ISGs studied, 1 out of 100 were differentially expressed because of age in females (figure 25A). Compliment factor H *(CFH)* was the only significantly differentially expressed in both sexes (P = <0.0001).

In males, a total of 24 out of 100 ISGs were differentially expressed (figure 25B), 20 lung ISGs were highly significant (P = < 0.0001): *RAB20, CD40, TMEM140, HLA-E, IFI27, BST2, C11orf96, PML, GTPBP1, OPTN, PLSCR4, C19orf66, GBP2, JAG1, PRKD2, PTGIR, SP100, OGFR, SLC25A28* and *CFH* (figure 25B). Where females had 2 lung ISGs uniquely differentially expressed, males had 43 lung ISGs that were significantly differentially expressed in males because of age that aren't in females (figure 25C).

Thus far we have shown there to be sex-dependent effects of age on constitutive expression of several ISGs in the lung. We have not yet shown how these changes occur. Next, we will look at two examples of ISGs that show a significant change in expression level over time (*CFH* and *JAG1*) and one that shows no significant expression (*TRIM25*).

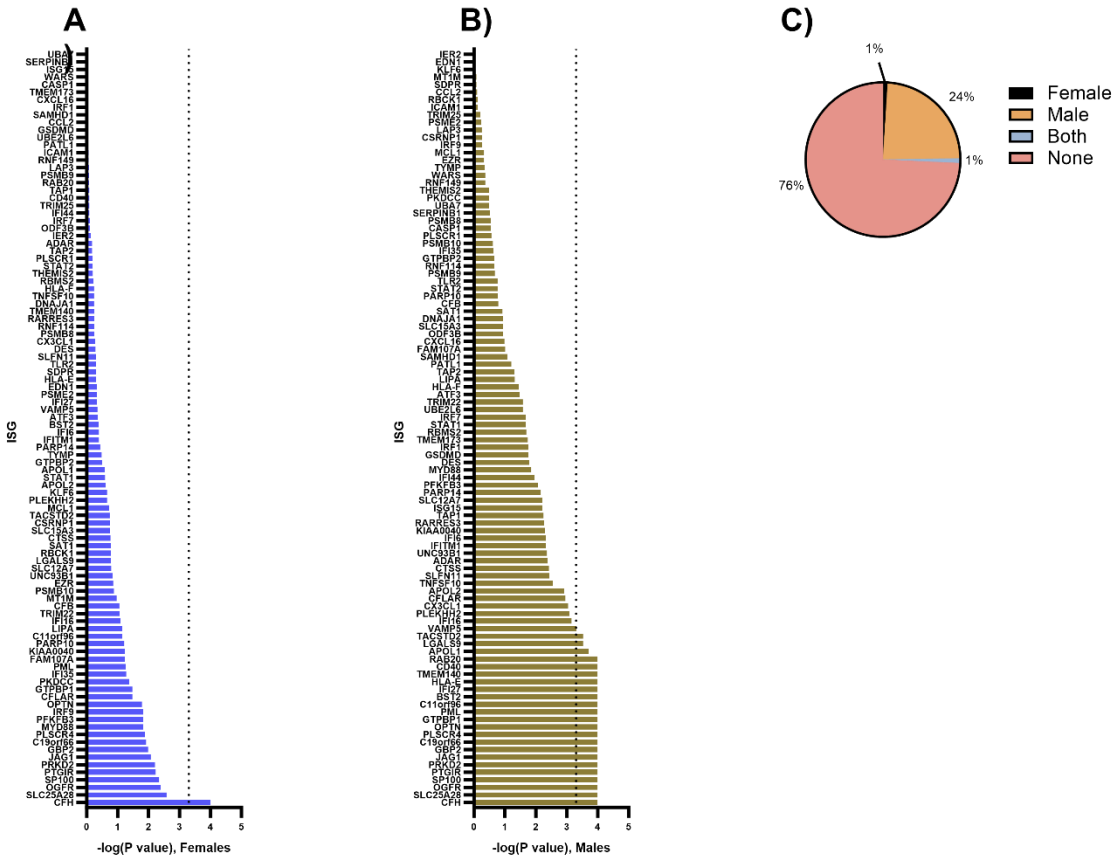

Figure 25. Identification of sex-dependent effects of age on constitutive levels of lung ISG expression. nTPMs of 100 lung ISGs where categorised by sex and age. Multiple-comparison ANOVA (Kruskal-Wallis) analysis was carried out for each ISG in both females and males to determine any significant effect of age on ISG constitutive expression levels. A) Significance testing of 100 lung ISGs constitutive expression between age groups in females. B) Significance testing of 100 lung ISGs constitutive expression between age groups in males. C) proportion of ISGs showing significant differences in constitutive expression because of age in females only, males only, both females and males, or ISGs showing no significant change in expression levels. Statistical test used: multiple-comparison Kruskal-Wallis.

3.4.2.7. CFH and JAG1 show a sex-dependent effect of age on constitutive expression in the lung

We chose two ISGs (*CFH* and *JAG1*) that were determined to have an age-dependent effect on ISG expression in both females and males (*CFH*) and males only (*JAG1*) as well as an ISG (*TRIM25*) that showed no statistically significant effect of age on ISG expression levels (figure 25) to expand and elucidate where exactly these changes in expression level occur.

Figure 25 showed expanded results for these genes, looking at expression levels between age cohorts of combined female and male expression levels, as well as females and males individually. All ISG expression levels were compared using multiple comparison Kruskal-Wallis ANOVA testing. *CFH* was shown to have a high level of differential expression between age cohorts for combined sex samples, (figure 26A), Age cohorts 50-59 and 60-79 had significantly less expression ($P = 0.0015$ and $P = <0.0001$, respectively). Expression levels significantly reduced between 30-39 to 60-79 ($P = 0.0004$). Similarly, a significant drop in expression levels was seen between ages 40-49 to 60-79 and 50-59 to 60-49 cohorts ($P = 0.0004$ and $P = 0.0026$, respectively). For *CFH* expression in females (figure 26B), there was a significant reduction in expression levels between the ages of 20-29 to 50-59 and 20-29 and 60-79 ($P = 0.00138$ and $P = 0.0004$, respectively). A significant reduction in expression levels was also seen between the ages of 30-39 to 40-49 ($P = 0.0327$). When looking at *CFH* expression levels in males (figure 26C), there was significant reduction in expression levels between the ages of 20-29 and 60-79 ($P = 0.0004$), as well as between the ages of 30-39 to 60-79 and 40-40 to 60-79 ($P = 0.0181$ and $P = 0.0172$, respectively). Finally, we saw a reduction in *CFH* expression in males between the ages of 50-59 and 60-79 ($P = 0.0044$).

JAG1 age-dependent expression levels in combined females and males (figure 26D) showed a similar trend as seen with *CFH*. There was a reduction in expression levels between the ages 20-29 to 60-79 and 30-39 and 60-79 ($P = 0.0002$ and $P = <0.0001$, respectively). JAG1 expression levels at ages 60-79 were similarly lower than ages 40-49 ($P = <0.0001$) and 50-59 ($P = 0.0075$). *JAG1* expression levels in females (figure 26E) showed a reduction in expression levels between the ages 30-39 and 60-79 ($P = 0.0397$). For *JAG1* expression in males (figure 26F), there were significant reduction in expression levels between the ages 20-29 and 50-59, as well as between 20-29 and 60-79 ($P = 0.0291$ and 0.0001, respectively). Lower expression levels of *JAG1* were seen in the age group 60-79 compared to 30-39, 40-49 and 50-59 ($P = 0.0014$, $P = 0.0025$ and $P = 0.0400$, respectively).

TRIM25 showed no significant difference in expression levels between any age cohorts when female and male expression levels were combined (Figure 26G). Similarly, no statistically significant change in expression levels were seen in females (figure 26H) and males (figure 26I).

To ensure that the differential expression level of certain lung ISGs identified in figures 23-25 are a result of gene-specific expression and not whole genome variation between sexes and over time, we will next select 2 commonly used reference genes in transcriptomic studies. We will compare the nTPM of these genes between females and males, and over time in both combined female and male samples, as well as female and male samples separately.

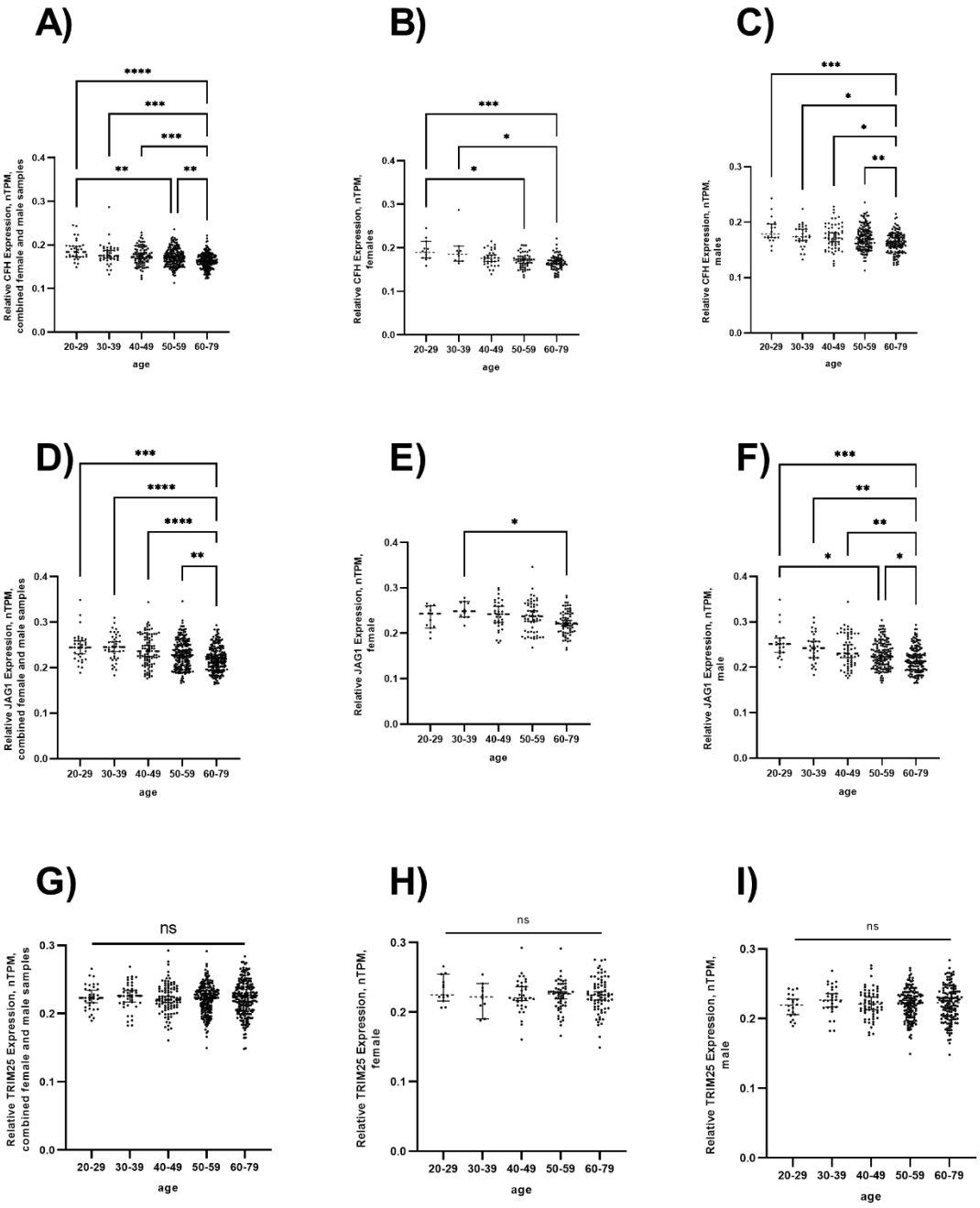

Figure 26. *CFH* and *JAG1* but not *TRIM25* are differentially expressed in response to changing age and sex. A) Combined female and male cohorts comparing *CFH* expression levels (nTPM) between sample groups. B) *CFH* expression for females at each age cohort. C) *CFH* expression for males at each age cohort. D) *JAG1* combined female and male nTPMs comparing expression between age cohorts. E) *JAG1* expression for females at each age cohort. F) *JAG1* expression for males at each age cohort. G) *TRIM25* combined female and male nTPMs comparing expression between age cohorts H) *TRIM25* expression for females at each age cohort I) *TRIM25* expression for males at each age cohort. Statistical test used: multiple comparison Kruskal-Wallis. Results denote median nTPM +/- 95% CI

3.4.2.8. *GAPDH* and *ACTB* constitutive expression in the lung is not affected by sex or age

In order to validate our findings of the effect of sex and age on constitutive expression of lung ISGs, we next chose two commonly used reference genes in influenza research Glyceraldehyde 3-phosphate dehydrogenase (*GAPDH)* and Actin (*ACTB*) (Suzuki et al., 2000). By analysing these reference genes, we can infer whether any changes in constitutive lung ISG expression are a result of genome-wide variation or are truly gene-specific.

GAPDH showed no significant difference in expression levels within the lung between females and males (figure 27A) (P = 0.9473). equally, when female and male samples are combined (figure 27B), there is no significant change in lung expression level as an effect of changing age (P = 0.5509). We tested the effect of age on both females and males (figure 27C and 27D respectively) and found no significant effect of age on either sex (P = 0.6594, and P = 0.1990 respectively). As with *GAPDH*, *ACTB* showed no significant difference in constitutive expression levels in the lung (figure 27E) (P = 0.8266). similarly, there was no significant effect of age when female and male samples were combined (figure 27F) (P = 0.2533). When female and male samples were tested separately for the effect of changing age on constitutive expression in the lung (figure 27G and 27H respectively), there was no significant change in expression levels over time for either sex (P = 0.6269, and P = 0.4554 respectively).

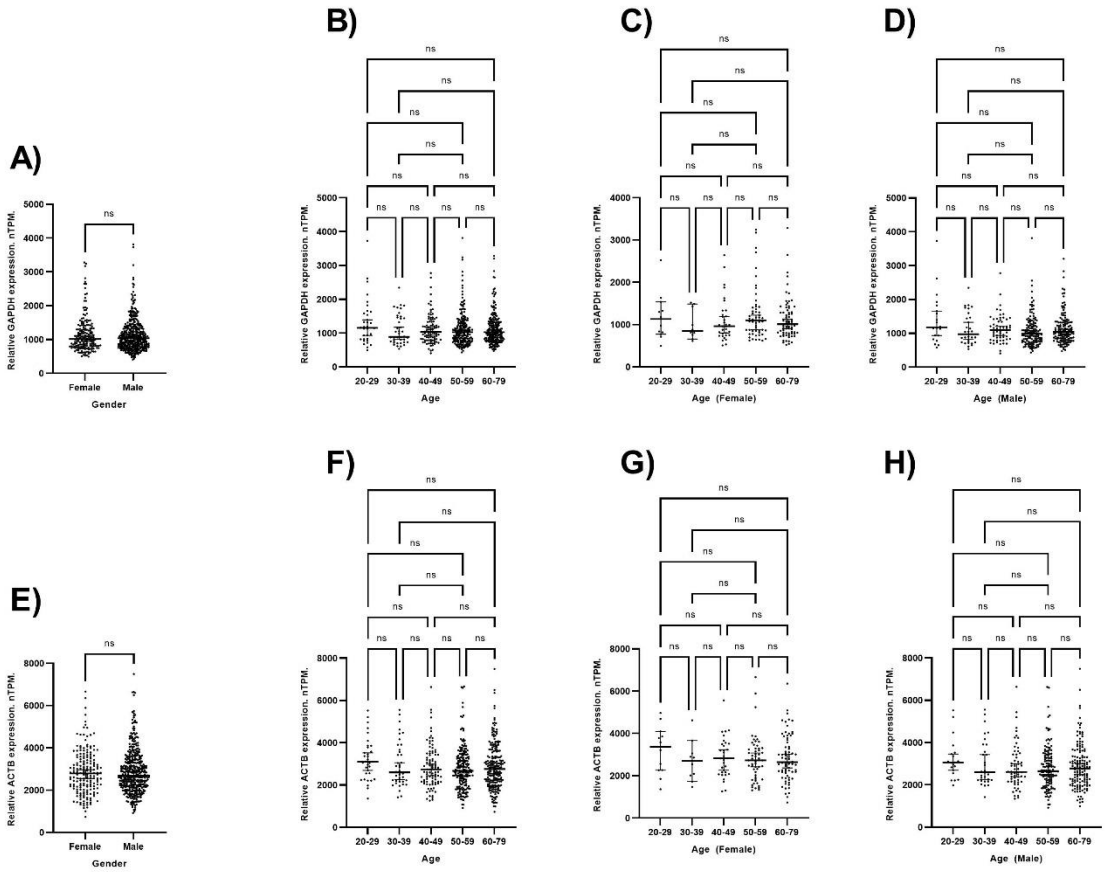

Figure 27. *GAPDH* and *ACTB* constitutive expression in the lung is not affected by sex or age. A) Constitutive expression of *GAPDH* between females and males. Statistical test used: Mann-Whitney U test. B) Effect of changing age on lung expression levels of *GAPDH* for combined female and male samples. C) Effect of changing age on constitutive expression levels of *GAPDH* in females. D) Effect of changing age on constitutive expression levels of *GAPDH* in males. Statistical test used: multiple comparison Kruskal-Wallis ANOVA. E) Constitutive expression of *ACTB* between females and males. Statistical test used: Mann-Whitney U test. F) Effect of changing age on lung expression levels of *ACTB* for combined female and male samples. G) Effect of changing age on constitutive expression levels of *ACTB* in females. H) Effect of changing age on constitutive expression levels of *ACTB* in males. Statistical test used: multiple comparison Kruskal-Wallis ANOVA. Violin plots denote median nTPM +/- 95% CI.

3.4.3. Conclusions and Next Steps

Our data suggest a donor-dependent effect on innate immune activation (figure 19), we therefore wanted to determine inherent variance within the population (constitutive ISG expression in the lung). To do this, we compared the expression of lung ISGs in 578 individuals in the absence of direct challenge/infection (Pontén et al., 2008). Our analysis shows that out of the 100 lung ISGs investigated, 7% showed a difference (but not statistically significant) in constitutive expression between males and females (figure 23B) and that for all of these 7 ISGs (*PML, DES, GTBP2, OGFR, PATL1, JAG1* and *SLC25A28*).

Of these genes, a number are involved in similar cellular functions. *PML, JAG1* and *SLC25A28* have all been shown to have roles in cell fate determination and apoptosis. *GTPBP2* and *PATL1* have roles in mRNA degradation and OGFR and DES have major functions in cell proliferation and cellular homeostasis, respectively (table 12). In determining the potential role of these ISGs during LAIV or IAV infection, we looked to the literature to determine the current understanding. Of these 7 genes, *PML* and *JAG1* are known to have direct anti-IAV activity, and these are described below. *PML* is a member of the tripartite motif protein family (TRIM) and is the basis of subnuclear structures known as *PML* nuclear bodies (*PML*-NBs). These PML-NBs act to localise a number of proteins within the cell that result in wide-ranging effects, this means PML-NBs are implicated in a wide range of cellular functions including cell cycle regulation, apoptosis and DNA damage responses (Bernardi and Pandolfi, 2007). *PML* has been shown to have anti-viral properties, including roles in inhibiting IAV replication (Li et al., 2009). *PML* acts to stabilise *RIG-I*, in doing so, promoting a Type 1 IFN response. Additionally, *PML* has been shown to stabilise FBXW7, a protein with roles in cell homeostasis and proliferation (Yan et al., 2021). Indeed, FBXW7 has been shown to be an important regulator of host susceptibility to Influenza, indeed in FBXW7-deficient mice, sensitivity to several viruses, including IAV, was increased (Song et al., 2017).

Having shown that none of the lung ISGs analysed here show a significant increase in constitutive expression in males compared to females (Figure 23), we next wanted to elucidate any significant changes in expression levels as a result of changing age. Within both males and females, we see that there is variation in constitutive expression in the vast majority of lung ISGs analysed here (figure 24A). to understand whether this is significant, we first combined sample cohorts of females and males, and ran a multiple-component ANOVA test between each age category for each ISG (figure 24B). We found that 32 out of 100 lung ISGs had a significant change in expression between at least two age cohorts. These data indicate that there is a significant effect of age on lung ISG expression levels. Interestingly, when samples of females and males for all ISGs are combined in each age category, we find there to be no significant difference in gene expression. These data suggests that there is a greater effect of changing age on lung ISG expression than sex.

Our next question was to understand whether the significant effect of age on lung ISG constitutive expression (figure 25) is equal between females and males. 1 out of 100 lung ISGs were differentially expressed as a result of changing age in females (figure 25A) compared to 24 out of 100 lung ISGs in males (figure 25B). These data suggest that there is a sex-dependent effect of age on the constitutive expression of lung ISGs. In support of this conclusion, surveillance studies looking at risk- and protective-factors for ARDS, a number of protective factors were noted, including vaccination status, and female sex (Bonmarin et al., 2015). Our data suggest that the steady state of lung ISG expression in females over time may play a role in this sex-dependent protective phenotype.

In elucidating the effect of age on constitutive lung ISG expression, we here discuss two ISGs (*CFH* and *JAG1*) that show significant differential expression as a result of age in both females and males (*CFH*) and males only (*JAG1*). Our data show that Complement Factor H (*CFH*) (also referred to as Factor H (FH)) constitutive expression levels show a negative correlation with age: as age increases, the expression level of *CFH* decreases. This is true for both females and males, and combined sexes.

CFH has a major role in regulating the complement pathway. The complement pathway provides means of recognising pathogenic microbes and other target cells, inducing an innate cell response leading to phagocytosis and cell lysis. To prevent this action being carried out on un-intended host targets, host cells incorporate a number of membrane-bound complement regulatory and inhibitory proteins, *CFH* being amongst these (Jozsi, 2017). *CFH* modulates the complement pathway by binding to C3b, a key component of the alternative pathway and the amplification loop, (figure 28). The age-associated decrease in FH expression seen in these samples accounts for known FH-mediated age-related macular degeneration (AMD) where any dysregulation in FH or NF-κB will alter the complement pathway and the pro-inflammatory response associated with AMD (Armento et al., 2021).

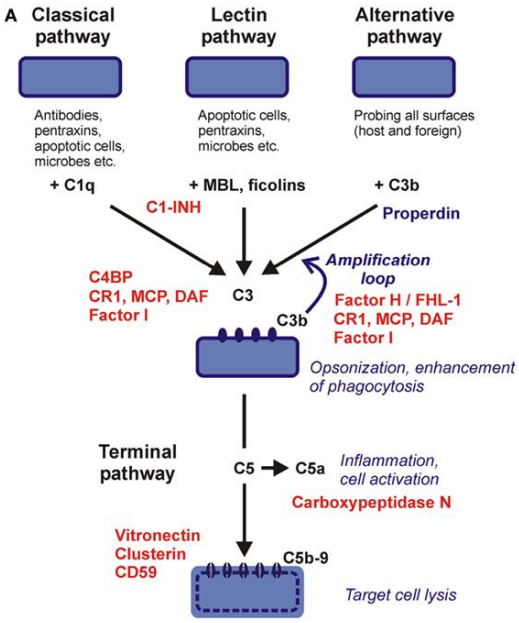

Figure 28. Factor H (CFH) acts to inhibit the alternative complement pathway. A) three pathways of the complement system, Classical, Lectin and Alternative pathways. Red font indicates complement inhibitors. adapted from Jozsi M. 2017 (Jozsi, 2017).

Interestingly, as well as roles in age-associated morbidities such as AMD outlined above, *CFH* has been shown to be an inhibitory to influenza infection. Containing specific binding regions to sialic acids (Bai et al., 2021) which enables direct competitive inhibition by binding competition to influenza virions (Murugaiah et al., 2020). Indeed it was shown that infection with influenza H1N1 (but not H3N2) subtypes in the presence of Factor H (FH), independent of its compliment-related activities, led to reduction in transcriptional levels of a number of immune genes (*IFN-α, TNF-α, IL-12, IL-6 IFN-α* and *RANTES*) (Murugaiah et al., 2020).

To understand how the decreasing levels of constitutive *CFH* expression between individuals of increasing age may impact IAV infection, we would require primary airway cells from individuals across all age-ranges included in this study. We would utilise PCR and RNA sequencing techniques to quantify *CFH* levels in the presence and absence of IAV/LAIV infection. Additionally, we would undergo growth kinetics studies in 3D-differentiated hAEC nasal and bronchial cells of donors with differing levels of *CFH* constitutive expression, we would also look to knock out *CFH* expression and measure the effect of its absence on the growth potential of IAV/LAIV.

Similar to *CFH*, *JAG1* showed a negative correlation in expression levels relative to age, as the age cohorts increased, the expression level of *JAG1* decreased. This trend was, however, seen more prominently in males (figure 26F), where there were five age comparisons showing significant drops in expression with increasing age, compared with only one in females between the ages of 30-39 and 60-79 (figure 26E). These data suggest that *JAG1* has a sex-dependent effect of age on constitutive expression levels.

JAG1 is one of five known mammalian ligands with roles in activating Notch signalling pathways; Delta-like (DLL) 1, Dll3, Dll4, Jagged-1 and Jagged 2 (Amsen et al., 2009). Notch signalling pathways have been shown to have roles in the immune response, including T-cell development, namely the differentiation of naive $CD8^+$ T-Cells into cytotoxic T lymphocytes that kill cells infected with virus (Radtke et al., 2010). Additionally, *JAG1* is known to play a role in Notch pathway associated T-helper cell differentiation to further induce a specific T-cell response to microbe infection (Radtke et al., 2010). The Notch pathway ligand DLL2 has been shown to be important for regulating influenza infection in macrophage cells. However, the role of the Notch pathway in epithelial cells is currently unknown (Ito et al., 2011).

Similar to *CFH*, to further elucidate the potential impact of changing expression levels of *JAG1* in response to host demographics (sex and age), we would require human airway cells where *JAG1* has been knocked down in order to assess its role in IAV/LAIV infection and host-cell responses. Using primary airway cells from different individuals of varying demographics, we can use RT-qPCR and sequencing methods to quantify relative *JAG1* expression levels, both at constitutive (untreated) and challenged (IAV/LAIV infection) states.

MX1 expression levels were not significantly different between females and males, similarly, changing age appeared to not significantly alter gene expression levels. There was a significant fall in *MX1* expression in males between the ages of 40-49 and 50-59, although this was the only significant difference. These data suggest that baseline expression of *MX1* is stable and unaffected by both sex and age. The ISG *MX1* is a protein belonging to the dynamin superfamily of large GTPases (Jimah and Hinshaw, 2019) that has been shown to have direct anti-influenza activity by preventing vRNPs from entering the nucleus, sequestering them in to the cells cytoplasm (Xiao et al., 2013, Haller and Kochs, 2020). As well as direct anti-influenza activity, *MX1* has been shown to have roles in promoting a pro-inflammatory response upon sensing infected epithelial cell inflammasome (Lee et al., 2019b).

Our data suggests that *MX1* constitutive expression in the lung is not significantly changed as a result of ageing, it has, however, been shown previously that in challenge to IAV (A/PR/8/34), circulating monocytes of older persons (65-89) had reduced Type 1 IFN responses relative to younger 20–30-year-olds, including *MX1* (Pillai et al., 2016). These data suggest that beyond differences in constitutive immune gene expression studied here, this may extend to host responses to IAV/LAIV infection. Although these studies were done with monocytes and not epithelial cells, and again the lowest age range was 20-30 yrs meaning that any direct inference to LAIV infection responses in airway epithelia must be made with relevant considerations.

Results in figure 22 suggest a sex-dependent effect of age on *OAS1* expression levels. Specifically, we show that constitutive expression of *OAS1* to reduce in males from ages 40-49 to 50-59. Interestingly, we show that between the age cohorts 50-59 and 60-79, there is a significant increase in *OAS1* constitutive expression (figure 22D). Conversely, in females we see no significant change in constitutive expression of *OAS1* in the lung (figure 22C). *OAS1* is an ISG that forms a part of the OAS protein family 2’-5’-oligoadenylate synthase consisting of 4 genes (OAS1, 2, 3 and 4). These proteins have a known and characterised anti-IAV role through cytosolic activation of RNaseL, resulting in the cleavage of viral RNA (Iwasaki and Pillai, 2014). These data further corroborate the suggestion that the previously seen protective factor of sex (female) (Bonmarin et al., 2015) may be in part due to a more stable level of constitutive ISG over time.

When relating these data to the potential impact of ISG constitutive expression on basal anti-viral state of host cells to LAIV infection, and how this is variable based on sex and age, there are several caveats. The first being that we were unable to obtain upper (nasal) tract transcriptomic data as this was not available in the GTEX study data. This is important to note as it has been shown that there are differences in the genetic and cellular make up of lower respiratory tissues compared to upper airway tissues. Advances in single-cell sequencing has shown the extent to which the upper and lower respiratory tract differ in the cellular composition (as reviewed by Hewitt R, and Lloyd C, 2021 (Hewitt and Lloyd, 2021), in particular noting the differences in the immunological potential at the mucosal surface that is dependent on a number of factors including temperature and bidirectional air flows. https://www.ncbi.nlm.nih.gov/pmc/articles/PMC7804588/ . Additionally, although LAIV is licenced for persons between the age of 2 yrs – 49 yrs, a major cohort of recipients are school-aged children who receive the Flumist/Fluenz vaccine, such as in school programs in the UK. With our youngest available data set from the GTEX study being 20 - 29 yrs, this obviously discounts the school-aged cohort we would be interested in studying.

Ideally, our analysis should have been conducted on transcriptome data derived from the nasal tract and include children aged 2 yrs – 19 yrs. These data would allow us to elucidate the variation in background ISG expression profiles in a manner more representative of the target demographic/tissue to which LAIV targets. Caution must be taken when drawing conclusions from the results here in chapter 3.4. Having conducted a large number of statistical tests per experiment, a correction calculation would provide a more accurate P value to take in to account the random chance of finding a significant test result. To do this, we could re analyse using corrections such as the Bonferroni test. This would increase the stringency of significance threshold relative to the number of genes tested.

Due to time constraints, these transcriptomic data have not been confirmed *in vitro*. To do this, we would perform single-cell and bulk-RNA sequencing on primary 3D-differentiated hAECn cells at base state and challenged after interferon challenge. We would utilise several hAECn cells covering the demographics studied sex and age groups. We would wish to infect these cells with LAIV also to understand how the baseline differences in ISG expression affect the host cell responses to LAIV. The difficulty would be in using enough hAECn donors to have sufficient power to conduct statistical analysis that will enable accurate conclusions resulting from biological phenomena between demographic cohorts and not because of inherent variation within such demographic cohorts.

4. Discussion

4.1. Choice of Cell Model is Important for Contextualising Experimental Results during IAV/LAIV Research and Development

The choice of which cell model to use in the study of Influenza immunobiology and LAIV development is vital to ensure conclusions drawn are correctly contextualised in relation to the question being asked. Our study corroborates previous findings by Charman et al 2021. (Charman et al., 2021) showing that MDCK cells are significantly more permissive to IAV infection than human airway epithelial cells (A549 and HBEC3-KT). This suggests that host cell responses to IAV are not equal between cell types, thus MDCK cells may be less physiologically representative of the human airway, potentially missing key host-virus interactions that will be present *in vivo* in the human airway that may influence the outcome of IAV infection. This is important in the case of LAIV development. During the annual development of LAIV (Flumist), MDCK cells are commonly used to determine the potency of LAIV strains through the use of FFU-assays to quantify viral infectious potential (Hawksworth et al., 2020). With cold-adapted LAIV being restricted to the upper respiratory tract, we assessed nasal airway epithelial cells for their viability as a more physiologically representative model system for medium-throughput virology assays. Our data shows that primary hAECn cells are significantly more restrictive to LAIV infection than MDCK cells. Moreover, we show that this restriction is not a result of LAIV being less efficient in the attachment or entry into hAECn cells. We hypothesised therefore that host-cell responses may vary different between cell types.

The use of primary cells for medium-throughput assays such as with LAIV titration assays (including, but not limited to FFU-assays), comes with a number of challenges. Firstly, use of primary cells comes with higher costs, including initial cell stock purchase relative to continuous cell lines such as MDCK cells, and comparatively expensive maintenance medium to maintain growth independently of the addition of foetal calf serum that can stimulate primary airway cell differentiation (Popov et al., 2019). Additionally primary hAECn cells require specialist maintenance media that incurs an additional expense. Adding to these costs is the short lifespan of primary airway cells due to the onset of cellular senescence. hAECn cells from Epithelix are recommended to be used up to passage 6 (Epithelix), however in our laboratory, hAECn cells were routinely viable up to passage 11. Thus, primary cells have considerably reduced lifespans relative to continuous cell lines, particularly MDCK or A549cells. This means that a greater number of cell aliquots will be required for primary hAECn infection immunobiology analysis, which in an industrial setting can amplify the experimental costs considerably. In order to circumvent this, we immortalised primary hAECn cells lentiviral transduction and expression of hTERT and CDK4 as previously described (Ramirez et al., 2004). However, we show that epithelial cell numbers

proportionally decreased on sequential passage (figure 10). This meant that cell sorting for immortalised epithelial cells would be required.

We attempted to utilise fluorescence-associated cell sorting (FACS) to positively select for epithelial cells by labelling epithelial cells with the epithelial cell marker EpCAM. Although cell sorting was successful, the viability of cells post-FACS was low, with cells being unable to survive past 2 passages post-sorting (data not shown). Alternative methods of immortalisation have been shown used such as lentiviral transduction with Simian Virus 40 (SV40) Large Antigen T (Bryan and Reddel, 1994). Additionally, alternative methods of cell sorting might increase cell viability of post-sorting, such as magnetic-associated cell sorting (MACS) (Deng and Lin, 2012).

4.2. LAIV restriction in MDCK cells relative to hAECn cells is not as a result of differential attachment/entry efficiencies

Our data suggest that where we see LAIV is restricted in MDCK cells relative to hAECn cells at single-cycle infection, this restriction is not due to differences in the attachment and entry efficiency of LAIV between cell lines. We show that for LAIV A/Slovenia/2903/2015, there was a statistically significant increase in intracellular virions at 2hpi in hAECn cells than in MDCK cells. Additionally, we see that LAIV A/Bolivia/559/2013 had no significant different in attachment/entry efficiencies between MDCK and hAECn cells. These data suggest that the restriction we see at single-cycle infection in hAECn cells relative to MDCK cells is likely a result of host cell innate immune responses to infection.

Beyond comparing the attachment/entry efficiencies of LAIV between cell types, we show that there are inter-strain differences in the relative number of intracellular virions at 2hpi. Our data suggest that LAIV A/Slovenia/2903/2015 has a significantly higher attachment/entry efficiency than LAIV A/Bolivia/559/2013 in all cell lines tested (MDCK, hAECn D1 and hAECn D2). We hypothesise that this strain-dependent differential internalisation rates of LAIV may contribute to the differential replication potential between the two LAIV strains as shown in previous studies (Dibben et al., 2021, Hawksworth et al., 2020).

With our data suggesting that hAECn host-responses to LAIV infection may contribute to differential infection potential between MDCK and hAECn cells at single-cycle infection, we next aimed to elucidate primary hAECn ISG responses to LAIV infection, using MX1 and OAS1 as markers of innate immune responses to IAV/LAIV infection as they have been well characterised for their anti-influenza activity as reviewed by Iwasaki A. 2014 (Iwasaki and Pillai, 2014). We had two objectives in this analysis: 1) to determine comparative ISG expression in primary hAECn cells between LAIV A/Slovenia/2903/2015 ad LAIV A/Bolivia/559/2013. And 2) To understand whether ISG expression levels differ between individual and pooled hAECn donors in response to LAIV infection (LAIV A/Slovenia/2903/2015).

4.3. LAIV A/Slovenia/2903/2015 indues a higher MX1 response (but not OAS1) than LAIV A/Bolivia/559/2013 in primary hAECn cells

VE studies have been undertaken to elucidate variable VE between LAIV strains over previous seasons. Together these data show that although LAIV-A strains differ in only 2 out of 8 gene segments (HA and NA) different strains of LAIV have different replication potential, particularly LAIV A/Bolivia/559/2013 reached a lower peak titre in 3D-differentiated airway epithelia compared to LAIV A/Slovenia/2903/2015 (Hawksworth et al., 2020). Additionally, studies by Dibben et al. 2019 showed that there is a competitive inhibition on strain-specific replication potential, showing that in a formulation of multivalent LAIV, LAIV A/Bolivia/559/20123 had a lower rate of replication than the other LAIV strains included (Dibben et al., 2021). Our data suggest that concurrent with this differential replication potential, there may be differences in the relative levels of ISG induction (*MX1*). We should take care when analysing ISG response to IAV/LAIV as it is known that during replication, IAV produces defective viral genomes (DVGs) that have been shown to induce an innate immune response irrespective of replication through the RIG-I pathway (Penn et al., 2022, Elshina and Te Velthuis, 2021). However, the LAIV formulations used in this thesis have been shown in previous studies by Ayaz S. et al. 2021 to have similar levels of DVGs, moreover, in this study, they found that DVG levels did not correlate with ISG expression (Ayaz et al., 2021). We are therefore confident that our results are indicative of host responses to competent LAIV virions and not a result of DVGs within the samples.

In order to perform unbiased and comprehensive analysis, we would require RNA sequence and differential gene expression (DEG) analysis to understand whether there are other ISGs beyond *MX1* that show differential expression in response to different LAIV strains. Additionally, we would look to confirm the necessity of active viral replication on the induction of ISG expression as previously reported (Iwasaki and Pillai, 2014). Such experiments could be achieved by the infection hAECn cells with LAIV in the presence of favipiravir to block viral replication by inhibiting viral RNA polymerase, then utilise two-step RT-PCR to quantify relative levels of ISG expression. This would tie in our preliminary understanding of host responses to LAIV to that of VE studies focussing on differential rates of replication between LAIV strains to their relative immune responses to infection (Dibben et al., 2021, Hawksworth et al., 2020).

4.4. hAECn Cells from Different Donors Differ Significantly in their Innate Immune Response to LAIV Infection

We aimed to elucidate how hAECn cells from individual different donors, and pooled donors respond to LAIV infection. Using LAIV A/Slovenia/2903/2015 as a model strain, we found that of the three donors we used, there were significant differences in *MX1* expression. Additionally, we found that when pooling these donors, there was no significant difference in *MX1* expression between the pooled culture and its constituent individual donors. These data suggest that when using primary 2D hAECn cells for IAV/LAIV studies, a pooled donor culture would provide a response within range of individual donors, limiting biassing the response due to inherent genetic variation between donors. Our study used three donors, this is limiting the power of our study, to verify inter-donor differences in innate immune responses to LAIV, we would require a larger sample size of donors, based on our results from chapter 3.4, we would recommend a minimum of 3 donors from each demographic cohort in order to increase the chances of encompassing the range of demographics shown to be a potential factor in differential ISG constitutive expression (sex and age). We hypothesise that there is natural genetic variation within the population in relation to both the constitutive expression of ISGs, and the level of innate immune activation in response to LAIV. Previous proteomic studies of A/California/07/2009 infection in NHBE cells from 3 different donors showed significant differences in both pro- and anti-viral protein expression (Mindaye et al., 2017) including *MX1*, corroborating our *MX1* transcript analysis. To elucidate the former, we used open-access GTEX portal transcriptomic data from 578 individuals to understand the variation in constitutive lung ISG expression between females and males, and between differing age groups.

4.5. There is no Significant Difference in Constitutive Expression of Lung ISGs Between Females and Males.

7% of lung ISGs tested within this study trended to a higher constitutive expression level in males compared to females, though not to a statistically significant degree (chapter 3.4 figure 23), these genes cover a range of cellular functions including programmed cell death and cellular homeostasis (Table 13). These data suggest a state of propensity for programmed cell death in response to pathogens in males that is relatively reduced in females. Validation studies would be required to understand how potential differential expression of these ISGs between the sexs effect the replication ability of IAV/LAIV. To do this, we would require a large sample size of donors covering males and females of a wide range of ages. We would quantify the relative expression level of these ISGs in the absence- and presence of LAIV/IAV infection.

Alongside this, we would ideally run bulk RNA-sequencing to understand the wider genome and which genes are significantly altered between females and males beyond the 100 ISGs tested here. Together these data suggest an inherent variation in baseline innate immune gene expression that must be considered when using primary human airway cells from single donors for IAV/LAIV research and development.

4.6. Sex-Associated Effect of Age on Constitutive Expression of ISGs in the Lung

We previously show that of the 7 lung ISGs showing a trend in differential constitutive expression between females and males, all of them are expressed to a higher level in males than females. Interestingly when we look at the effect of age on constitutive lung ISG expression, there is a clear difference between females and males. In males, there were 58 out of 100 ISGs that were significantly differentiated as a result of changing age compared to 17 in females. These data provide further evidence for the requirement of understanding the biology and genetics of any primary human airway epithelial cell donor if used for IAV/LAIV development. Interestingly when we looked at MX1 and OAS1 constitutive expression in these samples, we found no evidence differential expression levels as a result of sex, additionally, in terms of age, we found differences in males.

The skewing of ISG constitutive expression towards males may be a result of a number of factors, as reviewed by Jaillon S et al. 2017. Such factors include the location of a number of innate immune genes on the X chromosome as well as the influence of sex-associated dominant hormones such as oestrogen and testosterone, testosterone in particular has been shown to be immunosuppressive to individuals post vaccination (Furman et al., 2014), interestingly it has been noted that females have enhanced innate and adaptive responses relative to males, as such males are more susceptible to pathogens such as bacteria, viruses, parasites and fungi (Jaillon et al., 2019). Indeed studies have shown that women have lower survival rates to pandemic influenza, yet respond with higher levels of neutralizing antibodies post-vaccination (Giefing-Kröll et al., 2015), although these studies were conducted in the elderly population with IIVs (Wang et al., 2002, Cook et al., 2006, Nichol et al., 2007, Engler et al., 2008, Falsey et al., 2009, Furman et al., 2014) The effect of sex on innate immune responses to LAIV is less well understood.

The main limitation of this study is the lack of upper airway tract transcriptomic data. Using lung transcriptomics analysis allows us to make inferences on the nature of ISG expression between different demographics (sex and age) across the airway tract. Studies have shown differences in children regarding immune responses between the upper and lower tract both at a basal level, and in response to SARS-CoV-2 (Saheb Sharif-Askari et al., 2022, Alfi et al., 2021) showing the importance of studying the appropriate tissue relative to the infectious agent under investigation.

4.7. Thoughts and Potential Implications for LAIV/IAV Research and Development

The aim of this thesis was to understand the host cell responses of primary hAECn cells in order to determine the pros and cons of replacing non physiological cell culture systems like MDCK cells in IAV/LAIV immunobiology research and vaccine development. Many of the medium-throughput assays used with MDCK cells include TCID50, FFU and PFU assays. Although MDCK cells provide a cost-effective, fast growing and highly susceptible to infection, they do not physiologically reflect the upper respiratory tract to which IAV/LAIV primarily targets. Thus, discoveries in such model systems may inadvertently mislead the development of LAIV vaccines due to their relative hyper-permissivity.

Our data suggest that immortalising primary nasal cells to increase their longevity and cost-effectiveness may not be the complete answer due to individual donor immune response variation but could act as an intermediate stepping point by providing a more physiological model system for infection However, inter-donor variation is likely to account for some of the variance observed in VE between vaccination seasons. Pooling of multiple donors to avoid donor-dependent immune bias is likely to help to improve LAIV VE by providing a model system that has an in-tact host response mechanism against LAIV, more closely resembling that of the human airway. Whilst 3D-differentiated airway epithelia may provide the optimal *in vitro* model in terms of physiological relevance. Their slow rate of growth as well as their high cost and comparatively higher skill level in handling, makes them less suitable for medium-throughput assays than 2D cultures during LAIV research and development.

Our data provides preliminary understanding of how different strains of LAIV may result in different levels of innate immune activation (MX1 expression), adding further to our understanding of why there is variation in VE between LAIV strains over previous vaccination seasons. We suggest further work is required to understand how this differential ISG expression incurred by different LAIV strains. We suggest looking in to how multivalency may impact upon such ISG responses through experimentation described in Chapter 3.3.

5. Future Work

Our data suggests that LAIV H1N1 strains (LAIV A/Slovenia/2903/2015 and LAIV A/Bolivia/559/2013) result in significantly different expression levels of *MX1* (but not *OAS1*). To first understand whether this result is specific to *MX1*, a genome-wide approach would be required. In order to do this, bulk-RNA sequencing should be undertaken on primary hAECn cells in 2D infected with LAIV and mock-infection. This would allow for determining any patterns of differential expression including particular pathways as well as individual ISGs. Studies in 3D-differentiated epithelial cells have shown cellular response to LAIV infection. (Forero et al., 2017) , therefore these differentiated nasal epithelia should be included as a comparison between 2D and 3D cell culture systems also. Where our studies compared LAIV strains in monovalent infection settings, we did not analyse the effect of multivalency on the induction of innate immune responses (ISG expression). This is important as LAIV is developed and delivered as a quadrivalent formulation consisting of 2 A-strains and 2 B-strains (AstraZeneca, 2023). We therefore propose expanding our current understanding of differential ISG expression in hAECn cells between LAIV strains, to elucidate the innate immune activation potential of multivalent formulations compared to the constitutive monovalent strains.

LAIV quadrivalent formulations are created with equal titres of all four constitutive strains. We propose infecting both 2D and 3D-differentiated primary human nasal epithelial cells with formulations of quadrivalent LAIV containing both equal, and adjusted ratios of constitutive LAIV strains. Alongside we would run infections with monovalent LAIV strains for direct comparison of host immune responses to Quadrivalent LAIV and the individual monovalent LAIV strain infections. We recommend using both single cell sequencing technologies as well as bulk RNA sequencing to ascertain sub-populations of cells containing monovalent, bivalent, trivalent, quadrivalent and no LAIV strains. Indeed single-cell sequencing technologies have been used to show that there are specific immune markers of cells that have active influenza infection distinct from bystander cells (Steuerman et al., 2018), showing the potential of such assays to elucidate host cell responses to influenza infection.

Using strain-specific HA as a signature for each LAIV strain, we can utilise sequencing technologies and PCR platforms (RT-qPCR and absolute quantification by ddPCR) to determine the relative replicative fitness of each strain, comparing the effect equal or adjusted levels of constituent strains within a LAIV formulation. Figure 29 shows a schematic of a proposed experimental plan to elucidate the effect of multivalency on host cell responses. Understanding innate immune responses to LAIV is informative as it has been shown that a strong innate immune

response is required for the establishment of a robust adaptive immune response (Medzhitov and Janeway, 1997), required for vaccine-associated protection against incoming wild-type influenza virus.

Together with the data in this thesis, such experimental workflows will further elucidate host-cell responses to LAIV in both monovalent and quadrivalent formulations of equal and adjusted ratios of constituent strains. This will further our understanding of potential causes of variable VE seen with LAIV in previous vaccination seasons, and work to provide evidence for the necessity (or not) of adjusted the ratios of LAIV within a Quadrivalent LAIV formulation to maximise the VE of each constituent strain.

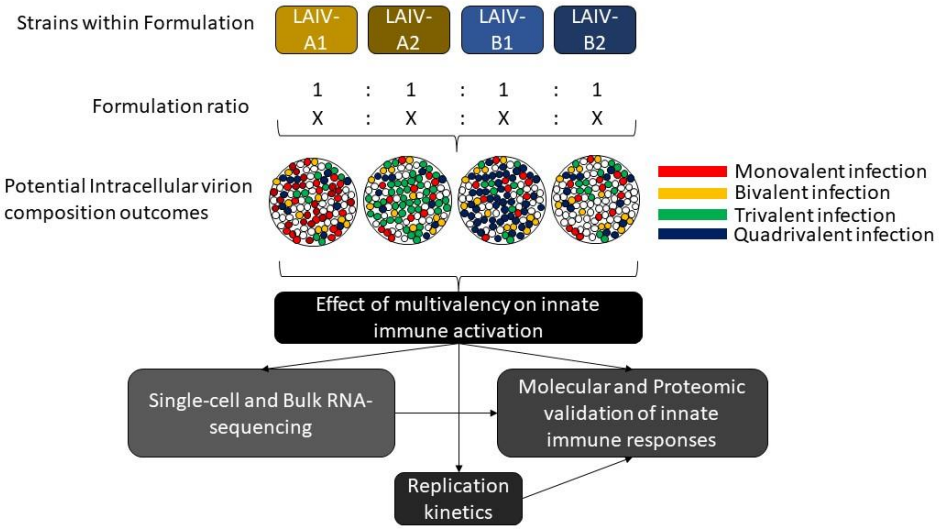

Figure 29. Determining the effect of LAIV multivalency on the activation of innate immune responses in primary human nasal cells, schematic of proposed future research. Infection pooled-donor human nasal epithelial cells with LAIV formulations at equal (1:1:1:1 genome copies) or differential ratios of individual input LAIV strains (X). This will lead to sub-populations of cells infected with monovalent bivalent, trivalent or quadrivalent (intended outcome) LAIV strains. We will utilise single cell and bulk RNA sequencing to determine LAIV strain replication fitness and activation of innate immune responses.

References

Burden of Flu [Online]. Available: https://www.cdc.gov/flu/about/burden/index.html [Accessed 27.04.2023 2023].

The Human Protein Atlas [Online]. Available: https://www.proteinatlas.org/about [Accessed 14/04/2023 2023].

2018. Influenza Virus: Dealing with a Drifting and Shifting Pathogen. *Viral Immunology,* 31**,** 174-183.

2019. Peramivir for influenza. *Aust Prescr,* 42**,** 143.

2021. Guidence on use of antiviral agents for the treatment and prophylaxis of seasonal influenza. 11 ed.

ACIP 2016. ACIP votes down use of LAIV for 2016-2017 flu season.

AGNETTI, G., HERRMANN, H. & COHEN, S. 2022. New roles for desmin in the maintenance of muscle homeostasis. *Febs j,* 289**,** 2755-2770.

AHMED, F. & HUSAIN, M. 2021. Human N-Alpha-Acetyltransferase 60 Promotes Influenza A Virus Infection by Dampening the Interferon Alpha Signaling. *Front Immunol,* 12**,** 771792.

ALBRECHT, R. A. & GARCÍA-SASTRE, A. 2008. Suppression of innate immunity by Orthomyxoviruses. *Cellular Signaling and Innate Immune Responses to RNA Virus Infections***,** 267-286.

ALFI, O., YAKIREVITCH, A., WALD, O., WANDEL, O., IZHAR, U., OIKNINE-DJIAN, E., NEVO, Y., ELGAVISH, S., DAGAN, E., MADGAR, O., FEINMESSER, G., PIKARSKY, E., BRONSTEIN, M., VORONTSOV, O., JONAS, W., IVES, J., WALTER, J., ZAKAY-RONES, Z., OBERBAUM, M., PANET, A. & WOLF, D. G. 2021. Human Nasal and Lung Tissues Infected Ex Vivo with SARS-CoV-2 Provide Insights into Differential Tissue-Specific and Virus-Specific Innate Immune Responses in the Upper and Lower Respiratory Tract. *J Virol,* 95**,** e0013021.

AMBROSE, C. S., WU, X., JONES, T. & MALLORY, R. M. 2012. The role of nasal IgA in children vaccinated with live attenuated influenza vaccine. *Vaccine,* 30**,** 6794-801.

AMSEN, D., ANTOV, A. & FLAVELL, R. A. 2009. The different faces of Notch in T-helper-cell differentiation. *Nat Rev Immunol,* 9**,** 116-24.

AREVALO, C. P., BOLTON, M. J., LE SAGE, V., YE, N., FUREY, C., MURAMATSU, H., ALAMEH, M.-G., PARDI, N., DRAPEAU, E. M., PARKHOUSE, K., GARRETSON, T., MORRIS, J. S., MONCLA, L. H., TAM, Y. K., FAN, S. H. Y., LAKDAWALA, S. S., WEISSMAN, D. & HENSLEY, S. E. 2022. A multivalent nucleoside-modified mRNA vaccine against all known influenza virus subtypes. *Science,* 378**,** 899-904.

ARMENTO, A., SCHMIDT, T. L., SONNTAG, I., MERLE, D. A., JARBOUI, M. A., KILGER, E., CLARK, S. J. & UEFFING, M. 2021. CFH Loss in Human RPE Cells Leads to Inflammation and Complement System Dysregulation via the NF-κB Pathway. *Int J Mol Sci,* 22.

ASTRAZENECA. 2023. *The only needle-free nasal spray flu vaccine* [Online]. Available: https://www.flumistquadrivalent.com/ [Accessed 13.03.2023 2023].

ATCC.

AUDSLEY, J. M. & TANNOCK, G. A. 2004. The role of cell culture vaccines in the control of the next influenza pandemic. *Expert Opin Biol Ther,* 4**,** 709-17.

AYAZ, S., DIBBEN, O. & CHAPMAN, D. 2021. Presence of defective viral genes in H1N1 live attenuated influenza vaccine strains is not associated with reduced human cell fitness or vaccine effectiveness. *Vaccine,* 39**,** 6735-6745.

BADHAM, M. D. & ROSSMAN, J. S. 2016. Filamentous Influenza Viruses. *Curr Clin Microbiol Rep,* 3**,** 155-161.

BAI, L., XIE, Q., XIA, M., GONG, K., WANG, N., CHEN, Y. & ZHAO, M. 2021. The importance of sialic acid, pH and ion concentration on the interaction of uromodulin and complement factor H. *J Cell Mol Med,* 25**,** 4316-4325.

BARBERIS, I., MYLES, P., AULT, S. K., BRAGAZZI, N. L. & MARTINI, M. 2016. History and evolution of influenza control through vaccination: from the first monovalent vaccine to universal vaccines. *J Prev Med Hyg,* 57**,** E115-e120.

BARR, I. G. & JELLEY, L. L. 2012. The coming era of quadrivalent human influenza vaccines: who will benefit? *Drugs,* 72**,** 2177-85.

BARRÍA, M. I., GARRIDO, J. L., STEIN, C., SCHER, E., GE, Y., ENGEL, S. M., KRAUS, T. A., BANACH, D. & MORAN, T. M. 2013. Localized mucosal response to intranasal live attenuated influenza vaccine in adults. *J Infect Dis,* 207**,** 115-24.

BERNARDI, R. & PANDOLFI, P. P. 2007. Structure, dynamics and functions of promyelocytic leukaemia nuclear bodies. *Nat Rev Mol Cell Biol,* 8**,** 1006-16.

BERTRAMS, W., HONZKE, K., OBERMAYER, B., TONNIES, M., BAUER, T. T., SCHNEIDER, P., NEUDECKER, J., RUCKERT, J. C., STIEWE, T., NIST, A., EGGELING, S., SUTTORP, N., WOLFF, T., HIPPENSTIEL, S., SCHMECK, B. & HOCKE, A. C. 2022. Transcriptomic comparison of primary human lung cells with lung tissue samples and the human A549 lung cell line highlights cell type specific responses during infections with influenza A virus. *Sci Rep,* 12**,** 20608.

BLOCK, S. L., REISINGER, K. S., HULTQUIST, M. & WALKER, R. E. 2007. Comparative immunogenicities of frozen and refrigerated formulations of live attenuated influenza vaccine in healthy subjects. *Antimicrob Agents Chemother,* 51**,** 4001-8.

BONMARIN, I., BELCHIOR, E., BERGOUNIOUX, J., BRUN-BUISSON, C., MÉGARBANE, B., CHAPPERT, J. L., HUBERT, B., LE STRAT, Y. & LÉVY-BRUHL, D. 2015. Intensive care unit surveillance of influenza infection in France: the 2009/10 pandemic and the three subsequent seasons. *Euro Surveill,* 20.

BOTH, G. W., SLEIGH, M. J., COX, N. J. & KENDAL, A. P. 1983. Antigenic drift in influenza virus H3 hemagglutinin from 1968 to 1980: multiple evolutionary pathways and sequential amino acid changes at key antigenic sites. *J Virol,* 48**,** 52-60.

BRASS, A. L., HUANG, I. C., BENITA, Y., JOHN, S. P., KRISHNAN, M. N., FEELEY, E. M., RYAN, B. J., WEYER, J. L., VAN DER WEYDEN, L., FIKRIG, E., ADAMS, D. J., XAVIER, R. J., FARZAN, M. & ELLEDGE, S. J. 2009. The IFITM proteins mediate cellular resistance to influenza A H1N1 virus, West Nile virus, and dengue virus. *Cell,* 139**,** 1243-54.

BRYAN, T. M. & REDDEL, R. R. 1994. SV40-induced immortalization of human cells. *Crit Rev Oncog,* 5**,** 331-57.

BUCHAN, S. A., BOOTH, S., SCOTT, A. N., SIMMONDS, K. A., SVENSON, L. W., DREWS, S. J., RUSSELL, M. L., CROWCROFT, N. S., LOEB, M., WARSHAWSKY, B. F. & KWONG, J. C. 2018. Effectiveness of Live Attenuated vs Inactivated Influenza Vaccines in Children During the 2012-2013 Through 2015-2016 Influenza Seasons in Alberta, Canada: A Canadian Immunization Research Network (CIRN) Study. *JAMA Pediatr,* 172**,** e181514.

BYRD-LEOTIS, L., JIA, N., MATSUMOTO, Y., LU, D., KAWAOKA, Y., STEINHAUER, D. A. & CUMMINGS, R. D. 2022. Sialylated and sulfated N-Glycans in MDCK and engineered MDCK cells for influenza virus studies. *Sci Rep,* 12**,** 12757.

ÇAĞLAYAN, E. & TURAN, K. 2022. Effects of Some Interferon-Related Proteins on Influenza A Viruse RNA Polymerase Activity. *Turk J Pharm Sci,* 19**,** 552-559.

CALDER, L. J., WASILEWSKI, S., BERRIMAN, J. A. & ROSENTHAL, P. B. 2010. Structural organization of a filamentous influenza A virus. *Proc Natl Acad Sci U S A,* 107**,** 10685-90.

CARITHERS, L. J., ARDLIE, K., BARCUS, M., BRANTON, P. A., BRITTON, A., BUIA, S. A., COMPTON, C. C., DELUCA, D. S., PETER-DEMCHOK, J., GELFAND, E. T., GUAN, P., KORZENIEWSKI, G. E., LOCKHART, N. C., RABINER, C. A., RAO, A. K., ROBINSON, K. L., ROCHE, N. V., SAWYER, S. J., SEGRÈ, A. V., SHIVE, C. E., SMITH, A. M., SOBIN, L. H., UNDALE, A. H., VALENTINO, K. M., VAUGHT, J., YOUNG, T. R. & MOORE, H. M. 2015. A Novel Approach to High-Quality Postmortem Tissue Procurement: The GTEx Project. *Biopreserv Biobank,* 13**,** 311-9.

CARTER, N. J. & CURRAN, M. P. 2011. Live attenuated influenza vaccine (FluMist®; Fluenz™): a review of its use in the prevention of seasonal influenza in children and adults. *Drugs,* 71**,** 1591-622.

CASPARD, H., GAGLANI, M., CLIPPER, L., BELONGIA, E. A., MCLEAN, H. Q., GRIFFIN, M. R., TALBOT, H. K., POEHLING, K. A., PETERS, T. R., VENEY, N. & AMBROSE, C. S. 2016. Effectiveness of live attenuated influenza vaccine and inactivated influenza vaccine in children 2-17 years of age in 2013-2014 in the United States. *Vaccine,* 34**,** 77-82.

CASPARD, H., MALLORY, R. M., YU, J. & AMBROSE, C. S. 2017. Live-Attenuated Influenza Vaccine Effectiveness in Children From 2009 to 2015-2016: A Systematic Review and Meta-Analysis. *Open Forum Infect Dis,* 4**,** ofx111.

CASTELLI, J. C., HASSEL, B. A., WOOD, K. A., LI, X. L., AMEMIYA, K., DALAKAS, M. C., TORRENCE, P. F. & YOULE, R. J. 1997. A study of the interferon antiviral mechanism: apoptosis activation by the 2-5A system. *J Exp Med,* 186**,** 967-72.

CDC. 2022a. *Flu Symtoms & Complications* [Online]. Available: https://www.cdc.gov/flu/symptoms/symptoms.htm [Accessed 21.03.2023 2023].

CDC. 2022b. *Influenza (Flu) Antiviral Drugs and Related Information* [Online]. Available: https://www.fda.gov/drugs/information-drug-class/influenza-flu-antiviral-drugs-and-related-information [Accessed 2023].

CHAKRABARTI, A., GHOSH, P. K., BANERJEE, S., GAUGHAN, C. & SILVERMAN, R. H. 2012. RNase L triggers autophagy in response to viral infections. *J Virol,* 86**,** 11311-21.

CHARMAN, M., MCFARLANE, S., WOJTUS, J. K., SLOAN, E., DEWAR, R., LEEMING, G., AL-SAADI, M., HUNTER, L., CARROLL, M. W., STEWART, J. P., DIGARD, P., HUTCHINSON, E. & BOUTELL, C. 2021. Constitutive TRIM22 Expression in the Respiratory Tract Confers a Pre-Existing Defence Against Influenza A Virus Infection. *Front Cell Infect Microbiol,* 11**,** 689707.

CHEN, C. & ZHUANG, X. 2008. Epsin 1 is a cargo-specific adaptor for the clathrin-mediated endocytosis of the influenza virus. *Proc Natl Acad Sci U S A,* 105**,** 11790-5.

CHENG, F., MCLAUGHLIN, P. J., VERDERAME, M. F. & ZAGON, I. S. 2009. The OGF-OGFr axis utilizes the p16INK4a and p21WAF1/CIP1 pathways to restrict normal cell proliferation. *Mol Biol Cell,* 20**,** 319-27.

CHERUKURI, A., SERVAT, E. & WOO, J. 2012. Vaccine-specific antibody secreting cells are a robust early marker of LAIV-induced B-cell response in ferrets. *Vaccine,* 30**,** 237-46.

CHIVUKULA, S., PLITNIK, T., TIBBITTS, T., KARVE, S., DIAS, A., ZHANG, D., GOLDMAN, R., GOPANI, H., KHANMOHAMMED, A., SARODE, A., COOPER, D., YOON, H., KIM, Y., YAN, Y., MUNDLE, S. T., GROPPO, R., BEAUVAIS, A., ZHANG, J., ANOSOVA, N. G., LAI, C., LI, L., ULINSKI, G., PIEPENHAGEN, P., DINAPOLI, J., KALNIN, K. V., LANDOLFI, V., SWEARINGEN, R., FU, T. M., DEROSA, F. & CASIMIRO, D. 2021. Development of multivalent mRNA vaccine candidates for seasonal or pandemic influenza. *NPJ Vaccines,* 6**,** 153.

CLOHISEY, S. & BAILLIE, J. K. 2019. Host susceptibility to severe influenza A virus infection. *Crit Care,* 23**,** 303.

COELINGH, K., OLAJIDE, I. R., MACDONALD, P. & YOGEV, R. 2015. Efficacy and effectiveness of live attenuated influenza vaccine in school-age children. *Expert Rev Vaccines,* 14**,** 1331-46.

COHEN, M., ZHANG, X. Q., SENAATI, H. P., CHEN, H. W., VARKI, N. M., SCHOOLEY, R. T. & GAGNEUX, P. 2013. Influenza A penetrates host mucus by cleaving sialic acids with neuraminidase. *Virol J,* 10**,** 321.

COOK, I. F., BARR, I., HARTEL, G., POND, D. & HAMPSON, A. W. 2006. Reactogenicity and immunogenicity of an inactivated influenza vaccine administered by intramuscular or subcutaneous injection in elderly adults. *Vaccine,* 24**,** 2395-402.

COUCEIRO, J. N., PAULSON, J. C. & BAUM, L. G. 1993. Influenza virus strains selectively recognize sialyloligosaccharides on human respiratory epithelium; the role of the host cell in selection of hemagglutinin receptor specificity. *Virus Res,* 29**,** 155-65.

COX, N. J. & SUBBARAO, K. 2000. Global epidemiology of influenza: past and present. *Annu Rev Med,* 51**,** 407-21.

COX, R. J., BROKSTAD, K. A., ZUCKERMAN, M. A., WOOD, J. M., HAAHEIM, L. R. & OXFORD, J. S. 1994. An early humoral immune response in peripheral blood following parenteral inactivated influenza vaccination. *Vaccine,* 12**,** 993-9.

CROCE, M. V., COLUSSI, A. G., PRICE, M. R. & SEGAL-EIRAS, A. 1999. Identification and characterization of different subpopulations in a human lung adenocarcinoma cell line (A549). *Pathol Oncol Res,* 5**,** 197-204.

CROSS, K. J., BURLEIGH, L. M. & STEINHAUER, D. A. 2001. Mechanisms of cell entry by influenza virus. *Expert Rev Mol Med,* 3**,** 1-18.

CRYSTAL, R. G., RANDELL, S. H., ENGELHARDT, J. F., VOYNOW, J. & SUNDAY, M. E. 2008. Airway epithelial cells: current concepts and challenges. *Proc Am Thorac Soc,* 5**,** 772-7.

DE VRIES, E., TSCHERNE, D. M., WIENHOLTS, M. J., COBOS-JIMÉNEZ, V., SCHOLTE, F., GARCÍA-SASTRE, A., ROTTIER, P. J. & DE HAAN, C. A. 2011. Dissection of the influenza A virus endocytic routes reveals macropinocytosis as an alternative entry pathway. *PLoS Pathog,* 7**,** e1001329.

DENG, X. L. & LIN, F. Q. 2012. [Magnetic activated cell sorting and its application in the studies of male infertility]. *Zhonghua Nan Ke Xue,* 18**,** 70-3.

DIBBEN, O., CROWE, J., COOPER, S., HILL, L., SCHEWE, K. E. & BRIGHT, H. 2021. Defining the root cause of reduced H1N1 live attenuated influenza vaccine effectiveness: low viral fitness leads to inter-strain competition. *NPJ Vaccines,* 6**,** 35.

DIEBOLD, S. S., KAISHO, T., HEMMI, H., AKIRA, S. & REIS E SOUSA, C. 2004. Innate antiviral responses by means of TLR7-mediated recognition of single-stranded RNA. *Science,* 303**,** 1529-31.

DONABEDIAN, A. M., DEBORDE, D. C. & MAASSAB, H. F. 1987. Genetics of cold-adapted B/Ann Arbor/1/66 influenza virus reassortants: the acidic polymerase (PA) protein gene confers temperature sensitivity and attenuated virulence. *Microb Pathog,* 3**,** 97-108.

DOROSHENKO, A. & HALPERIN, S. A. 2009. Trivalent MDCK cell culture-derived influenza vaccine Optaflu (Novartis Vaccines). *Expert Rev Vaccines,* 8**,** 679-88.

DOU, D., REVOL, R., ÖSTBYE, H., WANG, H. & DANIELS, R. 2018. Influenza A Virus Cell Entry, Replication, Virion Assembly and Movement. *Front Immunol,* 9**,** 1581.

DUFRASNE, F. 2021. Baloxavir Marboxil: An Original New Drug against Influenza. *Pharmaceuticals (Basel),* 15.

EISFELD, A. J., NEUMANN, G. & KAWAOKA, Y. 2015. At the centre: influenza A virus ribonucleoproteins. *Nat Rev Microbiol,* 13**,** 28-41.

ELLIOTT, M. 2001. Zanamivir: from drug design to the clinic. *Philos Trans R Soc Lond B Biol Sci,* 356**,** 1885-93.

ELSHINA, E. & TE VELTHUIS, A. J. W. 2021. The influenza virus RNA polymerase as an innate immune agonist and antagonist. *Cell Mol Life Sci,* 78**,** 7237-7256.

ENGLER, R. J., NELSON, M. R., KLOTE, M. M., VANRADEN, M. J., HUANG, C. Y., COX, N. J., KLIMOV, A., KEITEL, W. A., NICHOL, K. L., CARR, W. W. & TREANOR, J. J. 2008. Half- vs full-dose trivalent inactivated influenza vaccine (2004-2005): age, dose, and sex effects on immune responses. *Arch Intern Med,* 168**,** 2405-14.

EPITHELIX. *FAQs* [Online]. Available: https://www.epithelix.com/faq [Accessed 27.03.2023 2023].

EPITHELIX. 2023. Available: https://www.epithelix.com/products/haec-upper-airway [Accessed].

FAHY, J. V. & DICKEY, B. F. 2010. Airway mucus function and dysfunction. *N Engl J Med,* 363**,** 2233-47.

FALSEY, A. R., TREANOR, J. J., TORNIEPORTH, N., CAPELLAN, J. & GORSE, G. J. 2009. Randomized, double-blind controlled phase 3 trial comparing the immunogenicity of high-dose and standard-dose influenza vaccine in adults 65 years of age and older. *J Infect Dis,* 200**,** 172-80.

FDA. 2023. *Vaccines Licensed for Use in the United States* [Online]. Available: https://www.fda.gov/vaccines-blood-biologics/vaccines/vaccines-licensed-use-united-states [Accessed 29.03.2023 2023].

FELDMAN, R. A., FUHR, R., SMOLENOV, I., MICK RIBEIRO, A., PANTHER, L., WATSON, M., SENN, J. J., SMITH, M., ALMARSSON, Ö., PUJAR, H. S., LASKA, M. E., THOMPSON, J., ZAKS, T. & CIARAMELLA, G. 2019. mRNA vaccines against H10N8 and H7N9 influenza viruses of pandemic potential are immunogenic and well tolerated in healthy adults in phase 1 randomized clinical trials. *Vaccine,* 37**,** 3326-3334.

FISCHER, W. A., 2ND, CHASON, K. D., BRIGHTON, M. & JASPERS, I. 2014. Live attenuated influenza vaccine strains elicit a greater innate immune response than antigenically-matched seasonal influenza viruses during infection of human nasal epithelial cell cultures. *Vaccine,* 32**,** 1761-7.

FISCHER, W. A., 2ND, KING, L. S., LANE, A. P. & PEKOSZ, A. 2015. Restricted replication of the live attenuated influenza A virus vaccine during infection of primary differentiated human nasal epithelial cells. *Vaccine,* 33**,** 4495-504.

FORERO, A., FENSTERMACHER, K., WOHLGEMUTH, N., NISHIDA, A., CARTER, V., SMITH, E. A., PENG, X., HAYES, M., FRANCIS, D., TREANOR, J., MORRISON, J., KLEIN, S. L., LANE, A., KATZE, M. G. & PEKOSZ, A. 2017. Evaluation of the innate immune responses to influenza and live-attenuated influenza vaccine infection in primary differentiated human nasal epithelial cells. *Vaccine,* 35**,** 6112-6121.

FRENSING, T., KUPKE, S. Y., BACHMANN, M., FRITZSCHE, S., GALLO-RAMIREZ, L. E. & REICHL, U. 2016. Influenza virus intracellular replication dynamics, release kinetics, and particle morphology during propagation in MDCK cells. *Appl Microbiol Biotechnol,* 100**,** 7181-92.

FURMAN, D., HEJBLUM, B. P., SIMON, N., JOJIC, V., DEKKER, C. L., THIÉBAUT, R., TIBSHIRANI, R. J. & DAVIS, M. M. 2014. Systems analysis of sex differences reveals an immunosuppressive role for testosterone in the response to influenza vaccination. *Proc Natl Acad Sci U S A,* 111**,** 869-74.

GACK, M. U., ALBRECHT, R. A., URANO, T., INN, K. S., HUANG, I. C., CARNERO, E., FARZAN, M., INOUE, S., JUNG, J. U. & GARCÍA-SASTRE, A. 2009. Influenza A virus NS1 targets the ubiquitin ligase TRIM25 to evade recognition by the host viral RNA sensor RIG-I. *Cell Host Microbe,* 5**,** 439-49.

GAGNEUX, P., CHERIYAN, M., HURTADO-ZIOLA, N., VAN DER LINDEN, E. C., ANDERSON, D., MCCLURE, H., VARKI, A. & VARKI, N. M. 2003. Human-specific regulation of alpha 2-6-linked sialic acids. *J Biol Chem,* 278**,** 48245-50.

GAUSH, C. R. & SMITH, T. F. 1968. Replication and plaque assay of influenza virus in an established line of canine kidney cells. *Appl Microbiol,* 16**,** 588-94.

GENZEL, Y. & REICHL, U. 2009. Continuous cell lines as a production system for influenza vaccines. *Expert Rev Vaccines,* 8**,** 1681-92.

GIARD, D. J., AARONSON, S. A., TODARO, G. J., ARNSTEIN, P., KERSEY, J. H., DOSIK, H. & PARKS, W. P. 1973. In vitro cultivation of human tumors: establishment of cell lines derived from a series of solid tumors. *J Natl Cancer Inst,* 51**,** 1417-23.

GIEFING-KRÖLL, C., BERGER, P., LEPPERDINGER, G. & GRUBECK-LOEBENSTEIN, B. 2015. How sex and age affect immune responses, susceptibility to infections, and response to vaccination. *Aging Cell,* 14**,** 309-21.

GOLEBIEWSKI, L., LIU, H., JAVIER, R. T. & RICE, A. P. 2011. The avian influenza virus NS1 ESEV PDZ binding motif associates with Dlg1 and Scribble to disrupt cellular tight junctions. *J Virol,* 85**,** 10639-48.

GREEN, I. J. 1962. Serial propagation of influenza B (Lee) virus in a transmissible line of canine kidney cells. *Science,* 138**,** 42-3.

GROHSKOPF, L. A., SOKOLOW, L. Z., FRY, A. M., WALTER, E. B. & JERNIGAN, D. B. 2018. Update: ACIP Recommendations for the Use of Quadrivalent Live Attenuated Influenza Vaccine (LAIV4) - United States, 2018-19 Influenza Season. *MMWR Morb Mortal Wkly Rep,* 67**,** 643-645.

GU, Y., ZUO, X., ZHANG, S., OUYANG, Z., JIANG, S., WANG, F. & WANG, G. 2021. The Mechanism behind Influenza Virus Cytokine Storm. *Viruses,* 13.

GUAN, D. & KAO, H. Y. 2015. The function, regulation and therapeutic implications of the tumor suppressor protein, PML. *Cell Biosci,* 5**,** 60.

GUO, X. J. & THOMAS, P. G. 2017. New fronts emerge in the influenza cytokine storm. *Semin Immunopathol,* 39**,** 541-550.

HALLER, O. & KOCHS, G. 2020. Mx genes: host determinants controlling influenza virus infection and trans-species transmission. *Hum Genet,* 139**,** 695-705.

HARRIS, A., CARDONE, G., WINKLER, D. C., HEYMANN, J. B., BRECHER, M., WHITE, J. M. & STEVEN, A. C. 2006. Influenza virus pleiomorphy characterized by cryoelectron tomography. *Proc Natl Acad Sci U S A,* 103**,** 19123-7.

HAWKSWORTH, A., LOCKHART, R., CROWE, J., MAESO, R., RITTER, L., DIBBEN, O. & BRIGHT, H. 2020. Replication of live attenuated influenza vaccine viruses in human nasal epithelial cells is associated with H1N1 vaccine effectiveness. *Vaccine,* 38**,** 4209-4218.

HEROLD, S., BECKER, C., RIDGE, K. M. & BUDINGER, G. R. 2015. Influenza virus-induced lung injury: pathogenesis and implications for treatment. *Eur Respir J,* 45**,** 1463-78.

HEWITT, R. J. & LLOYD, C. M. 2021. Regulation of immune responses by the airway epithelial cell landscape. *Nature Reviews Immunology,* 21**,** 347-362.

HOFFMANN, E., MAHMOOD, K., CHEN, Z., YANG, C. F., SPAETE, J., GREENBERG, H. B., HERLOCHER, M. L., JIN, H. & KEMBLE, G. 2005. Multiple gene segments control the temperature sensitivity and attenuation phenotypes of ca B/Ann Arbor/1/66. *J Virol,* 79**,** 11014-21.

HOVANESSIAN, A. G. 2007. On the discovery of interferon-inducible, double-stranded RNA activated enzymes: the 2'-5'oligoadenylate synthetases and the protein kinase PKR. *Cytokine Growth Factor Rev,* 18**,** 351-61.

ICHINOHE, T., PANG, I. K., KUMAMOTO, Y., PEAPER, D. R., HO, J. H., MURRAY, T. S. & IWASAKI, A. 2011. Microbiota regulates immune defense against respiratory tract influenza A virus infection. *Proceedings of the National Academy of Sciences,* 108**,** 5354-5359.

ILYUSHINA, N. A., DICKENSHEETS, H. & DONNELLY, R. P. 2019. A comparison of interferon gene expression induced by influenza A virus infection of human airway epithelial cells from two different donors. *Virus Res,* 264**,** 1-7.

ILYUSHINA, N. A., IKIZLER, M. R., KAWAOKA, Y., RUDENKO, L. G., TREANOR, J. J., SUBBARAO, K. & WRIGHT, P. F. 2012. Comparative study of influenza virus replication in MDCK cells and in primary cells derived from adenoids and airway epithelium. *J Virol,* 86**,** 11725-34.

ISAKA, T., NESTOR, A. L., TAKADA, T. & ALLISON, D. C. 2003. Chromosomal variations within aneuploid cancer lines. *J Histochem Cytochem,* 51**,** 1343-53.

ITO, T., ALLEN, R. M., CARSON, W. F. T., SCHALLER, M., CAVASSANI, K. A., HOGABOAM, C. M., LUKACS, N. W., MATSUKAWA, A. & KUNKEL, S. L. 2011. The critical role of Notch ligand Delta-like 1 in the pathogenesis of influenza A virus (H1N1) infection. *PLoS Pathog,* 7**,** e1002341.

ITO, T., COUCEIRO, J. N., KELM, S., BAUM, L. G., KRAUSS, S., CASTRUCCI, M. R., DONATELLI, I., KIDA, H., PAULSON, J. C., WEBSTER, R. G. & KAWAOKA, Y. 1998. Molecular basis for the generation in pigs of influenza A viruses with pandemic potential. *J Virol,* 72**,** 7367-73.

IULIANO, A. D., ROGUSKI, K. M., CHANG, H. H., MUSCATELLO, D. J., PALEKAR, R., TEMPIA, S., COHEN, C., GRAN, J. M., SCHANZER, D., COWLING, B. J., WU, P., KYNCL, J., ANG, L. W., PARK, M., REDLBERGER-FRITZ, M., YU, H., ESPENHAIN, L., KRISHNAN, A., EMUKULE, G., VAN ASTEN, L., PEREIRA DA SILVA, S., AUNGKULANON, S., BUCHHOLZ, U., WIDDOWSON, M. A. & BRESEE, J. S. 2018. Estimates of global seasonal influenza-associated respiratory mortality: a modelling study. *Lancet,* 391**,** 1285-1300.

IWASAKI, A. & PILLAI, P. S. 2014. Innate immunity to influenza virus infection. *Nat Rev Immunol,* 14**,** 315-28.

JACKSON, L. A., HOLMES, S. J., MENDELMAN, P. M., HUGGINS, L., CHO, I. & RHORER, J. 1999. Safety of a trivalent live attenuated intranasal influenza vaccine, FluMist, administered in addition to parenteral trivalent inactivated influenza vaccine to seniors with chronic medical conditions. *Vaccine,* 17**,** 1905-9.

JAILLON, S., BERTHENET, K. & GARLANDA, C. 2019. Sexual Dimorphism in Innate Immunity. *Clin Rev Allergy Immunol,* 56**,** 308-321.

JIMAH, J. R. & HINSHAW, J. E. 2019. Structural Insights into the Mechanism of Dynamin Superfamily Proteins. *Trends Cell Biol,* 29**,** 257-273.

JIN, H., LU, B., ZHOU, H., MA, C., ZHAO, J., YANG, C. F., KEMBLE, G. & GREENBERG, H. 2003. Multiple amino acid residues confer temperature sensitivity to human influenza virus vaccine strains (FluMist) derived from cold-adapted A/Ann Arbor/6/60. *Virology,* 306**,** 18-24.

JOZSI, M. 2017. Factor H Family Proteins in Complement Evasion of Microorganisms. *Front Immunol,* 8**,** 571.

KIA'I, N. & BAJAJ, T. 2023. Histology, Respiratory Epithelium. *StatPearls.* Treasure Island (FL) ineligible companies. Disclosure: Tushar Bajaj declares no relevant financial relationships with ineligible companies.

KING, J. C., JR., STODDARD, J. J., GAGLANI, M. J., MOORE, K. A., MAGDER, L., MCCLURE, E., RUBIN, J. D., ENGLUND, J. A. & NEUZIL, K. 2006. Effectiveness of school-based influenza vaccination. *N Engl J Med,* 355**,** 2523-32.

KLENK, H. D., ROTT, R., ORLICH, M. & BLÖDORN, J. 1975. Activation of influenza A viruses by trypsin treatment. *Virology,* 68**,** 426-39.

KONGSOMROS, S., MANOPWISEDJAROEN, S., CHAOPREECHA, J., WANG, S. F., BORWORNPINYO, S. & THITITHANYANONT, A. 2021. Rapid and Efficient Cell-to-Cell Transmission of Avian Influenza H5N1 Virus in MDCK Cells Is Achieved by Trogocytosis. *Pathogens,* 10.

KOWALINSKI, E., LUNARDI, T., MCCARTHY, A. A., LOUBER, J., BRUNEL, J., GRIGOROV, B., GERLIER, D. & CUSACK, S. 2011. Structural basis for the activation of innate immune pattern-recognition receptor RIG-I by viral RNA. *Cell,* 147**,** 423-35.

KRAMMER, F., SMITH, G. J. D., FOUCHIER, R. A. M., PEIRIS, M., KEDZIERSKA, K., DOHERTY, P. C., PALESE, P., SHAW, M. L., TREANOR, J., WEBSTER, R. G. & GARCÍA-SASTRE, A. 2018. Influenza. *Nature Reviews Disease Primers,* 4**,** 3.

LACTMED 2006. COVID-19 Vaccines. *Drugs and Lactation Database (LactMed®).* Bethesda (MD): National Institute of Child Health and Human Development.

LAGACHE, T., SIEBEN, C., MEYER, T., HERRMANN, A. & HOLCMAN, D. 2017. Stochastic Model of Acidification, Activation of Hemagglutinin and Escape of Influenza Viruses from an Endosome. *Frontiers in Physics,* 5.

LANTHIER, P. A., HUSTON, G. E., MOQUIN, A., EATON, S. M., SZABA, F. M., KUMMER, L. W., TIGHE, M. P., KOHLMEIER, J. E., BLAIR, P. J., BRODERICK, M., SMILEY, S. T. & HAYNES, L. 2011. Live attenuated influenza vaccine (LAIV) impacts innate and adaptive immune responses. *Vaccine,* 29**,** 7849-56.

LAWKO, N., PLASKASOVITIS, C., STOKES, C., ABELSETH, L., FRASER, I., SHARMA, R., KIRSCH, R., HASAN, M., ABELSETH, E. & WILLERTH, S. M. 2021. 3D Tissue Models as an Effective Tool for Studying Viruses and Vaccine Development. *Frontiers in Materials,* 8.

LEE, K. H., GORDON, A., SHEDDEN, K., KUAN, G., NG, S., BALMASEDA, A. & FOXMAN, B. 2019a. The respiratory microbiome and susceptibility to influenza virus infection. *PLoS One,* 14**,** e0207898.

LEE, S., ISHITSUKA, A., NOGUCHI, M., HIROHAMA, M., FUJIYASU, Y., PETRIC, P. P., SCHWEMMLE, M., STAEHELI, P., NAGATA, K. & KAWAGUCHI, A. 2019b. Influenza restriction factor MxA functions as inflammasome sensor in the respiratory epithelium. *Sci Immunol,* 4.

LEMESSURIER, K. S., TIWARY, M., MORIN, N. P. & SAMARASINGHE, A. E. 2020. Respiratory Barrier as a Safeguard and Regulator of Defense Against Influenza A Virus and Streptococcus pneumoniae. *Front Immunol,* 11**,** 3.

LI, J., ARÉVALO, M. T., CHEN, Y., CHEN, S. & ZENG, M. 2014. T-cell-mediated cross-strain protective immunity elicited by prime-boost vaccination with a live attenuated influenza vaccine. *Int J Infect Dis,* 27**,** 37-43.

LI, M. L., RAO, P. & KRUG, R. M. 2001. The active sites of the influenza cap-dependent endonuclease are on different polymerase subunits. *Embo j,* 20**,** 2078-86.

LI, W., WANG, G., ZHANG, H., ZHANG, D., ZENG, J., CHEN, X., XU, Y. & LI, K. 2009. Differential suppressive effect of promyelocytic leukemia protein on the replication of different subtypes/strains of influenza A virus. *Biochem Biophys Res Commun,* 389**,** 84-9.

LIU, Q., ZHOU, Y. H. & YANG, Z. Q. 2016. The cytokine storm of severe influenza and development of immunomodulatory therapy. *Cell Mol Immunol,* 13**,** 3-10.

LUGOVTSEV, V. Y., MELNYK, D. & WEIR, J. P. 2013. Heterogeneity of the MDCK cell line and its applicability for influenza virus research. *PLoS One,* 8**,** e75014.

MAASSAB, H. F. 1967. Adaptation and growth characteristics of influenza virus at 25 degrees c. *Nature,* 213**,** 612-4.

MAIR, C. M., LUDWIG, K., HERRMANN, A. & SIEBEN, C. 2014. Receptor binding and pH stability - how influenza A virus hemagglutinin affects host-specific virus infection. *Biochim Biophys Acta,* 1838**,** 1153-68.

MALIK, G. & ZHOU, Y. 2020. Innate Immune Sensing of Influenza A Virus. *Viruses,* 12.

MANZOOR, R., IGARASHI, M. & TAKADA, A. 2017. Influenza A Virus M2 Protein: Roles from Ingress to Egress. *International Journal of Molecular Sciences,* 18**,** 2649.

MARTÍNEZ-SOBRIDO, L., PEERSEN, O. & NOGALES, A. 2018. Temperature Sensitive Mutations in Influenza A Viral Ribonucleoprotein Complex Responsible for the Attenuation of the Live Attenuated Influenza Vaccine. *Viruses,* 10.

MCAULEY, J. L., CORCILIUS, L., TAN, H. X., PAYNE, R. J., MCGUCKIN, M. A. & BROWN, L. E. 2017. The cell surface mucin MUC1 limits the severity of influenza A virus infection. *Mucosal Immunol,* 10**,** 1581-1593.

MCCLELLAN, K. & PERRY, C. M. 2001. Oseltamivir. *Drugs,* 61**,** 263-283.

MCKIMM-BRESCHKIN, J. L. 2013. Influenza neuraminidase inhibitors: antiviral action and mechanisms of resistance. *Influenza Other Respir Viruses,* 7 Suppl 1**,** 25-36.

MEDZHITOV, R. & JANEWAY, C. A., JR. 1997. Innate immunity: impact on the adaptive immune response. *Curr Opin Immunol,* 9**,** 4-9.

MIBAYASHI, M., MARTÍNEZ-SOBRIDO, L., LOO, Y. M., CÁRDENAS, W. B., GALE, M., JR. & GARCÍA-SASTRE, A. 2007. Inhibition of retinoic acid-inducible gene I-mediated induction of beta interferon by the NS1 protein of influenza A virus. *J Virol,* 81**,** 514-24.

MIFSUD, E. J., KUBA, M. & BARR, I. G. 2021. Innate Immune Responses to Influenza Virus Infections in the Upper Respiratory Tract. *Viruses,* 13.

MINDAYE, S. T., ILYUSHINA, N. A., FANTONI, G., ALTERMAN, M. A., DONNELLY, R. P. & EICHELBERGER, M. C. 2017. Impact of Influenza A Virus Infection on the Proteomes of Human Bronchoepithelial Cells from Different Donors. *J Proteome Res,* 16**,** 3287-3297.

MOHN, K. G., BREDHOLT, G., BROKSTAD, K. A., PATHIRANA, R. D., AARSTAD, H. J., TØNDEL, C. & COX, R. J. 2015. Longevity of B-cell and T-cell responses after live attenuated influenza vaccination in children. *J Infect Dis,* 211**,** 1541-9.

MOHN, K. G., BROKSTAD, K. A., PATHIRANA, R. D., BREDHOLT, G., JUL-LARSEN, A., TRIEU, M. C., LARTEY, S. L., MONTOMOLI, E., TONDEL, C., AARSTAD, H. J. & COX, R. J. 2016a. Live Attenuated Influenza Vaccine in Children Induces B-Cell Responses in Tonsils. *J Infect Dis,* 214**,** 722-31.

MOHN, K. G., BROKSTAD, K. A., PATHIRANA, R. D., BREDHOLT, G., JUL-LARSEN, Å., TRIEU, M. C., LARTEY, S. L., MONTOMOLI, E., TØNDEL, C., AARSTAD, H. J. & COX, R. J. 2016b. Live Attenuated Influenza Vaccine in Children Induces B-Cell Responses in Tonsils. *J Infect Dis,* 214**,** 722-31.

MOLINARI, N. A., ORTEGA-SANCHEZ, I. R., MESSONNIER, M. L., THOMPSON, W. W., WORTLEY, P. M., WEINTRAUB, E. & BRIDGES, C. B. 2007. The annual impact of seasonal influenza in the US: measuring disease burden and costs. *Vaccine,* 25**,** 5086-96.

MORIYAMA, M., CHEN, I. Y., KAWAGUCHI, A., KOSHIBA, T., NAGATA, K., TAKEYAMA, H., HASEGAWA, H. & ICHINOHE, T. 2016. The RNA- and TRIM25-Binding Domains of Influenza Virus NS1 Protein Are Essential for Suppression of NLRP3 Inflammasome-Mediated Interleukin-1β Secretion. *J Virol,* 90**,** 4105-4114.

MOULÈS, V., TERRIER, O., YVER, M., RITEAU, B., MORISCOT, C., FERRARIS, O., JULIEN, T., GIUDICE, E., ROLLAND, J. P., ERNY, A., BOUSCAMBERT-DUCHAMP, M., FROBERT, E., ROSA-CALATRAVA, M., PU LIN, Y., HAY, A., THOMAS, D., SCHOEHN, G. & LINA, B. 2011. Importance of viral genomic composition in modulating glycoprotein content on the surface of influenza virus particles. *Virology,* 414**,** 51-62.

MURUGAIAH, V., VARGHESE, P. M., SALEH, S. M., TSOLAKI, A. G., ALROKAYAN, S. H., KHAN, H. A., COLLISON, K. S., SIM, R. B., NAL, B., AL-MOHANNA, F. A. & KISHORE, U. 2020. Complement-Independent Modulation of Influenza A Virus Infection by Factor H. *Front Immunol,* 11**,** 355.

NELSON, S. W., LORBACH, J. N., NOLTING, J. M., STULL, J. W., JACKWOOD, D. J., DAVIS, I. C. & BOWMAN, A. S. 2019. Madin-Darby canine kidney cell sialic acid receptor modulation

induced by culture medium conditions: Implications for the isolation of influenza A virus. *Influenza Other Respir Viruses,* 13**,** 593-602.

NEUZIL, K. M., ZHU, Y., GRIFFIN, M. R., EDWARDS, K. M., THOMPSON, J. M., TOLLEFSON, S. J. & WRIGHT, P. F. 2002. Burden of interpandemic influenza in children younger than 5 years: a 25-year prospective study. *J Infect Dis,* 185**,** 147-52.

NICHOL, K. L., NORDIN, J. D., NELSON, D. B., MULLOOLY, J. P. & HAK, E. 2007. Effectiveness of influenza vaccine in the community-dwelling elderly. *N Engl J Med,* 357**,** 1373-81.

NICHOLSON, K. G., WOOD, J. M. & ZAMBON, M. 2003. Influenza. *Lancet,* 362**,** 1733-45.

NODA, T. 2011. Native morphology of influenza virions. *Front Microbiol,* 2**,** 269.

NODA, T., MURAKAMI, S., NAKATSU, S., IMAI, H., MURAMOTO, Y., SHINDO, K., SAGARA, H. & KAWAOKA, Y. 2018. Importance of the 1+7 configuration of ribonucleoprotein complexes for influenza A virus genome packaging. *Nat Commun,* 9**,** 54.

NOGALES, A. & MARTÍNEZ-SOBRIDO, L. 2016. Reverse Genetics Approaches for the Development of Influenza Vaccines. *Int J Mol Sci,* 18.

NOGALES, A., MARTINEZ-SOBRIDO, L., TOPHAM, D. J. & DEDIEGO, M. L. 2018. Modulation of Innate Immune Responses by the Influenza A NS1 and PA-X Proteins. *Viruses,* 10.

O'NEILL, R. E., TALON, J. & PALESE, P. 1998. The influenza virus NEP (NS2 protein) mediates the nuclear export of viral ribonucleoproteins. *EMBO J,* 17**,** 288-96.

OH, D. Y., BARR, I. G., MOSSE, J. A. & LAURIE, K. L. 2008. MDCK-SIAT1 cells show improved isolation rates for recent human influenza viruses compared to conventional MDCK cells. *J Clin Microbiol,* 46**,** 2189-94.

OMEIR, R. L., TEFEREDEGNE, B., FOSEH, G. S., BEREN, J. J., SNOY, P. J., BRINSTER, L. R., COOK, J. L., PEDEN, K. & LEWIS, A. M., JR. 2011. Heterogeneity of the tumorigenic phenotype expressed by Madin-Darby canine kidney cells. *Comp Med,* 61**,** 243-50.

OVERTON, E. T., GOEPFERT, P. A., CUNNINGHAM, P., CARTER, W. A., HORVATH, J., YOUNG, D. & STRAYER, D. R. 2014. Intranasal seasonal influenza vaccine and a TLR-3 agonist, rintatolimod, induced cross-reactive IgA antibody formation against avian H5N1 and H7N9 influenza HA in humans. *Vaccine,* 32**,** 5490-5.

PALESE, P. & SHAW, M. 2007. Fields virology. *Orthomyxoviridae: The Viruses and Their Replication, 5th ed.; Lippincott Williams & Wilkins, Wolters Kluwer Business: Philadelphia, PA, USA***,** 1647-1689.

PALESE, P., TOBITA, K., UEDA, M. & COMPANS, R. W. 1974. Characterization of temperature sensitive influenza virus mutants defective in neuraminidase. *Virology,* 61**,** 397-410.

PAULIN, D. & LI, Z. 2004. Desmin: a major intermediate filament protein essential for the structural integrity and function of muscle. *Exp Cell Res,* 301**,** 1-7.

PAVLOVIC, J., HALLER, O. & STAEHELI, P. 1992. Human and mouse Mx proteins inhibit different steps of the influenza virus multiplication cycle. *J Virol,* 66**,** 2564-9.

PENN, R., TREGONING, J. S., FLIGHT, K. E., BAILLON, L., FRISE, R., GOLDHILL, D. H., JOHANSSON, C. & BARCLAY, W. S. 2022. Levels of Influenza A Virus Defective Viral Genomes Determine Pathogenesis in the BALB/c Mouse Model. *J Virol,* 96**,** e0117822.

PETER M. HOWLEY, D. M. K. 2020. *Fields Virology: Emerging Viruses*.

PILLAI, P. S., MOLONY, R. D., MARTINOD, K., DONG, H., PANG, I. K., TAL, M. C., SOLIS, A. G., BIELECKI, P., MOHANTY, S., TRENTALANGE, M., HOMER, R. J., FLAVELL, R. A., WAGNER, D. D., MONTGOMERY, R. R., SHAW, A. C., STAEHELI, P. & IWASAKI, A. 2016. Mx1 reveals innate pathways to antiviral resistance and lethal influenza disease. *Science,* 352**,** 463-6.

PLESCHKA, S. 2013. Overview of influenza viruses. *Curr Top Microbiol Immunol,* 370**,** 1-20.

PLOTCH, S. J., TOMASZ, J. & KRUG, R. M. 1978. Absence of detectable capping and methylating enzymes in influenza virions. *J Virol,* 28**,** 75-83.

PONTÉN, F., JIRSTRÖM, K. & UHLEN, M. 2008. The Human Protein Atlas--a tool for pathology. *J Pathol,* 216**,** 387-93.

POPOV, A., SCOTCHFORD, C., GRANT, D. & SOTTILE, V. 2019. Impact of Serum Source on Human Mesenchymal Stem Cell Osteogenic Differentiation in Culture. *Int J Mol Sci,* 20.

RADTKE, F., FASNACHT, N. & MACDONALD, H. R. 2010. Notch signaling in the immune system. *Immunity,* 32**,** 14-27.

RAMIREZ, R. D., SHERIDAN, S., GIRARD, L., SATO, M., KIM, Y., POLLACK, J., PEYTON, M., ZOU, Y., KURIE, J. M., DIMAIO, J. M., MILCHGRUB, S., SMITH, A. L., SOUZA, R. F., GILBEY, L., ZHANG, X., GANDIA, K., VAUGHAN, M. B., WRIGHT, W. E., GAZDAR, A. F., SHAY, J. W. & MINNA, J. D. 2004. Immortalization of human bronchial epithelial cells in the absence of viral oncoproteins. *Cancer Res,* 64**,** 9027-34.

REYNOLDS, S. D., HILL, C. L., ALSUDAYRI, A., LALLIER, S. W., WIJERATNE, S., TAN, Z. H., CHIANG, T. & CORMET-BOYAKA, E. 2022. Assemblies of JAG1 and JAG2 determine tracheobronchial cell fate in mucosecretory lung disease. *JCI Insight,* 7.

ROBINSON, M. D. & OSHLACK, A. 2010. A scaling normalization method for differential expression analysis of RNA-seq data. *Genome Biology,* 11**,** R25.

ROY, A. M., PARKER, J. S., PARRISH, C. R. & WHITTAKER, G. R. 2000. Early stages of influenza virus entry into Mv-1 lung cells: involvement of dynamin. *Virology,* 267**,** 17-28.

SAHEB SHARIF-ASKARI, N., SAHEB SHARIF-ASKARI, F., HAFEZI, S., KALAJI, Z., TEMSAH, M., ALMUHSEN, S., ALSAFAR, H. S., HAMID, Q. & HALWANI, R. 2022. Airways tissue expression of type I interferons and their stimulated genes is higher in children than adults. *Heliyon,* 8**,** e11724.

SASAKI, S., JAIMES, M. C., HOLMES, T. H., DEKKER, C. L., MAHMOOD, K., KEMBLE, G. W., ARVIN, A. M. & GREENBERG, H. B. 2007. Comparison of the influenza virus-specific effector and memory B-cell responses to immunization of children and adults with live attenuated or inactivated influenza virus vaccines. *J Virol,* 81**,** 215-28.

SCHELLER, N., RESA-INFANTE, P., DE LA LUNA, S., GALAO, R. P., ALBRECHT, M., KAESTNER, L., LIPP, P., LENGAUER, T., MEYERHANS, A. & DIEZ, J. 2007. Identification of PatL1, a human homolog to yeast P body component Pat1. *Biochim Biophys Acta,* 1773**,** 1786-92.

SCHLEE, M., ROTH, A., HORNUNG, V., HAGMANN, C. A., WIMMENAUER, V., BARCHET, W., COCH, C., JANKE, M., MIHAILOVIC, A., WARDLE, G., JURANEK, S., KATO, H., KAWAI, T., POECK, H., FITZGERALD, K. A., TAKEUCHI, O., AKIRA, S., TUSCHL, T., LATZ, E., LUDWIG, J. & HARTMANN, G. 2009. Recognition of 5' triphosphate by RIG-I helicase requires short blunt double-stranded RNA as contained in panhandle of negative-strand virus. *Immunity,* 31**,** 25-34.

SEHGAL, P. B., YUAN, H., SCOTT, M. F., DENG, Y., LIANG, F. X. & MACKIEWICZ, A. 2020. Murine GFP-Mx1 forms nuclear condensates and associates with cytoplasmic intermediate filaments: Novel antiviral activity against VSV. *J Biol Chem,* 295**,** 18023-18035.

SEMPERE BORAU, M. & STERTZ, S. 2021. Entry of influenza A virus into host cells - recent progress and remaining challenges. *Curr Opin Virol,* 48**,** 23-29.

SHANNON, I., WHITE, C. L. & NAYAK, J. L. 2020. Understanding Immunity in Children Vaccinated With Live Attenuated Influenza Vaccine. *J Pediatric Infect Dis Soc,* 9**,** S10-s14.

SHAW, A. E., HUGHES, J., GU, Q., BEHDENNA, A., SINGER, J. B., DENNIS, T., ORTON, R. J., VARELA, M., GIFFORD, R. J., WILSON, S. J. & PALMARINI, M. 2017. Fundamental properties of the mammalian innate immune system revealed by multispecies comparison of type I interferon responses. *PLoS Biol,* 15**,** e2004086.

SHORT, K. R., KROEZE, E., FOUCHIER, R. A. M. & KUIKEN, T. 2014. Pathogenesis of influenza-induced acute respiratory distress syndrome. *Lancet Infect Dis,* 14**,** 57-69.

SIDORENKO, Y. & REICHL, U. 2004. Structured model of influenza virus replication in MDCK cells. *Biotechnol Bioeng,* 88**,** 1-14.

SIECZKARSKI, S. B. & WHITTAKER, G. R. 2002. Influenza virus can enter and infect cells in the absence of clathrin-mediated endocytosis. *J Virol,* 76**,** 10455-64.

SKEHEL, J. J. & WILEY, D. C. 2000. Receptor binding and membrane fusion in virus entry: the influenza hemagglutinin. *Annu Rev Biochem,* 69**,** 531-69.

SOBIESK, J. L. & MUNAKOMI, S. 2023. Anatomy, Head and Neck, Nasal Cavity. *StatPearls.* Treasure Island (FL) ineligible companies. Disclosure: Sunil Munakomi declares no relevant financial relationships with ineligible companies.

SONG, Y., LAI, L., CHONG, Z., HE, J., ZHANG, Y., XUE, Y., XIE, Y., CHEN, S., DONG, P., CHEN, L., CHEN, Z., DAI, F., WAN, X., XIAO, P., CAO, X., LIU, Y. & WANG, Q. 2017. E3 ligase FBXW7 is critical for RIG-I stabilization during antiviral responses. *Nat Commun,* 8**,** 14654.

SRIDHAR, S., BEGOM, S., BERMINGHAM, A., HOSCHLER, K., ADAMSON, W., CARMAN, W., BEAN, T., BARCLAY, W., DEEKS, J. J. & LALVANI, A. 2013. Cellular immune correlates of protection against symptomatic pandemic influenza. *Nat Med,* 19**,** 1305-12.

STEINHAUER, D. A., DOMINGO, E. & HOLLAND, J. J. 1992. Lack of evidence for proofreading mechanisms associated with an RNA virus polymerase. *Gene,* 122**,** 281-8.

STEUERMAN, Y., COHEN, M., PESHES-YALOZ, N., VALADARSKY, L., COHN, O., DAVID, E., FRISHBERG, A., MAYO, L., BACHARACH, E., AMIT, I. & GAT-VIKS, I. 2018. Dissection of Influenza Infection In Vivo by Single-Cell RNA Sequencing. *Cell Syst,* 6**,** 679-691.e4.

SUZUKI, T., HIGGINS, P. J. & CRAWFORD, D. R. 2000. Control selection for RNA quantitation. *Biotechniques,* 29**,** 332-7.

TAWA, K., YAMAMURA, S., SASAKAWA, C., SHIBATA, I. & KATAOKA, M. 2016. Sensitive Detection of Cell Surface Membrane Proteins in Living Breast Cancer Cells Using Multicolor Fluorescence Microscopy with a Plasmonic Chip. *ACS Appl Mater Interfaces,* 8**,** 29893-29898.

TISA, V., BARBERIS, I., FACCIO, V., PAGANINO, C., TRUCCHI, C., MARTINI, M. & ANSALDI, F. 2016. Quadrivalent influenza vaccine: a new opportunity to reduce the influenza burden. *J Prev Med Hyg,* 57**,** E28-33.

UJIE, M., TAKADA, K., KISO, M., SAKAI-TAGAWA, Y., ITO, M., NAKAMURA, K., WATANABE, S., IMAI, M. & KAWAOKA, Y. 2019. Long-term culture of human lung adenocarcinoma A549 cells enhances the replication of human influenza A viruses. *J Gen Virol,* 100**,** 1345-1349.

WALL, D. J., PATEL, M. M., CHUNG, J. R., LEE, B. & DAWOOD, F. S. 2021. Antibody Response and Protection After Receipt of Inactivated Influenza Vaccine: A Systematic Review. *Pediatrics,* 147.

WANG, C. S., WANG, S. T. & CHOU, P. 2002. Efficacy and cost-effectiveness of influenza vaccination of the elderly in a densely populated and unvaccinated community. *Vaccine,* 20**,** 2494-9.

WANG, Z., KEDZIERSKI, L., NUESSING, S., CHUA, B. Y. L., QUIÑONES-PARRA, S. M., HUBER, V. C., JACKSON, D. C., THOMAS, P. G. & KEDZIERSKA, K. 2016. Establishment of memory CD8+ T cells with live attenuated influenza virus across different vaccination doses. *J Gen Virol,* 97**,** 3205-3214.

WEIS, W., BROWN, J. H., CUSACK, S., PAULSON, J. C., SKEHEL, J. J. & WILEY, D. C. 1988. Structure of the influenza virus haemagglutinin complexed with its receptor, sialic acid. *Nature,* 333**,** 426-31.

WELLINGTON, D., LAURENSON-SCHAFER, H., ABDEL-HAQ, A. & DONG, T. 2019. IFITM3: How genetics influence influenza infection demographically. *Biomed J,* 42**,** 19-26.

WHO. 2023a. *Global Influenza Surveillance and Response System (GISRS)* [Online]. Available: https://www.who.int/initiatives/global-influenza-surveillance-and-response-system [Accessed 30.03.2023 2023].

WHO. 2023b. *Influenza (Seasonal)* [Online]. Available: https://www.who.int/en/news-room/fact-sheets/detail/influenza-(seasonal) [Accessed 23.03.2023 2023].

WILEY, D. C., WILSON, I. A. & SKEHEL, J. J. 1981. Structural identification of the antibody-binding sites of Hong Kong influenza haemagglutinin and their involvement in antigenic variation. *Nature,* 289**,** 373-8.

WONG, S. S. & WEBBY, R. J. 2013. Traditional and new influenza vaccines. *Clin Microbiol Rev,* 26**,** 476-92.

WRIGHT, P., NEUMANN, G. & KAWAOKA, Y. 2007. Orthomyxoviruses. Fields Virology. *Fields virology. Lippincott-Williams & Wilkins, Philadelphia***,** 1691-1740.

WU, M., ZHOU, E., SHENG, R., FU, X., LI, J., JIANG, C. & SU, W. 2022. Defective Interfering Particles of Influenza Virus and Their Characteristics, Impacts, and Use in Vaccines and Antiviral Strategies: A Systematic Review. *Viruses,* 14.

XIAO, H., KILLIP, M. J., STAEHELI, P., RANDALL, R. E. & JACKSON, D. 2013. The human interferon-induced MxA protein inhibits early stages of influenza A virus infection by retaining the incoming viral genome in the cytoplasm. *J Virol,* 87**,** 13053-8.

YAN, H. Y., WANG, H. Q., ZHONG, M., WU, S., YANG, L., LI, K. & LI, Y. H. 2021. PML Suppresses Influenza Virus Replication by Promoting FBXW7 Expression. *Virol Sin,* 36**,** 1154-1164.

YAN, N. & CHEN, Z. J. 2012. Intrinsic antiviral immunity. *Nat Immunol,* 13**,** 214-22.

YANG, X., STEUKERS, L., FORIER, K., XIONG, R., BRAECKMANS, K., VAN REETH, K. & NAUWYNCK, H. 2014. A beneficiary role for neuraminidase in influenza virus penetration through the respiratory mucus. *PLoS One,* 9**,** e110026.

YOUIL, R., SU, Q., TONER, T. J., SZYMKOWIAK, C., KWAN, W. S., RUBIN, B., PETRUKHIN, L., KISELEVA, I., SHAW, A. R. & DISTEFANO, D. 2004. Comparative study of influenza virus replication in Vero and MDCK cell lines. *J Virol Methods,* 120**,** 23-31.

ZENS, K. D., CHEN, J. K. & FARBER, D. L. 2016. Vaccine-generated lung tissue-resident memory T cells provide heterosubtypic protection to influenza infection. *JCI Insight,* 1.

ZHANG, J., HU, Y., MUSHARRAFIEH, R., YIN, H. & WANG, J. 2019. Focusing on the Influenza Virus Polymerase Complex: Recent Progress in Drug Discovery and Assay Development. *Curr Med Chem,* 26**,** 2243-2263.

ZHANG, Z., GUO, M., SHEN, M., KONG, D., ZHANG, F., SHAO, J., TAN, S., WANG, S., CHEN, A., CAO, P. & ZHENG, S. 2020. The BRD7-P53-SLC25A28 axis regulates ferroptosis in hepatic stellate cells. *Redox Biol,* 36**,** 101619.

ZHAO, C. & PU, J. 2022. Influence of Host Sialic Acid Receptors Structure on the Host Specificity of Influenza Viruses. *Viruses,* 14**,** 2141.

ZHOU, A., PARANJAPE, J., BROWN, T. L., NIE, H., NAIK, S., DONG, B., CHANG, A., TRAPP, B., FAIRCHILD, R., COLMENARES, C. & SILVERMAN, R. H. 1997. Interferon action and apoptosis are defective in mice devoid of 2',5'-oligoadenylate-dependent RNase L. *Embo j,* 16**,** 6355-63.

ZINOVIEV, A., GOYAL, A., JINDAL, S., LACAVA, J., KOMAR, A. A., RODNINA, M. V., HELLEN, C. U. T. & PESTOVA, T. V. 2018. Functions of unconventional mammalian translational GTPases GTPBP1 and GTPBP2. *Genes Dev,* 32**,** 1226-1241.